Development of Catalytic Processes for the Transformation of Low Value Chemical Feedstocks to Value Added Chemicals

David B. Lao

A dissertation submitted in partial fulfillment of the
requirements for the degree of:

Doctor of Philosophy

University of Washington

2013

Reading Committee:

James M. Mayer, Chair

D. Michael Heinekey

Karen I. Goldberg

Program Authorized to Offer Degree: Department of Chemistry

University of Washington

Abstract

Development of Catalytic Processes for the Transformation of Low Value Chemical Feedstocks to Value Added Chemicals

David B. Lao

Chair of the Supervisory Committee:

Professor James M. Mayer

Department of Chemistry

Dwindling oil reserves have necessitated the shift to alternative sources for fuels and commodity chemicals. This thesis describes fundamental studies and development of catalytic processes for the transformation of abundant, low value chemical resources into value added chemicals. Chapter 1 of this work gives a brief overview of the motivation, challenges, prior work for the catalytic conversion of methane to methanol, methane to ethane and higher alkanes, and glycerol to 1,3-propanediol. Chapter 2 describes efforts to study the kinetics of methanol oxidation by aqueous sodium periodate. The presence of methane pressure in these reactions hinders the rate of methanol oxidation. These fundamental studies may provide novel strategies to prevent the over-oxidation of methane in gas-to-liquid conversion chemistry. The effect of methane pressure, ionic

strength effects, and pH dependence on reaction kinetics was studied, but was complicated by the precipitation and thermal decomposition of sodium periodate. In addition, oxidation of cyclopropyl carbinol was studied to determine the mechanism of periodate oxidation. The lack of ring opening products mitigated against a radical chain mechanism. Chapter 3 discusses attempts to develop a complete catalytic cycle for methyl and aryl coupling using Pt and Pd complexes. These studies introduce potential new strategies for the utilization of methane as a chemical feedstock and catalytic aryl coupling. The formation of biphenyl from monophenyl-Pd^{II} complexes was demonstrated. Attempts to achieve base assisted methane activation with a series of Pt complexes were complicated by ligand incompatibility with bases. Finally, Chapter 4 details the development of a homogeneous iridium pincer catalyst for the catalytic deoxygenation of glycerol, a waste stream from biodiesel production, to 1,3-propanediol and 1-propanol. The tandem catalytic sequence with acid catalyzed dehydration followed by metal catalyzed hydrogenation is a rare example of a homogeneous system that yields 1,3-propanediol from glycerol, albeit in lower yields than 1-propanol. Mechanistic studies suggest that an iridium dihydrogen hydride complex may be the active catalyst in these reactions.

Table of Contents

List of Figures

List of Schemes

List of Tables

Acknowledgements

This thesis is a testament to my last five years of hard work and dedication. As I look back now, it seems somewhat surreal and a tear comes to my eye. Like all great accomplishments, I would not have been here if not for all the great people that have accompanied me on this journey.

I must first thank my two advisors, Jim Mayer and Mike Heinekey. When I first decided to join Jim's lab, I told him that I wanted to join his group because I knew he would make me a better scientist. Although I knew I would become a better scientist, I am still amazed by how much I have grown as a scientist and a person under his guidance. He has always been there to give me a push when needed and challenged me to be the best scientist that I could be. During my final year and a half of graduate school, Mike also contributed greatly to my scientific and personal development. One could not ask for two better advisors than Jim and Mike. It has been a pleasure to work with both of them and I will be forever thankful for all they have done for me.

Next, I must thank my undergraduate research advisors, Larry Dalton and Phil Reid. Larry and Phil gave me the opportunity to join their labs even though I had only just completed general chemistry. Without their mentorship, I may never have pursued graduate school.

As an undergraduate in the Dalton lab, I was supervised and trained by a number of graduate students and post docs to whom I am forever indebted. Kim Firestone and Denise Bale gave me my first hands-on research experience. Phil Sullivan, Samy Elangovan, and Josh Davies taught me all the organic synthesis techniques I know. Samy's words of encouragement and confidence in me as a scientist have stuck with me always.

Although I started as an organic student, joining the inorganic division may be one of the best decisions of my life. I have had the honor of working with and befriending many wonderful individuals including Kate Allen, Shoshanna Barnett, Johanna Blacquiere, Miles Braten, Colin Carver, Mauricio Cattaneo, Samantha Connelly, Alex Fox, Jon Goldberg, Rebecca Hayoun, Jessica Hoover, Mike Lanci, Steve Matthews, Joe Meredith, Alex Miller, Alisa Owens, Lisa Park-Gehrke, Michael Pegis, Jennifer Peper, Tom Porter, Ian Rhile, Carlos Rodriguez del Rio, Caroline Sauoma, Joel Schrauben, Adam Tenderholt, Sophia Tran, Tristan Tronic, Carolyn Valdez, Alex Wallner, Jeff Warren, Derek Wasylenko, Jessica Wittman, and Gene Wong. It's been a real pleasure to have spent time with all these talented people and I expect great things out of them in the future.

There are a few individuals who I feel had a huge impact on my time as a graduate student. Rebecca Hayoun helped train me and get settled when I first joined the lab. She also provided me with very useful discussions on my first project. Mike Lanci trained me to be an organometallic chemist. It was a privilege to have collaborated with him on methane oligomerization (even though he is a Philadelphia Eagles fan). Jeff

Warren is one of the most unforgettable people I've met in my life. I have always enjoyed the many interesting conversations we've shared pertaining to chemistry and his life experiences. Lisa Park-Gehrke is one of the most positive and cheerful people I've ever met. I am in awe of how she was able to keep that demeanor throughout five years of graduate school. Tristan Tronic's quiet and calm presence brought a nice balance to the lab. I often looked to Tristan as an example of a model graduate student. Tom Porter and Sophia Tran have been my best friends in graduate school. I'm glad to have had Tom and Sophia around to share inside jokes and stories. I think I have shared more laughs with them than anyone else in the department. Sophia has always been willing to lend me an ear and chat whenever I was down about something. Despite what I have joked about in the past, I will miss having her as a co-worker.

CENTC has given me the opportunity to collaborate with Melanie Sanford and Karen Goldberg. Their scientific expertise and insight were always of tremendous help during my scientific pursuits. Collaborations through CENTC also allowed me to meet Matt Remy, Monica Lotz, and Gene Wong. I have enjoyed getting to know them on a scientific and personal level.

I must thank all the great classmates and friends that I have made through my studies in chemical engineering and chemistry. Will Gibbons, Andy Steiner, Nick Cummings, and Skye Mitchell endured the rigor of chemical engineering courses with me. I will always cherish our late night cramming sessions, sleepless nights in the Benson Hall computer lab, and post exam celebrations. I entered graduate school with Nick Cox, Richard Rucker, Micah Uehling, Aaron Whittaker, Alicia McGhee and Erica Ingalls. I'm glad that they have been a part of my life and I'm excited to see all the great things they will accomplish in the future. Anh Nguyen and Klay Jones are two of my favorite people that I have met during my time at the UW. They are extremely loyal friends and have always been there to cheer me on.

I regard Pablo Basilio, Raymond Chung, Aaron Freidenberg, James Kuo, Alex Lee, Gabino Mabalay, Eric Miller, Ben Omura, Tomas Pulmano, Brian Steinberg, and Jeff Yoshida as my brothers. I'm very fortunate to have grown up with them over the past 14 plus years. They have been there for me through the highest and lowest points of my life and they are the best friends that a person could ask for. Brothers to the end.

My acknowledgements wouldn't be complete without thanking Emiley Hwang who stuck with me throughout graduate school. Most of my happiest moments during graduate school were shared with her and I don't think I would have made it through it if I didn't have her in my life. She's my best friend and I'll always love her.

Finally, I need to thank my family. My sister Lily and nephews Steven and Tyler have always been there to support me. My mom Xiao Hong and dad Zan Chao want me to succeed in life more than anyone else in the world. My parents would be willing to sacrifice anything so that I could pursue my dreams. I love my family and am very grateful to have them in my life.

Dedication

To Mom and Dad
and
all those who believed that I could do this.

1 – Introduction

1.1 Introduction

The current petrochemical industry is vital for providing both fuel and commodity chemicals. In a typical barrel of oil, the majority of the components are used for transportation fuels and the remaining components can be converted to polymers, lubricants, and aromatics for fine chemicals. As oil reserves are depleted, new alternatives for fuels and commodity chemicals must be developed.

Methane is an intriguing chemical feedstock and supplemental fuel that has garnered much attention in the past forty years.[1,2] Methane is an abundant hydrocarbon source and reserves continue to be discovered. Although abundant, it is energy intensive and expensive to capture and transport as methane reserves are commonly found in remote and off-shore areas. Methane is often flared at remote sites because it is a more effective green house gas than CO_2, but it is estimated that 500 teragrams of methane are still released into the atmosphere annually. [3,4] Rather than allowing this resource to be wasted, processes are needed to convert methane into higher value chemicals.

While methane may serve as a supplemental fuel and chemical feedstock for the near future, eventual independence from fossil fuels will be necessary. Biomass is a promising carbon source for the future. Although biomass is cheap, abundant, and renewable, new technologies must be developed to convert carbohydrates and polyalcohols into useful fuels and chemicals. Compared to the extensive studies for the

functionalization of hydrocarbons, there is relatively little work done with biomass products and it is a relatively new field of chemistry.[5]

One important bio-derived feedstock is glycerol, the waste product from biodiesel production. Biodiesel production has continued to grow since 2000 and it is estimated that close to 1.1 billion gallons will be produced in 2013.[6] Although glycerol has uses as a commodity chemical, the rate of growth of the biodiesel industry has resulted in a surplus of glycerol. As a result of overproduction, glycerol is often burned as a fuel for the biodiesel production process. Developing technologies to convert glycerol into a higher value chemical would be make biodiesel production into a much greener and profitable industry.[7,8,9]

1.2 Methane: Challenges and Outlooks

1.2.1 Methane to Methanol

The direct catalytic conversion of methane to methanol has been an area of great interest for the past several decades. The conversion of a gas to liquid fuel would greatly reduce storage and transportation costs, and allow for methane to be a viable supplemental fuel source. The current technology for the conversion of methane to methanol involves a two step procedure of steam reforming of methane followed by reduction of carbon monoxide with hydrogen over a copper and zinc catalyst. While this industrial procedure is highly selective, the high temperatures and pressures required for this process make it very energy intensive and expensive.

The main challenge in direct conversion of methane to methanol is the activation of the 105 kJ/mol C-H bond in methane, which is the strongest C-H bond of all aliphatic hydrocarbons and is relatively unreactive.[10] The conversion of methane to methanol is further complicated because under the conditions for which methane can be oxidized, further oxidation of methanol to formaldehyde and carbon dioxide is also facile.[11,12]

The earliest work for homogeneous C-H activation and functionalization of methane was by Shilov.[13] Shilov reported the activation of methane in aqueous solutions via initial C-H activation of methane by a Pt^{II} salt to form Pt^{II}-CH_3, oxidation of Pt^{II}-CH_3 to Pt^{IV}-CH_3 by a Pt^{IV} salt, and reductive elimination of methanol or methylchloride upon nucleophilic attack by hydroxide or chloride. Although these catalysts were capable of this transformation, the reaction is slow and requires the use of stoichiometric Pt^{IV} as an oxidant.

Periana has reported one of the most successful catalysts to date for the oxidation of methane.[12] Periana reported the conversion of methane to methyl sulfate using a Pt 2,2'-bipyrimidine complex in sulfuric acid and sulfur trioxide. By forming the methyl sulfate, further oxidation of the product is avoided. Although the oxidation of methane to methyl sulfate can be achieved in high selectivity, the reaction is hindered upon the formation of water over the course of the reaction.

As new technologies are developed for the oxidation of methane to methanol, new strategies are required to increase selectivity. Following the work of Dehestani for OsO_4 reduction by dihydrogen[14] and Bales' reports of the oxidation of alkanes by OsO_4[15],

Osako demonstrated that aqueous solutions of OsO_4 and $NaIO_4$ were capable of converting methane to methanol, formaldehyde (hydrolyzed to methanediol), and carbon dioxide.[16] Furthermore it was observed that a steady-state concentration of methanol was achieved within four hours of reaction and remained relatively constant for several days.

Osako also demonstrated that methanol oxidation to methanediol and CO_2 by OsO_4 and $NaIO_4$ was inhibited by the presence of methane.[17] When the analogous reactions are performed under argon or vacuum, the oxidation of methanol was a thousand times faster. A similar, but much less dramatic, inhibition effect was observed for the oxidation of methanol by aqueous solutions of $NaIO_4$. The inhibition of methanol oxidation by methane is unprecedented. Chapter 2 details efforts to elucidate the origin of this inhibition effect in hopes that these studies will aid in developing selective strategies for the oxidation of methane to methanol.

1.2.2 Methane to Ethane and Higher Alkanes

An alternative to methane upgrading is the formation of ethane via activation of methane followed by C-C bond formation. When ethane is dehydrogenated to ethylene, it can be used as to produce polyethylene, the most widely used plastic in the world. Current technologies for ethylene formation involve the steam cracking of higher value, long chain hydrocarbons. Catalytic oxidative coupling of methane has been studied using heterogeneous metal oxides, but these reactions require high temperatures and suffer from low conversions.[18] A direct and efficient catalytic route from methane to ethane

under mild conditions would be highly desirable. Such a route may also allow for the formation of higher alkanes for fuels.

A catalytic cycle for methane to ethane conversion can be generally envisioned as reductive elimination of ethane from a dimethyl metal complex followed by regeneration of the original species via C-H activation of methane. Reductive eliminations to form C-C bonds from transition metal complexes are well studied.[19,20] Specifically, the reductive elimination of ethane from a five-coordinate trimethyl Pt^{IV} complexes has been reported by Puddephatt[21] with 1,2-bis(diphenylphosphino)ethane and Goldberg[22] with β-diketiminate ligands. Reductive elimination from polymethyl Pd complexes have also been reported in the literature. Stille has reported the formation of ethane from dimethyl Pd^{II} and trimethyl Pd^{IV} complexes with phosphine ligands.[23] Canty has reported similar chemistry with dimethyl alkyl Pd^{IV} tris(pyrazo1-1-y1)methane complexes.[24]

Although numerous complexes of Pd and Pt have been reported to form ethane, none of these complexes have been reported to activate methane. Tilset[25] and Bercaw[26] have reported *N*,*N*′-diaryl-2,3-dimethyl-1,4-diaza-1,3-butadiene (DAB) Pt complexes capable of methane activation. Encouraged by these results, Lanci has demonstrated that upon oxidation, (DAB)$Pt(CH_3)_2$ complexes undergo oxidative disproportionation to form a $[(DAB)Pt(CH_3)_3]^+$ complex.[27] Reductive elimination of ethane can be promoted from these complexes by working in weakly coordinated solvents and increasing steric bulk around the metal center with substitution on the ligand aryl groups.

In order to complete the catalytic cycle, (DAB)Pt(CH_3)$_2$ must be regenerated from the formed [(DAB)Pt(CH_3)]$^+$ complex. While Tilset and Bercaw have reported that these types of complexes activate methane, they undergo methyl exchange rather than formation of additional Pt-C bonds. In chapter 3, studies to understand strategies for C-H activation of methane and efforts to achieve a complete catalytic cycle for C-C bond formation will be discussed.

1.3 Glycerol: Challenges and Outlook

Glycerol can be converted to several higher value chemicals, but one of the most attractive is 1,3-propanediol (1,3-PD). 1,3-PD is a component in the production of polyesters, polyurethanes, and polyethers. One widely produced polyester synthesized from 1,3-PD is polytrimethylene terephthalate, which is marketed by DuPont under the brand name Sorona™ and Shell Chemical under the brand name Corterra™. Current methods for the production of 1,3-PD are hydroformylation of ethylene oxide and biofermentation.[28] While these methods are practiced industrially, the use of waste stream glycerol with a highly selective and efficient catalytic system would be an attractive route to 1,3-PD.

The deoxygenation of glycerol to 1,3-PD can be envisioned as a tandem catalytic sequence with an initial acid catalyzed dehydration followed by metal catalyzed hydrogenation. Such reaction conditions require that catalysts for these processes be compatible under high temperatures and pressures and with water and acid. In addition to challenges with compatible catalysts, thermodynamic gas phase calculations have shown

that formation of 1,2-propanediol (1,2-PD) is favored over formation of 1,3-PD.[29, 30] Furthermore, Schlaf has suggested that in the reaction profile of homogeneous systems, acid catalyzed dehydration of glycerol has the highest activation barrier.[43] Therefore, under conditions where glycerol can be dehydrated, all subsequent steps for further dehydration and hydrogenation can also be achieved and 1,3-PD cannot be achieved selectively. Heterogeneous systems may circumvent this issue due to glycerol interaction with the catalyst surface.

Various heterogeneous catalysts have been developed for the deoxygenation of glycerol. Several copper[31,32,33] and ruthenium[34,35,36] catalysts have been reported, but the majority of them favor the formation of 1,2-PD over 1,3-PD. Pt catalysts have also been reported, several of which favor formation of 1,3-PD, but these catalysts still result in the formation of other products.[37,38,39] The highest selectivity for 1,3-PD using heterogeneous catalysts was reported by Tomishige using iridium nanoparticles on silica with rhenium oxides.[40] These catalyst were able to achieve up to 63% conversion with 49% selectivity to 1,3-PD, 10% selectivity to 1,2-PD, and 33% to 1-propanol (1-PO).

Despite all the reports of heterogeneous catalysts, there are relatively few reports of homogeneous catalysts. Che has reported the use of a $Rh(CO)_2$(acetylacetonate) complex for the conversion of glycerol to a 1:1 ratio of 1,3-PD and 1,2-PD.[41] More recent studies have not proven as successful for formation of 1,3-PD. Braca has reported a ruthenium iodocarbonyl catalyst which is 90% selective for the formation of 1-PO.[42]

Efforts by Schlaf using ruthenium aqua complexes with co-catalyst triflic acid afforded only propene formation.[43,44]

Ahmed-Foskey has reported the use of a homogeneous bis(phosphinite) (POCOP) iridium pincer catalyst for the catalytic deoxygenation of 1,2-PD to 1-PO in up to 95% yield.[45] Efforts to build upon this work to develop a catalytic system for the selective conversion of glycerol to 1,3-PD will be discussed in chapter 4.

1.4 Notes to Chapter 1

1 Conley, B. L.; Tenn III, W. J.; Young, K. J. H.; Ganesh, S. K.; Meier, S. K.; Ziatdinov, V. R.; Mironov, O.; Oxgaard, J.; Gonzales, J.; Goddard III, W. A.; Periana, R. A. *J. Mol. Catal. A: Chem.* **2006**, *251*, 8-23.

2 Bergman, R. G. *Nature* **2007**, *446*, 391-393.

3 Blasing, T. J.; Hand, K. *Tellus* **2007**, *59*, 15-21.

4 *Climate Change 2007: The Physical Science Basis. Contribution of Working Group I to the Fourth Assessment Report of the Intergovernmental Panel on Climate Change*; Solomon, S., D. Qin, M. Manning, Z. Chen, M. Marquis, K.B. Averyt, M.Tignor, H.L. Miller, Ed.; Cambridge University Press: New York, 2007.

5 Schalf, M. *Dalton Trans.* **2006**, 4645-4653.

6 National Biodiesel Board Annual Estimates. Biodiesel.org (accessed Apr 4, 2013).

7 Johnson, T. D.; Taconi, K. A. *Environmental Progress* **2007**, *26*, 338-348.

[8] Cheda, J. N.; Huber, G. W.; Dumesic, J. A. *Angew. Chem., Int. Ed.* **2007**, *46*, 7164-7183.

[9] Dam, J. T.; Hanefeld, U. *ChemSusChem* **2011**, *4*, 1017-1034.

[10] Berkowitz, J.; Ellison, G. B.; Gutman, D. *J. Phys. Chem.* **1994**, *98*, 2744-2765.

[11] Chen, G. S.; Labinger, J. A.; Bercaw, J. E. *Organometallics* **2009**, *28*, 4899-4901.

[12] Periana, R. A.; Taube, D. J.; Gamble, S.; Taube, H.; Satoh, T.; Fujii, H. *Science* **1998**, *280*, 560-564.

[13] Gol'dshleger, N. F.; Es'kova, V. V.; Shilov, A. E.; Shteinman, A. A. *Zh. Fiz. Khim.* **1972**, *46*, 1353.

[14] Dehestani, A.; Lam, W. H.; Hrovat, D. A.; Davidson, E. R.; Borden, W. T.; Mayer, J. M. *J. Am. Chem. Soc.* **2005**, *127*, 3423-3432.

[15] Bales, B. C.; Brown, P.; Dehestani, A.; Mayer, J. M. *J. Am. Chem. Soc.* **2005**, *127*, 2832-2833.

[16] Osako, T.; Watson, E. J.; Dehestani, A.; Bales, B. C.; Mayer, J. M. *Angew. Chem.* **2006**, *45*, 7433-7436.

[17] Osako, T.; Hayoun, R.; Mayer, J. M. 2007. Unpublished results.

[18] For example see: (a) Keller, G. E.; Bhasin, M. M. *J. Catal.* **1982**, *73*, 9-19. (b) Ito, T.; Lunsford, J. H. *Nature* **1985**, *314*, 721-722.

[19] Brown, J. M.; Cooley, N. A. *Chem. Rev.* **1988**, *88*, 1031-1046.

[20] Hartwig, J. Reductive Elimination. In *Organotransition Metal Chemistry From Bonding to Catalysis*; University Science Books: Sausalito, CA, 2010; 331-338.

[21] (a) Hill, G. S.; Puddephatt, R. J. *Organometallics* **1997**, *16*, 4522-4524. (b) Hill, G. S.; Yap, G. P. A.; Puddephatt, R. J. *Organometallics* **1999**, *18*, 1408-1418.

[22] Fekl, U.; Goldberg, K. I. *J. Am. Chem. Soc.* **2002**, *124*, 6804-6805.

[23] Moravskiy, A.; Stille, J. K. *J. Am. Chem. Soc.* **1981**, *103*, 4182-4186.

[24] Brown, D. G.; Byers, P. K.; Canty, A. J. *Organometallics* **1990**, *9*, 1231-1235.

[25] Johansson, L.; Ryan, O. B.; Tilset, M. *J. Am. Chem. Soc.* **1999**, *121*, 1974-1975.

[26] Owen, J. S.; Labinger, J. A.; Bercaw, J. E. *J. Am. Chem. Soc.* **2006**, *128*, 2005-2016.

[27] Lanci, M. P.; Remy, M. S.; Lao, D. B.; Sanford, M. S.; Mayer, J. M. *Organometallics* **2011**, *30*, 3704-3707.

[28] Kraus, G. A. *Clean Soil Air Water* **2008**, *36*, 648-651.

[29] Nimlos, M. R.; Blanksby, S. J.; Qian, X.; Himmel, M. E.; Johnosn, D. K. *J. Phys. Chem. A.* **2006**, *110*, 6145-6156.

[30] Coll, D.; Delbecq, F.; Aray, Y.; Sautet, P. Phys. *Chem. Chem. Phys.* **2011**, *13*, 1448-1456.

[31] Montassier, C.; Dumas, J. M.; Granger, P.; Barbier, *J. Appl. Cat. A: Gen.* **1995**, *121*, 231-244.

[32] Chaminand, J.; Djakovitch, L.; Gallezot, P.; Marion, P.; Pinel, C.; Rosier, C. *Green Chem.* **2004**. *6*, 359-361.

[33] Huang, L.; Zhu, Y.; Zheng, H.; Ding, G.; Li, Y. *Catal. Lett.* **2009**, *131*, 312-320.

[34] Miyazawa, T.; Koso, S.; Kunimori, K.; Tomishige, K.; *Appl. Cat. A: Gen.* **2007**, *318*, 244-251.

[35] Miyazawa, T.; Koso, S.; Kunimori, K.; Tomishige, K. *Appl. Cat. A: Gen.* **2007**, *329*, 30-35.

[36] Balaraju, M.; Rekha, V.; Devi, B. L. A. P.; Prasad, R. B. N.; Prasad, P. S. S.; Lingaiah, N. *Appl. Cat. A.: Gen.* **2010**, *384*, 107-114.

[37] Qin, L.; Song, M.; Chen. C. *Green Chem.* **2010**, *12*, 1466-1472.

[38] Gong, L.; Lu, Y.; Ding, Y.; Lin, R.; Li, J.; Dong, W.; Wang, T.; Chen, W. *Appl. Cat. A: Gen.* **2010**, *390*, 119–126.

[39] Gong, L.; Lu, Y.; Ding, Y.; Lin, R.; Li, J.; Dong, W.; Wang, T.; Chen, W. *Chin. J. Cat.* **2009**, *30*, 1189-1191.

[40] Nakagawa, Y.; Shinmi, Y.; Koso, S.; Tomishige, K. *J. Catal.* **2010**, *272*, 191-194.

[41] Che, M. US Pat., 4642394, 1987.

[42] Braca, G.; Galletti, A. M. R.; Sbrana, G. *J. Organomet. Chem.* **1991**, *417*, 41-49.

[43] Thibault, M. E.; DiMondo, D. V.; Jennings, M.; Abdelnur, P. V.; Eberlin, M. N.; Schlaf, M. *Green Chem.* **2011**, *13*, 357-366.

[44] Taher, D.; Thibault, M. E.; DiMondo, D.; Jennings, M.; Schlaf, M. *Chem. Eur. J.* **2009**, *15*, 10132-10143.

[45] Ahmed-Foskey, T. J.; Heinekey, D. M.; Goldberg, K. I.; *ACS Catal.* **2012**, *2*, 1285-1289.

2 – Oxidation of Methanol by Sodium Periodate

2.1 Introduction

2.1.1 General Introduction

Methane, CH_4, is the main component of natural gas and is produced in abundance by various anthropogenic and natural sources. Methane has garnered much attention in the past thirty years due to its use as a supplemental fuel and chemical feedstock.[1,2] It is estimated that over 500 teragrams of methane are released into the atmosphere annually.[3] In addition to being abundant, methane is the cleanest burning hydrocarbon, releasing the least CO_2 per joule upon combustion because it has the highest hydrogen-to-carbon ratio.

Despite its abundance, many natural gas wells are stranded off-shore or in remote locations such as Nigeria. Transporting methane from these locations to a desired locale costly due to the large amount of energy and equipment required for liquefaction or pipelining. As a result, most methane is consumed close to its place of origin.[4] Methane that cannot be easily transported is often flared. Flaring is preferential to releasing methane to the atmosphere because it is 63 times more effective as a greenhouse gas than CO_2 and it avoids potentially combustible conditions at locations around the gas well.[5] Approximately 1700 teragrams (2.4e12 m^3) of methane have been flared worldwide over the past 15 years.[6]

Rather than wasting these potential resources, it would be ideal to have a low cost method to transform methane into an easily transportable liquid such as methanol, CH_3OH. Unfortunately, the 105 kcal/mol C-H bonds in methane are the strongest of all aliphatic hydrocarbons and are relatively unreactive.[7] In addition, the oxidation of methane to methanol presents another challenge because further oxidation to formaldehyde, formic acid, and carbon dioxide becomes more facile.[8,9] Considerable effort has been made over the past several decades to develop reactions and catalysts that would be cost effective, selective, and yield high conversions and turnovers for the oxidation of methane to methanol.[1,2,10,11] The work presented here seeks to address the issue of selectivity. These studies investigate the methane inhibition of methanol oxidation by sodium periodate.

2.1.2 Previous Work

Dehestani and coworkers have previously shown that osmium tetroxide, OsO_4, is reduced by molecular hydrogen to Os(VI) dimers $L_2Os(O)_2(\mu\text{-}O)_2Os(O)_2L_2$ in the presence of ligands (L = pyridine or 1,10-phenanthroline) in organic media and $OsO_2(OH)_4^{2-}$ in basic aqueous media. The reduction is proposed to proceed via a [3+2] addition of hydrogen to two oxo groups on OsO_4. Other possible mechanisms were ruled out based on kinetic data and density functional theory calculations.[12]

The osmium work was continued by Bales and coworkers who showed that OsO_4 could oxidize alkanes under basic conditions. OsO_4 was found to oxidize isobutane,

cyclohexane, cyclopentane, toluene, ethane, and propane. These oxidations are proposed to proceed via a [3+2] addition mechanism, analogous to the OsO_4 and hydrogen systems previously described. Oxidation of isobutane was also found to proceed using catalytic OsO_4 with sodium periodate, $NaIO_4$, as the terminal oxidant.[13]

The previous findings described above led to the discovery by Osako and coworkers that aqueous solutions containing both OsO_4 and $NaIO_4$ under mild conditions oxidized methane to methanol, formaldehyde (hydrolyzed to methanediol), and carbon dioxide (Equation 2.1).[14]

$$CH_4 \xrightarrow[D_2O \text{ at } 50^oC]{OsO_4/NaIO_4} CH_3OH + H_2C(OH)_2 + CO_2 \qquad (2.1)$$

Only solutions containing both OsO_4 and $NaIO_4$ were found to oxidize methane to methanol. Under these conditions, the methanol product concentration was found to reach a steady-state concentration within 4 hours and remained relatively unchanged even after several days. This result was surprising due to the strong oxidizing conditions and well known over-oxidation of methanol.

Another unprecedented finding was that the oxidation rate of methanol by OsO_4 and $NaIO_4$ was inhibited by methane (Equation 2.2).

$$CH_3OH \xrightarrow[D_2O \text{ at } 50^oC \text{ under} CH_4]{OsO_4/NaIO_4} H_2C(OH)_2 + CO_2 \qquad (2.2)$$

Under vacuum or argon, the rate of oxidation of methanol is a thousand times faster than the same reaction under methane.

Later work by Osako showed that methanol is oxidized by $NaIO_4$ alone (Equation 2.3) and the oxidation rate was also inhibited by the presence of methane.[15]

$$CH_3OH \xrightarrow[\substack{\text{Phosphate Buffer in } D_2O \\ \text{at } 50^oC \text{ under } CH_4}]{NaIO_4} H_2C(OH)_2 + H_2CO + CO_2 \qquad (2.3)$$

Under 10 atm CH_4, the methanol oxidation rate was found to be about 23 times slower than under vacuum or argon. To date, there are still no explanations for the origin of this inhibition. Methane is considered to be relatively inert and spectroscopic data shows no interaction of methane with $NaIO_4$ or methanol.

There is no known precedence for the oxidation of methanol by $NaIO_4$ and very little literature on the uncatalyzed oxidation of alcohols by $NaIO_4$.[16,17,18,19,20] Periodate and periodic acid are more commonly used in the oxidative cleavage of glycols.[21] Most reports of alcohol oxidation by periodate in the literature often include transition metal catalysts. The work detailed herein furthers the understanding of uncatalyzed methanol oxidation by $NaIO_4$ and seeks to elucidate the origin of the methane inhibition effect in hopes that it may be applied to the challenge of selective methane activation.

2.2 Results and Discussion

2.2.1 Verifying the Methane Inhibition Effect

Results in this chapter will be discussed in the order obtained; therefore, many results reported in earlier sections will be further discussed in later sections. Initial efforts focused on reproducing the kinetic data collected by Osako and coworkers in order to verify the inhibition of methanol oxidation by methane.[15] Procedures reported by Osako

were closely followed so that comparisons could me made with previously determined rate constants. In this report, pD is used in place of pH because of the use of deuterated solvent. Conversion from pH to pD is obtained by adding 0.40 to the values obtained using a pH probe.[22] Past work completed by Osako and coworkers reported buffering reaction solutions at pD 6.4.[15] This pD was selected to mimic the OsO_4 chemistry where near neutral to high pD was required for the desired osmium species in solution.[12,13,14]

A 500 mM phosphate buffer, PB, solution at pD 6.4 was prepared with D_3PO_4 in D_2O. The pD of the buffer solution was adjusted with NaOD. A 95 mM stock solution of methanol in 500 mM PB solution at pD 6.4 was prepared. At pD 6.4, attempts to make a stock 200 mM sodium periodate solution in PB resulted in the precipitation of a white solid. To avoid using an unknown concentration stock solution, solid sodium periodate was weighed out and transferred directly into the reaction mixtures rather than using a stock solution.

Reaction solutions were prepared in medium-walled NMR tubes. Flame-sealed capillary standards containing hexamethylbenzene (δ 2.10, s, 18H) in benzene-d_6 were placed in the NMR tubes to quantify the integration of the methanol CH_3 ^{1}H-NMR chemical shift (δ 3.26, s, 3H). NMR tubes were charged with solid sodium periodate, methanol in PB solution, and PB solution. After connecting the tubes to a known volume gas bulb on a vacuum line, the NMR tubes were degassed with three freeze-pump-thaw cycles, and filled with a known pressure of argon or methane based on a Boyle's law calculation using the headspace in the NMR tube, the pressure in the bulb, and the

volume of the bulb. After pressurization with the desired gas, the tubes were flame sealed to the desired length.

Following flame sealing, the samples were kept frozen until immediately prior to ^{1}H-NMR analysis. Before recording a ^{1}H-NMR spectrum, the reaction solution was thawed, warmed to room temperature, and shaken vigorously. The formation of the previously described precipitate was observed in these solutions when a concentration greater than *ca.* 40 mM sodium periodate was used at pD 6.4.

After obtaining an initial ^{1}H-NMR spectrum, the tube was placed in an 80^{o}C oil bath controlled with a thermocouple. The precipitate in the reaction mixtures dissolved after approximately 24 hours in the oil bath. The tubes were periodically removed from the oil bath, cleaned with hexane, shaken, and cooled to room temperature to collect additional ^{1}H-NMR spectra. The reactions were monitored by ^{1}H-NMR spectroscopy following the disappearance of the methanol CH_3 peak. Complete oxidation of methanol was not always observed and the oxidation of methanol would appear to stop in some reactions. Reactions that proceeded for more than 10 days for complete oxidation were followed until the methanol concentration remained constant for more than four days. A set of example spectra are shown in Figure 2-1. Reaction time was measured as the time heated at 80^{o}C in the oil bath.

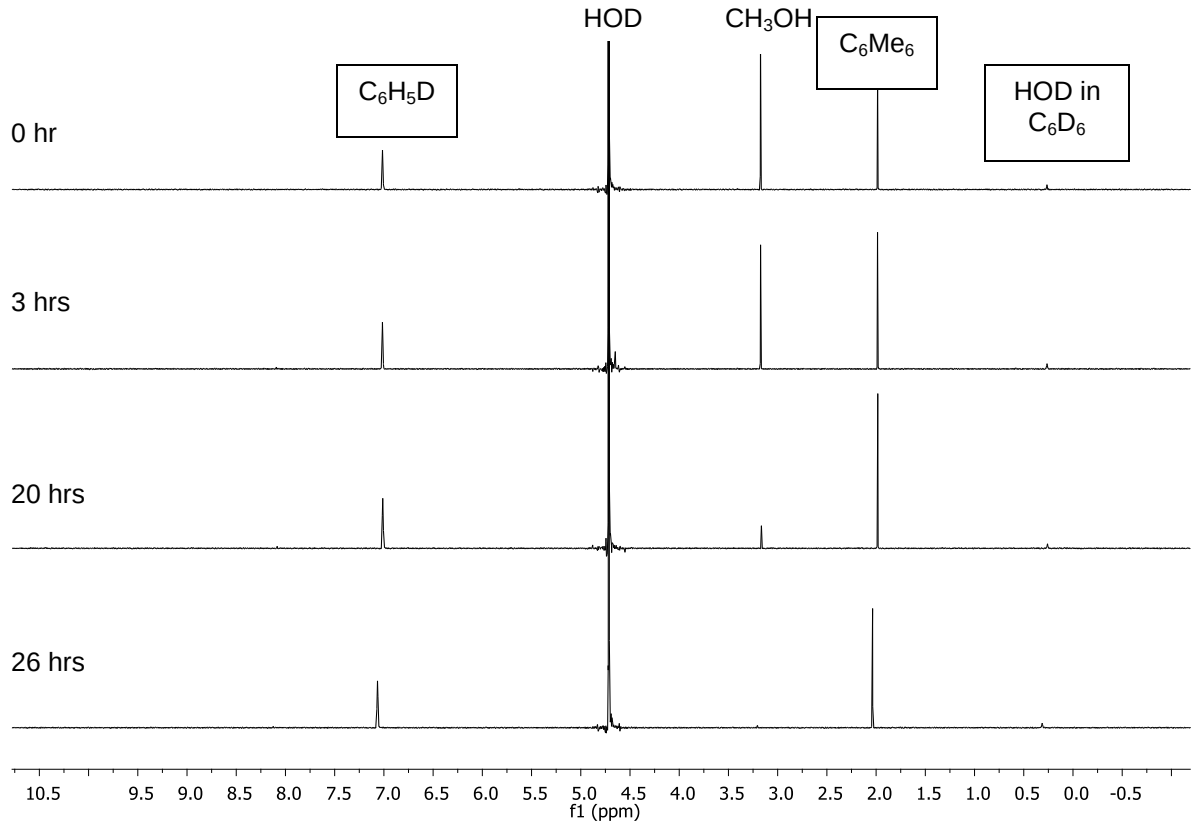

Figure 2-1. Typical ^{1}H-NMR spectra for the oxidation of CH_3OH by $NaIO_4$. Capillary standard peaks are shown in boxes. The CH_3OH NMR signal intensity decreases as it is oxidized.

After the reactions were complete, the exact initial concentrations of methanol in the reactions were quantified by opening the sealed NMR tube and introducing a known concentration of trimethylacetic acid (δ 1.13, s, 9H) in D_2O solution to calibrate the hexamethylbenzene capillary standard.

Based on the previous results obtained by Osako, the analysis of the kinetic data for oxidation of methanol by $NaIO_4$ has been assumed to obey elementary second order

kinetics, $-\frac{d[CH_3OH]}{dt} = k[NaIO_4][CH_3OH]$. The reactions were performed under pseudo-first order conditions with excess periodate, $-\frac{d[CH_3OH]}{dt} = k_{obs}[CH_3OH]$. The concentration of methanol versus time was plotted and fit to an exponential decay using Origin 6.1 to obtain k_{obs} for varying concentrations of sodium periodate. A linear fit of k_{obs} versus sodium periodate concentration was used to determine the rate constant, k. Under 3 atm of argon, the rate constant was calculated to be $k_{Ar} = (3.0 \pm 1.0) \times 10^{-4}$ $M^{-1}s^{-1}$. Under 3 atm of methane, the rate constant was calculated to be $k_{CH4} = (1.0 \pm 1.0) \times 10^{-4}$ $M^{-1}s^{-1}$. Under identical conditions, Osako reported $k_{Ar} = (6.9 \pm 0.5) \times 10^{-4}$ $M^{-1}s^{-1}$ and $k_{CH4} = (6.6 \pm 0.6) \times 10^{-5}$ $M^{-1}s^{-1}$.[15]

The rate constants demonstrate that the oxidation of methanol by $NaIO_4$ is inhibited by the presence of methane. Despite great effort to exactly reproduce previous experimental conditions, there were large variations in the measured rate constants. It was difficult to obtain reproducibility with Osako's results as well as between each sample run. These inconsistencies may be related to the formation of precipitate in these reactions or other as of yet unidentified factors. Osako and coworkers did not report observing insolubility of sodium periodate under these conditions.

In addition, methanol oxidation was often observed to stop after *ca.* 10 days and the methanol concentration remained constant even though reactions are performed with excess oxidant (Figure 2-2). Incomplete oxidation of methanol was also not reported by Osako and coworkers.

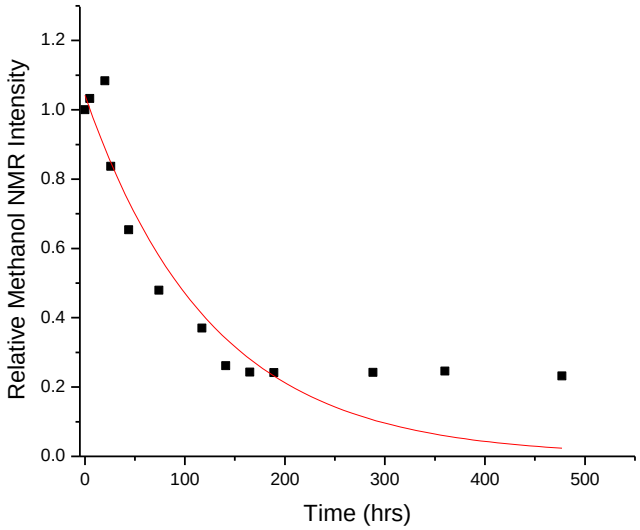

Figure 2-2. The ^{1}H-NMR kinetic data for 0.95 mM CH_3OH oxidation by 40 mM $NaIO_4$ in 500 mM PB under argon at 80^{o}C. Relative intensity of the CH_3OH ^{1}H-NMR integral is plotted versus time. Data are fit using an exponential decay function, $[CH_3OH] = [CH_3OH]_o e^{-k_{obs} \times t}$, rather than a shifted exponential decay function, $[CH_3OH] = [CH_3OH]_o e^{-k_{obs} \times t} + [CH_3OH]_f$, to illustrate that oxidation stops after *ca.* 10 days.

Due to the irreproducibility of the past results and inconsistent kinetic data between samples, research efforts focused on investigating several variables on the oxidation rate – methane pressure, ionic strength effects, and pH dependence. Research efforts also focused on probing the mechanism of the oxidation with periodate.

2.2.2 Methane Pressure Dependence Studies

Osako and coworkers reported a decrease in the oxidation rate of methanol at higher methane pressure. When the methane pressure was varied in the NMR tubes from

0 to 18.2 atm, calculated rate constants, k_{CH4}, ranged from $(6.9 \pm 0.5) \times 10^{-4}$ $M^{-1}s^{-1}$ to $(1.6 \pm 0.2) \times 10^{-5}$ $M^{-1}s^{-1}$.[15] The most marked changes in the rate constant were observed when the methane pressure was less than 3 atm.

For these studies, oxidation reactions under 1, 3, and 6 atm of methane (pressures at 25°C) were followed. At each pressure, a constant methanol concentration of 0.95 mM was used and $NaIO_4$ concentration was varied from 60, 40 and 20 mM. As a general trend, oxidation rates were observed to decrease as higher pressures of methane were used (Figure 2-3).

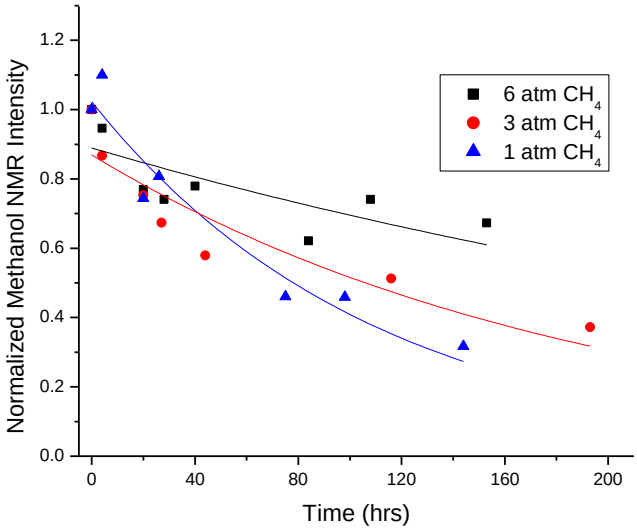

Figure 2-3. Kinetic data for the oxidation of 0.95 mM CH_3OH and 40 mM $NaIO_4$ heated at 80°C under 6, 3, and 1 atm of CH_4 (pressures at 25°C). Data are fit using exponential decay functions.

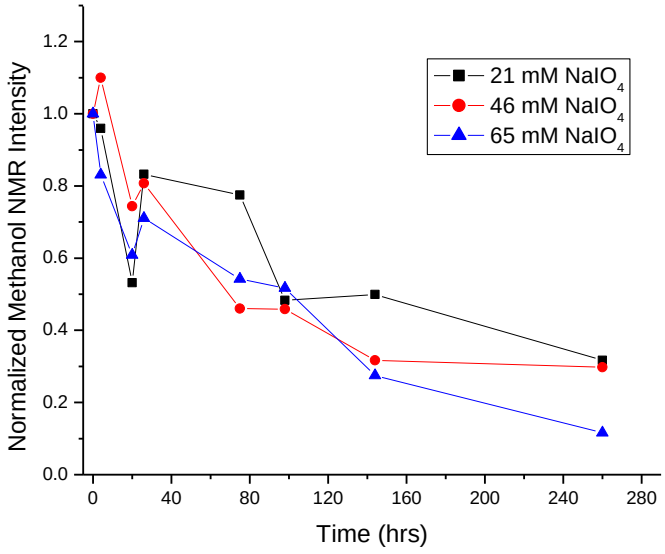

Figure 2-4. Kinetic data for the oxidation of 0.95 mM CH_3OH by various concentrations of $NaIO_4$ heated at 80°C under 1 atm CH_4 (pressure at 25°C). Data points are connected to show inconsistencies in the data.

However, the ^{1}H-NMR kinetic data were not of sufficient quality to be used to calculate a rate constant. The kinetic data obtained for a reaction carried out under 1 atm of methane is shown in Figure 2-4. The integration of the methanol peaks were observed to occasionally increase in intensity rather than continuously decrease in intensity. These increases in methanol peak intensity are attributed to instrumental errors rather than oxidation of methane. Methane is not observed to be oxidized by $NaIO_4$ alone.[14]

Inconsistent kinetic data were also observed as the concentration of oxidant at each pressure of methane was varied. The oxidation rates did not appear to vary much between 20 and 60 equivalents of $NaIO_4$. While the data shows solutions containing 20

equivalents $NaIO_4$ to have the slowest oxidation rate, solutions with 40 and 60 equivalents $NaIO_4$ have overlapping data points. In some instances, the data suggests using 40 equivalents of $NaIO_4$ yields a faster rate than 60 equivalents. This implies a zero-order dependence on periodate, which is not logical because methanol oxidation does not occur in the absence of periodate and periodate is consumed in these reactions.

A higher concentration of methanol, 7 mM, and increased NMR pulse delay times[23,24] (5 times the relaxation time) were used to achieve more accurate and consistent NMR integrations. These conditions resulted in larger integrals which had more consistency from spectrum to spectrum. Inconsistencies in NMR integrals from data point to data point were still observed, but the occurrence was less frequent and the overall variation in integration decreased.

Although this method allowed for higher accuracy of integrations, still no useful kinetic data could be obtained. Raising the concentration of oxidant again showed very little change in the oxidation rate. The oxidation rates show some overlap even when the equivalents of oxidant ranged from 14 to 42 versus methanol. As with previous experiments, the rate of oxidation also slowed to a stop after about 10 days. A more detailed analysis and possible cause for these observations will be suggested in later sections.

No quantitative rate constants were derived from these pressure dependence studies and therefore no direct comparison can be made with the rate constants obtained by Osako and coworkers. However, an increased inhibition on the oxidation rate with

increased methane pressure was qualitatively observed. Based on the solubility data series of methane under these conditions,[25] the concentrations of methane at 25°C are estimated to be 1.2 mM at 1 atm, 3.1 mM at 3 atm, and 5.5 mM at 6 atm. Based on these estimates, it is unlikely that methane inhibits these reactions through some direct interaction with periodate since the concentration of periodate (*ca.* 20-60 mM) is much greater than the concentration of methane in solution. It is possible that the inhibition occurs from an interaction between methane and some highly reactive and short lived species that arises from periodate. It is also possible that the inhibition is due to some interaction between methane and methanol.

2.2.3 Ionic Strength Effects

The effect of the phosphate buffer, PB, concentration on the oxidation rate was studied. Osako and coworkers previously observed that the oxidation rate of methanol by $NaIO_4$ under argon is approximately nine times faster in the presence of PB than in its absence.[15] This decrease in the oxidation rate in the absence of buffer was originally attributed to an ionic strength effect.

To further investigate whether this change in the rate constant is due to an ionic strength effect or buffer effect, reaction solutions of different salts with concentrations of identical ionic strength (Equation 2.4) were studied.

$$I = \frac{1}{2}\sum_{i=1}^{n}\left[[\text{concentration of ion i}]\times[\text{charge of ion i}]^2\right] \qquad (2.4)$$

Sodium periodate (40 mM) solutions containing only D_2O without other salts, D_2O with 500 mM PB, D_2O with 600 mM $NaNO_3$, and D_2O with 195 mM Na_2SO_4 were used in these studies. All these solutions have an ionic strength of approximately 0.63 M. The D_2O solution containing only $NaIO_4$ has an ionic strength of approximately 0.05 M.

pD dependence was not taken into account in these studies. Studies by Osako and coworkers showed very little change in the oxidation rates when reactions were studied between pD 4.4 to 7.4.[15] The solutions used in these studies had pDs ranging from 4.6 to 6.0 and the trends observed were assumed to be independent of pD effects. Additionally, these studies were meant to obtain qualitative information and no quantitative kinetic data was extracted.

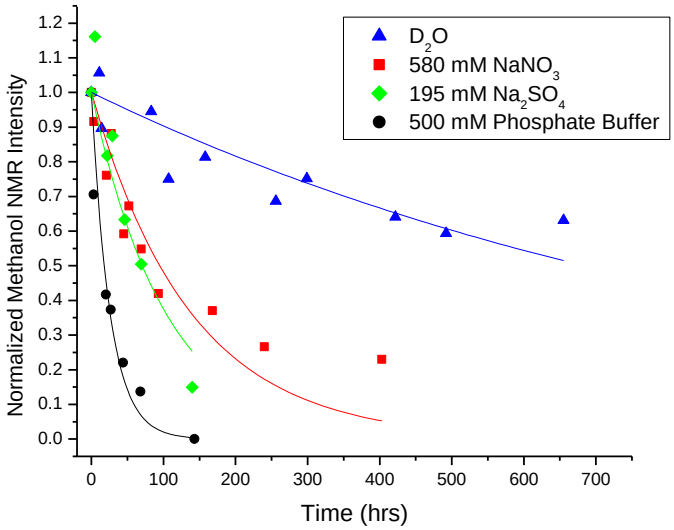

Figure 2-5. Kinetic data for the oxidation of 0.95 mM CH_3OH by 40 mM $NaIO_4$ in different salt solutions and D_2O at 80°C. Reactions are performed under argon. Data are fit using exponential decay functions.

The collected kinetic data for methanol oxidation by periodate in different salt solutions are shown in Figure 2-5. Reactions with just $NaIO_4$ in D_2O showed slower methanol oxidation rates than any of the solutions containing additional salts. Solutions that contained $NaNO_3$ and Na_2SO_4 showed nearly identical oxidation rates and were faster than the solutions containing only $NaIO_4$ in D_2O. Salt solutions of identical ionic strength that do not contain PB have half-lives that are 4 times longer than solutions containing PB. The fastest of the four reactions was the solution that contained PB.

While an ionic strength effect seems to affect the oxidation rate, these preliminary data also suggest the oxidation rate is affected by more than an ionic strength effect. It is possible that the increased rate of oxidation in phosphate buffer is due to both an ionic

strength and buffer effect. At the time of these studies, reaction conditions were not yet optimized and it is also possible that these preliminary results are due to the randomness in the kinetic data. Additional studies are necessary for a more definitive conclusion.

2.2.4 Periodate Speciation

Initial experiments herein used solutions buffered at pD 6.4 to test the reproducibility of past work. However, $NaIO_4$ solutions greater than 40 mM at pD 6.4 resulted in the formation of a white precipitate as previously described. This procedure was later deemed undesirable because it was unclear whether pseudo-first order kinetics were being obeyed in these heterogeneous mixtures.

The identity of the white precipitate was initially unknown and unreported by Osako and coworkers so characterization of the white precipitate was undertaken. Infrared spectroscopy of the white precipitate (Figure 2-6) exhibited a vibrational stretch at 740 cm^{-1} rather than the characteristic 853 cm^{-1} stretch of IO_4^-, suggesting the presence of an IO_6^{5-} salt.[26] The UV-Vis spectra of dissolved white precipitate in deionized water showed the characteristic absorbance of $NaIO_4$. A comparison of the extinction coefficient of pure $NaIO_4$ to the absorbance of a known mass of dissolved white precipitate in deionized water suggested the white powder contained *ca.* 80% $NaIO_4$ by mass. The IR and UV-Vis spectra support the findings by Hill (1928)[27] and Buist (1969)[28] that near neutral and mildly basic periodate solutions form insoluble $Na_2H_3IO_6$ and $Na_3H_2IO_6$ salts. Similar findings were reported by Panigrahi and Misro.[29] Attempts to obtain single crystals for an X-ray crystal structure of the white solid were unsuccessful.

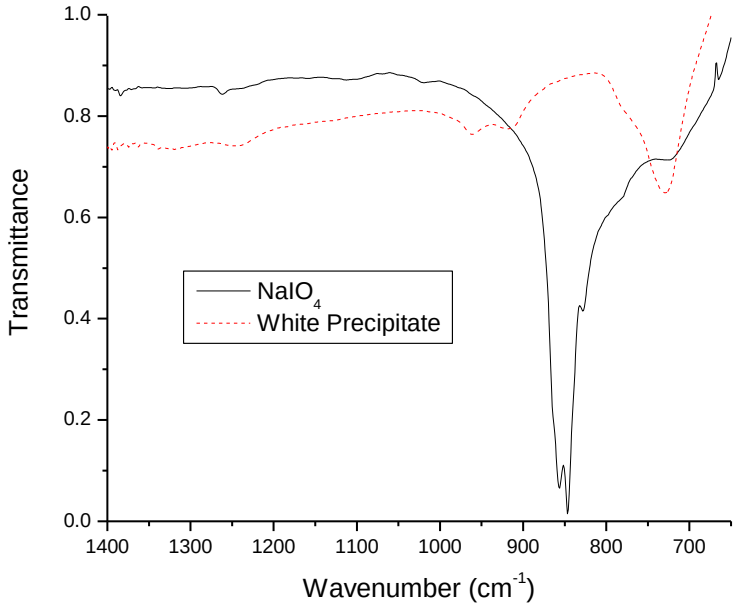

Figure 2-6. Infared absorbance spectra for $NaIO_4$ and the white precipitate formed by $NaIO_4$ in pD 6.4 buffer solutions. Spectra collected using KBr pellets.

In light of these findings, attempts to prepare homogenous periodate solutions were made using potassium periodate, KIO_4, in potassium phosphate buffer. The potassium salt has been reported to have greater solubility in basic solutions than the sodium salt.[27] Although no precipitate was observed, desired periodate concentrations could not be prepared due to low solubility of potassium periodate, perhaps due to the larger size of the potassium ion. It was later found that a homogenous, high concentration $NaIO_4$ solution could be prepared using a pD 4.4 buffer solution, the characteristic pD value of an aqueous 250 mM $NaIO_4$ solution. Due to the much improved solubility of $NaIO_4$ at low pD, reactions were studied below pD 4.6 from this point forward.

2.2.5 pD Dependence Studies

Osako and coworkers reported oxidation rates to be independent of pD between pD 4.4 to 7.4.[15] After it was determined that $NaIO_4$ had increased solubility at pD below 6.4, studies were carried out to probe the pD dependence between pD 2.0 and 6.4.

Methanol oxidation reactions at pD 2.1, 4.5, and 6.4 were compared. All reaction mixtures were under 3 atm of argon and contained 6.7 mM methanol, 280 mM $NaIO_4$, and 500 mM PB. The kinetic data for the reactions are shown in Figure 2-7.

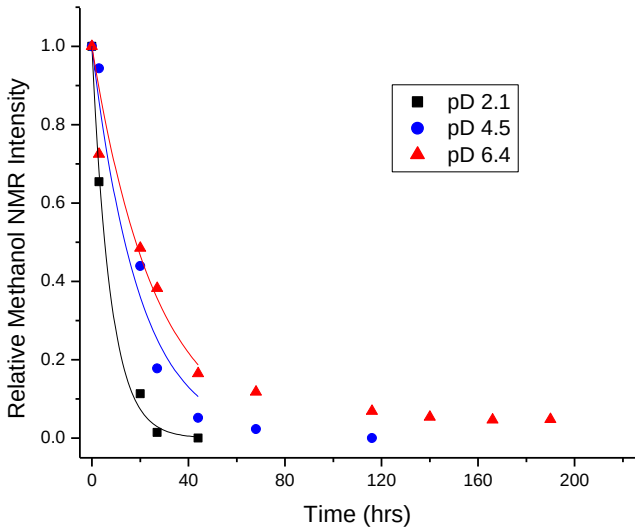

Figure 2-7. Kinetic data for the oxidation of 6.7 mM CH_3OH by 280 mM $NaIO_4$ in different pD buffer solutions under argon at 80°C. Data are fit using exponential decay functions.

The data show that reaction rates were faster at lower pD. The solution at pD 2.0 had a half-life of less than 12 hours at 80°C. The reaction rates of solutions at pD 4.5 and 6.4 had similar half-lives of approximately 24 hours, but the reaction rate of the solution

at pD 4.5 appeared slightly faster. Complete oxidation of methanol occurred after approximately 24 hours for the solution at pD 2.0 and 120 hours for the solution at pD 4.5. At pD 6.4, complete oxidation was not observed even after 8 days.

Initial attempts to reproduce kinetics at pD 2.0 were promising. There is a clear increase in oxidation rate as the pD is lowered in these reactions. Initial experiments also show reactions under these conditions to be inhibited by methane. Due to the faster kinetic rates, studies at low pD are desirable for future kinetic studies.

It is still unclear why these reactions are so much faster at low pD. Although acid dependence on periodate oxidation has not been reported, the oxidation of alcohols with chromic acid has been reported to be acid catalyzed with the oxidation rates shown to be a strong function of acidity.[30] Deuterated periodic acid, D_5IO_6, is expected to be the major species present at pD = 2 and some reports show the use of periodic acid in place of a periodate salt for oxidative cleavage of diols. [31,32]

2.2.6 Periodate Thermal Decomposition

Thermal decomposition experiments were performed in order to rationalize puzzling results obtained from reaction stoichiometry experiments. UV-Vis spectra were analyzed in order to determine the equivalents of sodium periodate consumed per equivalent of methanol. Osako and coworkers have previously reported reduction of periodate to iodate in these oxidation reactions.[15] The concentrations of periodate and iodate present in the reaction mixtures can be calculated based on the extinction coefficients of the two species present and UV-Vis spectra. By determining the

concentration of periodate in the reaction mixture prior to oxidation of methanol and after complete oxidation of methanol to CO_2, the reaction stoichiometry can be obtained.

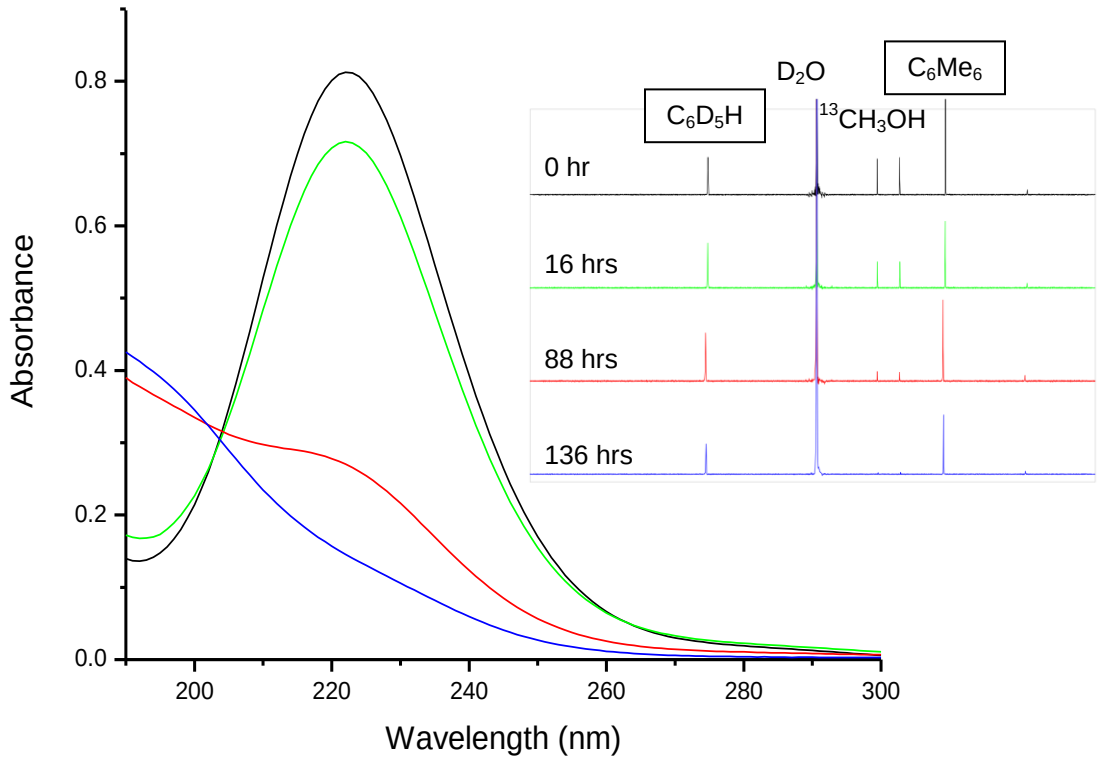

Figure 2-8. The absorbance spectra of the reaction solution of $^{13}CH_3OH$ oxidation by $NaIO_4$. Inset: The corresponding ^{1}H-NMR of the oxidation reaction. Capillary standard peaks are shown in boxes.

Initial attempts to determine reaction stoichiometry were performed by UV-Vis spectroscopy. A J. Young NMR tube under 1 atm argon was charged with a solution of 3.8 mM $^{13}CH_3OH$, 150 mM $NaIO_4$, and 500 mM PB at pD 4.0. After each ^{1}H-NMR spectrum was collected, the NMR tube was opened, 10 µL of the reaction mixture was

removed and diluted to 10 mL with deionized water, and a UV-Vis spectrum of the diluted solution mixture was collected. Dilutions are necessary due to the large extinction coefficient, 9500 $M^{-1}cm^{-1}$, at 222 nm for $NaIO_4$. The remaining reaction mixture in the J. Young NMR tube was flushed with nitrogen and returned to an 80°C oil bath. This process was repeated intermittently for *ca.* 140 hours. The collected ^{1}H-NMR and UV-Vis spectra are shown in Figure 2-8. As the oxidation reaction progressed, the characteristic peak of periodate (λ_{max} = 222 nm) decreased in intensity and the characteristic peak of iodate increased in intensity (λ_{max} below 190 nm detection limit of instrument).

After 8 days, it was observed that methanol oxidation had stopped and nearly all the periodate in solution had reduced to iodate. This would suggest a stoichiometric ratio of over 40 equivalents of periodate per equivalent of methanol. In order to rule out any interactions the reaction may have had with air, analogous experiments were also performed in flame-sealed NMR tubes containing the same concentrations of solution. The NMR tube was pressurized with 3 atm of argon, sealed, and not opened to air until the NMR tube was cut open for UV-Vis spectroscopy. The results were nearly identical with the previous experiments with *ca.* 40 equivalents periodate reducing to iodate by the end of the reaction.

Several control reactions were carried out to elucidate the cause of this reduction of periodate to iodate. Solutions of 300 mM $NaIO_4$ in 500 mM PB at pD 2.0, 300 mM $NaIO_4$ in 500 mM PB at pD 4.0, and 300 mM $NaIO_4$ in D_2O at pD 4.4 were used.

Solutions were heated at 80^{o}C in capped NMR tubes under air, in flame-sealed NMR tubes under argon, and in flame-sealed NMR tubes under methane. Half the tubes were wrapped in aluminum foil to avoid exposure to light. Solutions were heated for a week before 10 µL of each solution was diluted to 50 mL with deionized water. UV-Vis absorption spectra were collected for each solution. After a week, all solutions tested showed a majority of the periodate had been reduced to iodate.

Periodate has been shown to undergo photolysis to form iodate radical when exposed to ultraviolet radiation,[33,34,35] however, this reaction is likely insignificant under these conditions because solutions wrapped in foil still exhibit reduction of periodate. NMR tubes used are borosilicate glass and do not transmit significant light with wavelength less than 300 nm. In addition, stock solutions of $NaIO_4$ left on the bench top in glass scintillation vials show no reduction of periodate even after several months. Complete reaction of periodate with some trace impurity in the NMR tubes is unlikely due to the high concentration (300 mM) of periodate in these solutions. The decomposition of periodate to iodate under these conditions is most likely attributed to heating of the solutions at 80^{o}C.

These findings explain the strange results of the stoichiometry experiments. They also offer a reason as to why the oxidation of methanol stops after a week and suggest that the previously collected kinetic data did not obey pseudo-first order conditions.

One solution to this issue may arise from the previously discussed pD dependence studies. The reactions at pD 2.0 showed complete methanol oxidation within 24 hours.

Methanediol and formic acid were observed as intermediate products before being further oxidized to CO_2. A calculation of the periodate concentration based on the UV-Vis spectrum of the reaction mixture showed 3.4 equivalents of periodate were consumed per equivalent of methanol. This stoichiometric ratio is close to the 3 equivalents of periodate to 1 equivalent of methanol expected for a reaction in which methanol is oxidized completely to CO_2 and periodate is reduced to iodate (Equation 2.5).

$$3\,IO_4^- + CH_3OH \rightarrow CO_2 + 3\,IO_3^- + 2\,H_2O \qquad (2.5)$$

It also suggests very little periodate is thermally decomposing within 24 hours. Reactions at this pD may be useful for obtaining kinetic data that follows pseudo-first order conditions with constant periodate concentration.

2.2.7 Mechanistic Studies

Studies were undertaken to better understand the mechanism of aliphatic alcohol oxidation by periodate. To our knowledge, there are no reports of this mechanism. One mechanism that could explain the inhibition of methane involves a reactive iodyl or periodyl radical. There have been some reports in the literature suggesting the high reactivity of iodyl[36] and periodyl radicals.[35] Methane intercepting and terminating an iodyl or periodyl radical chain is one explanation for the inhibition.

Cyclopropyl carbinol was selected as a radical clock to detect the presence of radicals in the reaction pathway.[37,38,39,40] A radical mechanism, initiated by hydrogen atom abstraction from cyclopropyl carbinol, would form cyclopropyl carbinoyl radical. The presence of this radical intermediate would be indicated by the formation of several

ring-opened products. Formation of the corresponding oxidized products, cyclopropyl aldehyde and cyclopropyl carboxylic acid, would suggest the reaction does not proceed via a radical mechanism. This reaction pathway is shown in Scheme 2-1.

Scheme 2-1. Possible reaction pathway for reaction of cyclopropyl carbinol with $NaIO_4$ if ring opened products and oxidation products proceed through different intermediates.

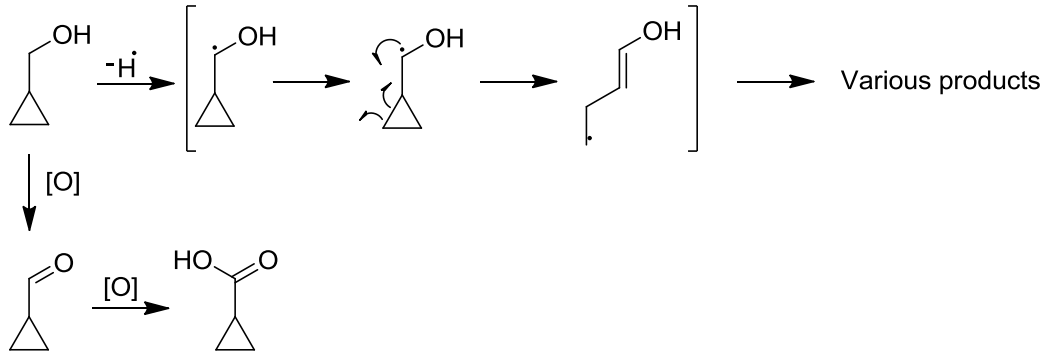

The formation of the corresponding oxidation products does not completely rule out a radical mechanism. An initial mechanistic step involving formation of a cyclopropyl carbinoyl radical could also proceed to cyclopropyl aldehyde and cyclopropyl carboxylic acid if the competing ring-opening step is much slower. This reaction pathway is shown in Scheme 2-2. Although there are many reports of ring-opening rate constants, k_{open}, for cyclopropyl carbinoyl and other derivatives,[41,42,43,44,45,46,47,48,49] the cyclopropyl carbinoyl radical could not be located in the literature. Recent correspondence with Newcomb, suggests these radicals would be destabilized in aqueous solution and have similarly fast ring-opening rate constants as the

alkyl derivative with k_{open} *ca.* 10^8 s^{-1}.[50] Reactions under several different concentrations were studied to thoroughly probe for the presence of radicals.

Scheme 2-2. Possible reaction pathway for reaction of cyclopropyl carbinol with $NaIO_4$ if ring open products and oxidation products proceed through the same cyclopropyl carbinoyl radical intermediate.

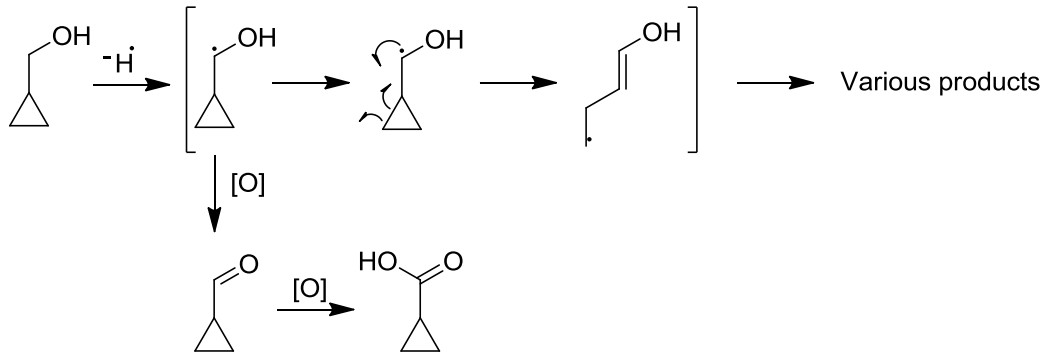

Reaction solutions were degassed and placed under 1 atm argon in J. Young NMR tubes with several different ratios of cyclopropyl carbinol to sodium periodate. Reaction conditions ranged from using excess alcohol, equal equivalents of alcohol and oxidant, and excess oxidant. Reactions were kept at pD 6.4 with phosphate buffer and heated at 80^{o}C to mimic standard reaction conditions for methanol oxidation. All reaction concentrations examined showed the oxidation of cyclopropyl carbinol (δ 0.01-0.07, m, 2H; 0.33-0.39, m, 2H; 0.82-0.95, m, 1H; 3.23-3.25, d, 2H) to cyclopropyl aldehyde (δ 1.00-1.11, m, 4H; 1.66-1.77, m, 1H; 8.52-8.55, d, 1H) and cyclopropyl carboxylic acid (δ 0.57-0.64, m, 4H; 1.26-1.34, m, 1H) by ^{1}H-NMR. Presence of cyclopropyl carboxylic acid was confirmed by spiking reaction solutions with commercially available cyclopropyl carboxylic acid and observing an increase in ^{1}H-NMR signal intensity.

Formation of ring-opened products was not observed, which may argue against a radical pathway.

Further reactions with sodium periodate and cyclopropyl carbinol were performed in the presence of dioxygen (O_2), a diffusion-limited alkyl radical trap,[51,52,53] to test if the rate of formation of the oxidized products was out competing a ring-opening step. Because no ring-opening rate is available, it is unclear whether the rate of cyclopropyl carbinoyl radical oxidation by $NaIO_4$ is faster than the rate of ring-opening. Dioxygen is expected to rapidly react with cyclopropyl carbinoyl radical and begin autoxidation chains indicated by an increased rate of alcohol consumption and possible formation of various side products.

Reactions were performed with 104 mM cyclopropyl carbinol, 6 mM $NaIO_4$, 500 mM phosphate buffer, and 1 atm dioxygen. Excess alcohol was used to ensure any cyclopropyl carbinoyl radicals would react with dioxygen rather than periodate. The concentration of dioxygen in these reactions, at 80^{o}C and 500 mM PB, is estimated to be 0.8 mM based on the solubility of O_2 in D_2O.[54] These reactions also yielded cyclopropyl aldehyde and cyclopropyl carboxylic acid with no observed increase in reaction rate, further suggesting a non-radical pathway.

Although these experiments are preliminary, no reaction conditions afforded ring-opened products. All reaction conditions afforded clean conversion to cyclopropyl aldehyde and cyclopropyl carboxylic acid. The reactions with cyclopropyl carbinol are evidence against a radical chain mechanism.

2.2.8 Oxidation of Other Alcohols

Prior to the findings that reactions at acidic pD had faster kinetics than those at near neutral pD, studies were aimed towards finding substrates that had faster kinetics than methanol oxidation. Because the only method available to follow these reactions is ^{1}H-NMR spectroscopy, faster kinetics are desired to shorten the required times for kinetic studies of the methane inhibition and alternate substrates would allow kinetic isotope effect studies. Initial studies focused on qualitative exploration of the oxidation of different alcohol substrates, and so kinetic data were not quantified. Reaction solutions under 1 atm argon in J. Young tubes contained 7 mM alcohol and 90 mM $NaIO_4$ in 500 mM PB at pD 6.4.

Isopropanol was the first substrate studied. ^{1}H-NMR showed *ca.* 25% conversion to acetic acid and formic acid, but the expected product, acetone, was not observed. These products were hypothesized to form from the cleavage of acetone rather than cleavage of isopropanol. Oxidation experiments of acetone with sodium periodate also showed the formation of acetic acid and formic acid, supporting this hypothesis. These findings have also been previously reported in the literature.[55] Due to complications from the cleavage of acetone, isopropanol was deemed undesirable for future kinetic isotope effect studies. Additionally, preliminary analysis of the kinetic data suggests that the oxidation of isopropanol is slower than methanol. This may be due to a steric hindrance effect of the secondary alcohol.

The oxidation of ethanol showed *ca.* 60% conversion to ethanal and acetic acid by ^{1}H-NMR spectroscopy. Preliminary data suggests that ethanol has a faster oxidation rate than isopropanol, possibly due to less steric hindrance. Further studies with ethanol may prove fruitful for kinetic isotope effect studies.

Aromatic alcohols could react more rapidly than aliphatic alcohols due to possible stabilization of intermediates by the aromatic ring. Oxidation of 4-methyl benzyl alcohol resulted in rapid decomposition of the aromatic ring. Reaction solutions placed in an 80^{o}C oil bath showed complete conversion to formic acid, acetic acid, and CO_2 (not observed, but assumed based on NMR yields of formic and acetic acid) within 2 hours. This carbon-carbon bond cleavage may be analogous to the cleavage of glycols. Attempts to slow the decomposition reaction were made by monitoring the reaction at room temperature. After 24 hours left on the bench top, no reaction was observed. The use of aromatic alcohols was eventually abandoned in light of the discovery that reaction kinetics are much faster at low pD.

2.3 Conclusions

The methane inhibition of methanol oxidation by $NaIO_4$ has been studied to develop a better understanding of this unprecedented result. Initial attempts to reproduce the kinetic data collected by Osako were not within error. Although similar qualitative observations could be made, experiments to quantitatively measure the methane pressure dependence on rate constants were inconclusive due to inconsistent kinetic data. As a

result, the previous experimental procedures were abandoned and work focused on further understanding the nature of these reactions.

Preliminary results show that these reactions are much faster in the presence of phosphate buffer compared to reactions in only D_2O and solutions of non-buffering salts. These results suggest both an ionic strength effect and a buffering effect on the reaction kinetics. The reaction kinetics were also found to be much faster in more acidic solutions. These findings are contrary to previous findings that there was no pD dependence between pD 4.4-7.4.

Reactions carried out at lower pD also allowed for higher solubility of $NaIO_4$. The sodium salts $Na_2H_3IO_6$ and $Na_3H_2IO_6$ were found to precipitate at pD greater than 4.4. These findings were not previously reported. Periodate was shown to thermally reduce to iodate. These findings suggest that previous work was not performed under the assumed pseudo-first order conditions with excess periodate.

Mechanistic studies with cyclopropyl carbinol as a radical clock suggested that methanol oxidation by periodate does not occur via a radical mechanism. Ethanol may be a possible substrate for future kinetic isotope effect studies.

2.4 Experimental

Materials. Solvents D_2O (Cambridge Isotope Labs, 99.9%, Low Paramagnetic) and benzene-d^6 (Cambridge Isotope Labs, 99.9%) were used as received without further purification. All reagents, methanol (Mallinckrodt), cyclopropyl carbinol (Aldrich, 95%),

cyclopropyl carboxylic acid (Sigma-Aldrich, 95%), acetone (J.T. Baker), isopropanol (Mallinckrodt), ethanol (Decon Labs, 200 proof), 4-methyl benzyl alcohol (Aldrich), $NaIO_4$ (Sigma-Aldrich, 99.8%), trimethylacetic acid (Aldrich), D_3PO_4 (Cambridge Isotope Labs, 85% in D_2O), NaOD (Cambridge Isotope Labs, 30% in D_2O), $NaNO_3$ (Sigma), and Na_2SO_4 (EMD), were used as received without further purification. Gases, argon (Praxair), methane (Matheson, 99.99%), and oxygen (Praxair), were used directly without further purification.

Instrumentation and Measurements. ^{1}H-NMR spectra were recorded on a Bruker AV300 spectrometer at 298K. Spectra are reported by referencing chemical shift, δ (assignment, multiplicity, and number of protons), to the residual solvent peak, HOD (4.79 ppm). Electronic absorption spectra were obtained with a Hewlett-Packard 8453 UV-Vis spectrophotometer using 1 cm pathlength quartz cuvettes and reported in λ/cm. IR absorption spectra were obtaining using KBr pellets on a Bruker Tensor 27 spectrometer at 4 cm^{-1} resolution and reported in cm^{-1}. pH measurements were obtained with a Fisher Scientific Accumet Excel XL50 pH meter equipped with a Hamilton spintrode electrode. pD values were obtained by adding 0.4 to the measured pH value.[22] Atomic emission spectra were obtained with a Jarrell Ash 955 Inductively Coupled Plasma spectrometer and reported in relative flame intensities.

Preparation of Phosphate Buffer Stock Solutions. A 50 mL volumetric flask was charged with D_3PO_4 (2.971 g, 25 mmol) and D_2O. To this solution was added NaOD until

the desired pH is achieved as measured by the pH meter. The solution was stored in a plastic bottle on the bench top.

Preparation of Alcohol Stock Solutions. A 10 mL volumetric flask was charged with CH_3OH (0.0304 g, 0.95 mmol) and phosphate buffer solution. The flask was stoppered and shaken to mix solution. The solution was stored in a scintillation vial on the bench top. Identical procedures for followed for other alcohol substrates: cyclopropyl carbinol (0.0342 g, 0.95 mmol), isopropanol (0.0571 g, 0.95 mmol), ethanol (0.0438 g, 0.95 mmol), and 4-methyl benzyl alcohol (0.0116 g, 0.095 mmol.)

Preparation of $NaIO_4$ Stock Solutions. A 10 mL volumetric flask was charged with $NaIO_4$ (0.6417 g, 3.00 mmol) and phosphate buffer solution (below pH 4.4 to avoid formation of insoluble $Na_2H_3IO_6$ and NaH_4IO_6).[27] The flask was stoppered and solution shaken to dissolve solids. Solution was stored in a scintillation vial on the bench top.

Preparation of Trimethylacetic Acid Stock Solution. A 10 mL volumetric flask was charged with trimethylacetic acid (0.1021 g, 1.00 mmol) and D_2O. The flask was stoppered, sonicated, and shaken to dissolve solids. Solution was stored in a scintillation vial on the bench top.

Procedure for Alcohol Oxidation in Flame-Sealed NMR Tube. An oven-dried medium-walled NMR tube with attached 14/20 ground glass joint and containing a hexamethylbenzene capillary standard (prepared by Takao Osako) was charged with methanol in 500 mM phosphate buffer solution (28.0 µL, 2.66 µmol) and $NaIO_4$ in 500 mM phosphate buffer solution (372 µL, 112 µmol.) The NMR tube was connected to a

known volume 7.2 mL gas bubble attached to a high vacuum line. The reaction solution was freeze-pump-thaw degassed three times. After the last degas cycle, the NMR tube was left in a Dewar flask containing LN_2, the gas bubble was charged with a known pressure of the desired gas (Ar or CH_4), and the tube was opened to the bubble to condense the gas into the tube. The tube was flame-sealed at a known length. The pressure of gas in the bubble was predetermined based on a Boyle's Law calculation with the desired pressure in the NMR tube headspace at room temperature, the sealed NMR tube length, and the volume of the gas bubble. Identical procedures were followed for all other alcohol substrates.

Procedure for Alcohol Oxidation in J-Young Top NMR Tube. An oven-dried J. Young top NMR tube containing a hexamethylbenzene capillary standard (prepared by Takao Osako) was charged with methanol in 500 mM phosphate buffer solution (28.0 µL, 2.66 µmol) and $NaIO_4$ in 500 mM phosphate buffer solution (372 µL, 112 µmol.) The tube was connected to a high vacuum line and the reaction solution was freeze-pump-thawed three times. After the last degas cycle, the reaction solution was removed from LN_2, partially thawed, filled with the desired gas (Ar, CH_4, or O_2), and closed. Identical procedures were followed for all other alcohol substrates.

Monitoring the Alcohol Oxidation Reaction. Following completion of sample preparation, samples were left in a freezer at -35^{o}C (flame-sealed NMR tubes) or in a refrigerator at 4^{o}C (J. Young top NMR tubes) until initial NMR spectra could be obtained. Prior to collecting NMR data, tubes were thawed, warmed to room temperature,

and shaken vigorously. Following the initial spectra, the NMR tubes were placed in an 80^{o}C oil bath. Tubes were intermittently removed from the oil bath, cleaned with hexane, shaken, and cooled to room temperature prior to obtaining NMR spectra. The oxidation of methanol was monitored by the disappearance of the methanol signal δ 3.26 (singlet, 3 protons). The reaction time was taken as the time spent in the oil bath.

Calibration of the Hexamethylbenzene Capillary Standard. Following the complete oxidation of the alcohol substrate, the reaction NMR tubes were opened and trimethylacetic acid solution (50 µL, 5 µmol) was added to the reaction mixture. Tubes were recapped, shaken to mix, and an NMR spectrum was collected. The trimethylacetic acid peak, δ 1.13 (singlet, 9 protons), was used to calibrate the concentration of the hexamethylbenzene peak, δ 2.10 (singlet, 18 protons.) The calibrated hexamethylbenzene concentration was then used to determine the methanol concentration in the reaction mixture.

2.5 Notes to Chapter 2

[1] Conley, B. L.; Tenn III, W. J.; Young, K. J. H.; Ganesh, S. K.; Meier, S. K.; Ziatdinov, V. R.; Mironov, O.; Oxgaard, J.; Gonzales, J.; Goddard III, W. A.; Periana, R. A. *J. Mol. Catal. A: Chem.* **2006**, *251*, 8-23.

[2] Bergman, R. G. *Nature* **2007**, *446*, 391-393.

[3] *Climate Change 2007: The Physical Science Basis. Contribution of Working Group I to the Fourth Assessment Report of the Intergovernmental Panel on Climate*

Change; Solomon, S., D. Qin, M. Manning, Z. Chen, M. Marquis, K.B. Averyt, M.Tignor, H.L. Miller, Ed.; Cambridge University Press: New York, 2007.

[4] Crabtree, R. H. *Chem. Rev.* **1995**, *95*, 987-1007.

[5] Blasing, T. J.; Hand, K. *Tellus* **2007**, *59*, 15-21.

[6] Elvidge, C.; Ziskin, D.; Baugh, K.; Tuttle, B.; Ghosh, T.; Pack, D.; Erwin, E.; Zhizhin, M. *Energies* **2009**, *2*, 595-622.

[7] Berkowitz, J.; Ellison, G. B.; Gutman, D. *J. Phys. Chem.* **1994**, *98*, 2744-2765.

[8] Chen, G. S.; Labinger, J. A.; Bercaw, J. E. *Organometallics* **2009**, *28*, 4899-4901.

[9] Periana, R. A.; Taube, D. J.; Gamble, S.; Taube, H.; Satoh, T.; Fujii, H. *Science* **1998**, *280*, 560-564.

[10] Gesser, H. D.; Hunter, N. R. *Catalysis Today* **1998**, *42*, 183-189.

[11] Labinger, J. A.; Bercaw, J. E. *Nature* **2002**, *417*, 507-514.

[12] Dehestani, A.; Lam, W. H.; Hrovat, D. A.; Davidson, E. R.; Borden, W. T.; Mayer, J. M. *J. Am. Chem. Soc.* **2005**, *127*, 3423-3432.

[13] Bales, B. C.; Brown, P.; Dehestani, A.; Mayer, J. M. *J. Am. Chem. Soc.* **2005**, *127*, 2832-2833.

[14] Osako, T.; Watson, E. J.; Dehestani, A.; Bales, B. C.; Mayer, J. M. *Angew. Chem.* **2006**, *45*, 7433-7436.

[15] Osako, T.; Hayoun, R.; Mayer, J. M. 2007. Unpublished results.

[16] Bugarcic, Z.; Novokmet, S.; Kostic, V. J. *Serb. Chem. Soc.* **2005**, *70*, 681-686.

[17] Dewkar, G. K.; Narina, S. V.; Sudalai, A. *Org. Lett.* **2003**, *5*, 4501-4504.

[18] Lei, M.; Hu, R.-J.; Wang, Y.-G. *Tetrahedron* **2006**, *62*, 8928-8932.

[19] Moghadam, M.; Tangestaninejad, S.; Mirkhani, V.; Karami, B.; Rashidi, N.; Ahmadi, H. *J. Iran. Chem. Soc.* **2006**, *3*, 64-68.

[20] Srivastava, S.; Srivastava, S.; Singh, S.; Parul *Int. J. Pure Appl. Chem.* **2008**, *3*, 17-20.

[21] Carey, F. A.; Sundberg, R. J. *Advanced Organic Chemistry Part B: Reactions and Synthesis*; Fifth Edition ed.; Springer: Charlottesville, 2007.

[22] Perrin, D. D.; Dempsey, B. *Buffers for pH and Metal Ion Control*; Halsted Press: New York, 1974.

[23] Weizman, H. *J. Chem. Educ.* **2008**, *85*, 294.

[24] Claridge, T. D. W. *High-Resolution NMR Techniques in Organic Chemistry*; Elsevier: Boston, 1999; Vol. 19.

[25] *IUPAC Solubility Data Series: Methane*; Clever, H. L.; Young, C. L., Eds.; Pergamon Press: New York, 1987; Vol. 27/28.

[26] Nakamoto, K. *Infared and Raman Spectra of Inorganic and Coordination Compounds*; 3rd ed.; Wiley-Interscience: New York, 1978.

[27] Hill, A. E. *J. Am. Chem. Soc.* **1928**, *50*, 2678-2692.

[28] Buist, G. J.; Hipperson, W. C. P.; Lewis, J. D. *J. Chem. Soc. A* **1969**, 307-312.

[29] Panigrahi, G. P.; Misro, P. K. *Indian J. Chem., Sect. A: Inorg., Bio-inorg., Phys., Theor. Anal. Chem.* **1977**, *15*, 1066-1069.

[30] Stewart, R. *Oxidation Mechanisms: Applications to Organic Chemistry*; W. A. Benjamin, Inc.: New York, 1964.

[31] Crouthamel, C. E.; Hayes, A. M.; Martin, D. S. *J. Am. Chem. Soc.* **1951**, *73*, 82-87.

[32] Price, C. C.; Knell, M. *J. Am. Chem. Soc.* **1942**, *64*, 552-554.

[33] Klaning, U. K.; Sehested, K. *J. Chem. Soc., Faraday Trans.* **1978**, *74*, 2818-2838.

[34] Lee, C.; Yoon, J. *J. Photochem. Photobiol., A* **2004**, *165*, 35-41.

[35] Tang, X.; Weavers, L. K. *J. Photochem. Photobiol., A* **2008**, *194*, 212-219.

[36] Nandibewoor, S. T.; Hiremath, G. A. *J. Indian Chem. Soc.* **1999**, *76*, 250-252.

[37] Griller, D.; Ingold, K. U. *Acc. Chem. Res.* **1980**, *13*, 317-323.

[38] Jin, Y.; Lipscomb, J. D. *Biochimica et Biophysica Acta (BBA) - Protein Structure and Molecular Enzymology* **2000**, *1543*, 47-59.

[39] Newcomb, M. *Tetrahedron* **1993**, *49*, 1151-1176.

[40] Wang, K.; Mayer, J. M. *J. Org. Chem.* **1997**, *62*, 4248-4252.

[41] Beckwith, A. L. J.; Bowry, V. W. *J. Am. Chem. Soc.* **1994**, *116*, 2710-2716.

[42] Beckwith, A. L. J.; Moad, G. *J. Chem. Soc., Perkin Trans. 2* **1980**, 1473-1482.

[43] Davies, A. G.; Muggleton, B.; Godet, J.-Y.; Pereyre, M.; Pommier, J.-C. *J. Chem. Soc., Perkin Trans. 2* **1976**, 1719-1724.

[44] Itzel, H.; Fischer, H. *Tetrahedron Lett.* **1975**, *16*, 563-564.

[45] Mathew, L.; Warkentin, J. *J. Am. Chem. Soc.* **1986**, *108*, 7981-7984.

[46] Newcomb, M.; Horner, J. H.; Emanuel, C. J. *J. Am. Chem. Soc.* **1997**, *119*, 7147-7148.

[47] Tanko, J. M.; Drumright, R. E.; Suleman, N. K.; Brammer, L. E. *J. Am. Chem. Soc.* **1994**, *116*, 1785-1791.

[48] Walborsky, H. M.; Plonsker, L. *J. Am. Chem. Soc.* **1961**, *83*, 2138-2144.

[49] Martinez, F. N.; Schlegel, H. B.; Newcomb, M. *J. Org. Chem.* **1998**, *63*, 3618-3623.

[50] Newcomb, M., Personal Communication with Jim Mayer; January 23, 2010.

[51] Maillard, B.; Ingold, K. U.; Scaiano, J. C. *J. Am. Chem. Soc.* **1983**, *105*, 5095-5099.

[52] Burton, G. W.; Ingold, K. U. *Acc. Chem. Res.* **1986**, *19*, 194-201.

[53] Sawyer, D. T. *Oxygen Chemistry*; Oxford University Press: New York, 1991.

[54] *IUPAC Solubility Data Series: Oxygen and Ozone*; Battino, R., Ed.; Pergamon Press: New York, 1987; Vol. 7.

[55] Panigrahi, G. P.; Misro, P. K. *Indian J. Chem., Sect. A: Inorg., Bio-inorg., Phys., Theor. Anal. Chem.* **1978**, *16*, 762-766.

3 – Development of Platinum and Palladium Catalysts for Methyl and Aryl Coupling

3.1 Introduction

3.1.1 General Introduction

Methane, the simplest hydrocarbon, has garnered much attention in the past thirty years due to its use as a supplemental fuel and chemical feedstock.[1] Unlike crude oil reserves which are slowly depleting, the rate of discovery of natural gas reserves is increasing.[2] However, due to the low value of natural gas and high cost involved in transporting gases, reserves in remote locations are often flared to avoid hazardous accumulation at drilling sites.[3] Conversion of methane to more valuable fuels is greatly desired. Extensive research in the past 40 years has focused on the catalytic oxidation of methane to methanol, a liquid fuel which is more cost effective to transport. Significant challenges are faced due to the high C-H bond strength of methane[4] and the ease of formation of over-oxidation products.[5]

An alternative approach to methane upgrading would be to develop a catalytic cycle for the oxidative dimerization of methane to ethane. Ethane can be dehydrogenated to ethylene, which can then be converted to polyethylene, the most widely used plastic in the world. The catalytic dimerization of methane would be a more economical route to ethylene, which is commonly formed by steam cracking of higher value, longer chain hydrocarbons. Although catalytic oxidative coupling of methane has been studied using

heterogeneous metal oxides, these reactions require high temperatures and suffer from low conversions.[6] The work reported herein aims to develop a homogeneous transition-metal catalyst that can be utilized for the catalytic dimerization of methane under mild conditions.

3.1.2 Previous Work

A potential catalytic cycle for the oxidative dimerization of methane is shown in Scheme 3-1. Such a cycle would involve oxidative disproportionation of a dimethyl-metal^{II} complex to half equivalents of a trimethyl-metal^{IV} complex and a monomethyl-metal^{II} complex. C-C bond forming reductive elimination from the trimethyl-metal^{IV} complex generates half equivalents of ethane and the monomethyl-metal^{II} complex. In the last step of the proposed cycle, methane activation with the monomethyl-metal^{II} complex regenerates a dimethyl-metal^{II} complex.

Scheme 3-1. Proposed catalytic cycle for the oxidative dimerization of methane.

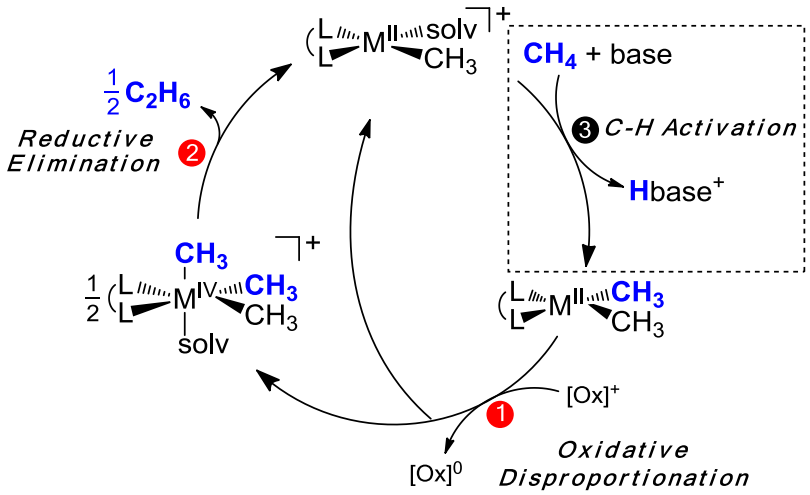

Steps 1 and 2 of the catalytic cycle in Scheme 3-1 have been extensively studied by our group using Pd[7] and Pt[8] catalysts. Most notably, our work has shown that Pt complexes with *N*,*N*′-diaryl-2,3-dimethyl-1,4-diaza-1,3-butadiene (DAB) ligands can undergo steps 1 and 2 of the catalytic cycle with proper steric bulk on the aryl substituents.[8] Reductive eliminations to form C-C bonds from transition metal complexes are well studied.[9,10] Specifically, reductive elimination of ethane has been demonstrated by Pt complexes bearing phosphine[11] or β-diketiminate[12] ligands and polymethyl Pd complexes[13], these complexes have not been shown to activate methane. Pt complexes with DAB ligands are of particular interest because they have been reported to activate methane and hence are promising candidates for achieving catalysis.[14]

Initial studies focused on steps 1 and 2 of the catalytic cycle with diphenyl-Pt^{II} complexes. Due to benzene activation being much more facile than methane activation, it was hoped that the analogous catalytic cycle to make biphenyl could be realized more easily. Guided by the previous report of ethane generation from monomethyl-Pd^{II} complexes with various X-type ligands,[15,16] monophenyl-Pd^{II} complexes were also developed and their reaction chemistry was investigated. Previously reported monoaryl-Pd^{II} complexes have been reported in the literature to achieve aryl-CF_3 reductive elimination in the presence of fluoropyridinium oxidants.[17] Additionally, the report of C-H activation with these types of complexes suggested that a catalytic process for aryl coupling could be achieved.[18]

The following section focuses on progress towards step 3 of the catalytic cycle - the generation of a dimethyl-Pt^{II} complex from a monomethyl-Pt^{II} complex via methane activation. C-H activation with Pt catalysts is well documented in the literature,[19] however, there are relatively few examples of Pt catalysts which forgo rapid reductive elimination of methane upon C-H activation. By the principle of microscopic reversibility, the mechanism of methane activation with $[(DAB)Pt(CH_3)(solvent)]^+$ complexes has been proposed to proceed through five-coordinate dimethyl-Pt^{IV} hydride cations, which rapidly reductively eliminate to release methane, Scheme 3-2 pathway **A**.[20] In order to generate a dimethyl-Pt^{II} complex following methane activation, base assisted C-H activation studies were undertaken to attempt to deprotonate a dimethyl-Pt^{IV} hydride intermediate, Scheme 3-2 pathway **B**.

Scheme 3-2. Pathway **A** shows the typical methyl exchange observed for methane activation with Pt^{II} complexes. Pathway **B** shows the potential generation of a dimethyl Pt^{II} complex by deprotonation of a dimethyl Pt^{II} hydride intermediate.

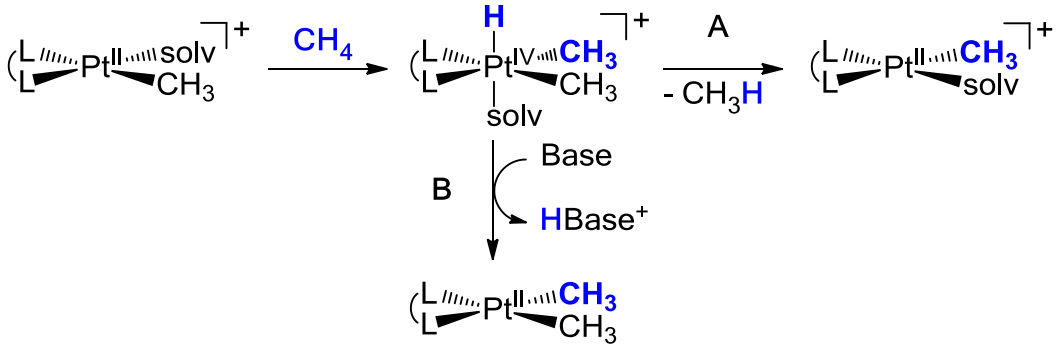

Studies were also undertaken to probe the ability of tridentate facial ligands to stabilize dimethyl-Pt^{IV} hydride intermediates in hopes of slowing reductive elimination of methane.

Finally, effort towards methane activation with Pt^{II} complexes containing large bite angle bidentate ligands with proton relays capable of dihydrogen activation will be presented.

3.2 Results and Discussion

3.2.1 Attempts at Developing a Catalytic Cycle for Aryl Coupling

In order to determine whether a catalytic cycle for phenyl coupling analogous to the methyl coupling chemistry in Scheme 3-1 could be developed, the oxidative disproportionation (Scheme 3-1, step 1) of diphenyl-Pt^{II} complexes was first studied. The diphenyl-Pt^{II} complexes bearing various DAB ligands used for these studies were prepared analogously to literature procedures[21] and are shown in Figure 3-1.

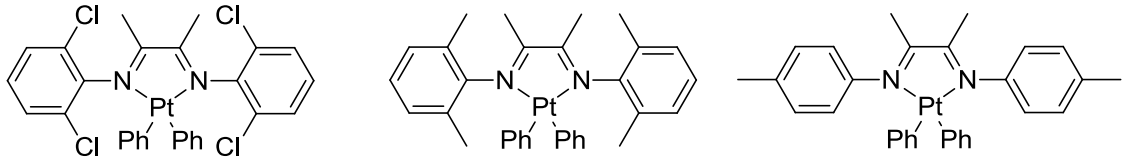

1 **2** **3**

Figure 3-1. (DAB)Pt(C_6H_5)$_2$ complexes studied for oxidative disproportionation and reductive elimination chemistry.

Reactions of these complexes with one equivalent of acylferrocenium resulted in formation of benzene and unidentified products by ^{1}H-NMR spectroscopy. The formation of triphenyl-Pt^{IV} complexes, monophenyl-Pt^{II} complexes, or biphenyl was not observed. Reactions in acetonitrile-d_3, acetone-d_6, and nitromethane-d_3 all yielded identical results.

To test whether the oxidative disproportionation formation of triphenyl-Pt^{IV} complexes was hindered by the steric crowding around the metal center, the diphenyl-Pt^{II} complexes were reacted with diphenyliodonium triflate, an oxidative phenyl transfer reagent. Reaction mixtures of diphenyliodonium triflate with the (DAB)Pt(C_6H_5)$_2$ complexes showed no formation of [(DAB)Pt(C_6H_5)$_3$]]$^+$. Heating reaction mixtures for 3 days at 50 ^{o}C showed only unreacted starting materials by ^{1}H-NMR spectroscopy. These findings suggest there is too much steric bulk around the metal center in these complexes for the oxidative addition of a phenyl cation. Oxidative addition of phenyl cation to the less sterically hindered (4,4'-ditertbutyl-2,2'-bipyridine)Pt(C_6H_5)$_2$ ((^{t}butylbipy)Pt(C_6H_5)$_2$) complex to form [(^{t}butylbipy)Pt(C_6H_5)$_3$]$^+$ is reported to be facile in the literature,[22] but there are no reports of formation of [(DAB)Pt(C_6H_5)$_3$]$^+$ complexes. Reductive elimination from [(^{t}butylbipy)Pt(C_6H_5)$_3$]$^+$ was not investigated because Pt complexes with ^{t}butylbipy are not reported to activate C-H bonds.

Due to the difference in reactivity between (DAB)Pt(C_5H_6)$_2$ and (DAB)Pt(CH_3)$_2$ complexes with one electron oxidants and their inability to form biphenyl, it was concluded that these complexes could not be used to develop a catalytic cycle for aryl coupling and this work was discontinued.

Guided by the previous report of oxidative methyl coupling from monomethyl-Pd^{II} complexes,[15,16] the analogous monophenyl-Pd^{II} trifluoromethyl complexes were prepared (Figure 3-2).

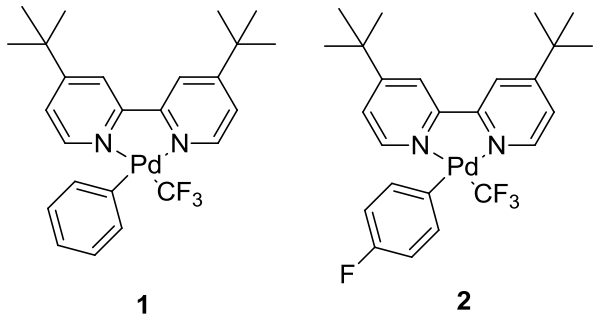

1 **2**

Figure 3-2. (^{t}butylbipy)Pd(C_6H_5)(CF_3) and (^{t}butylbipy)Pd(C_6H_4F)(CF_3) complexes studied for oxidative disproportionation and reductive elimination chemistry.

Oxidation of the (^{t}butylbipy)Pd(C_6H_5)(CF_3), Figure 3-2-**1**, with acylferrocenium in acetone-d_6 over 32 hours at room temperature resulted in the formation of biphenyl in ca. 50% expected stoichiometric yield. Benzene formation was not observed. Due to formation of various unidentified side-products, it was unclear why only ca. 50% yield was achieved. Reaction mixtures characterized by ^{19}F-NMR spectroscopy showed a broad resonance presumed to be [(^{t}butylbipy)Pd(CF_3)(solvent)]$^+$ as the major inorganic product.

In order to better track the side-products of the reaction by ^{19}F-NMR spectroscopy, (^{t}butylbipy)Pd(C_6H_4F)(CF_3) (Figure 3-2-**2**) was prepared. Oxidation of (^{t}butylbipy)Pd(C_6H_4F)(CF_3) with acylferrocenium in acetone-d_6 over 72 hours at room temperature resulted in formation of 4,4'-difluorobiphenyl in ca. 50% yield.

Fluorobenzene was not observed. Monitoring reactions by ^{19}F-NMR spectroscopy showed formation of [(^{t}butylbipy)Pd(CF_3)(solvent)]$^+$, 4,4'-difluorobiphenyl, and three unidentified fluoro-phenyl products. The unidentified fluorophenyl products were formed in roughly 1:1 ratio with 4,4'-difluorobiphenyl. Attempts to isolate the unidentified fluoro-phenyl products were unsuccessful. Filtering reaction solutions through silica to remove inorganic products showed 4,4'-difluorobiphenyl as the only organic product by ^{1}H-NMR spectroscopy.

To investigate the mechanism for the reaction, (^{t}butylbipy)Pd(C_6H_5)(CF_3) was treated with one equivalent of diphenyliodonium triflate. 100% yield of biphenyl was observed after 60 hours at room temperature. Although a diphenyl Pd^{IV} intermediate was not observed, the formation of biphenyl with diphenyliodonium triflate suggests that biphenyl is formed via reductive elimination from diphenyl Pd^{IV}.

Studying mechanism of these reactions is difficult due to the higher oxidation potential of (^{t}butylbipy)Pd(C_6H_5)(CF_3) compared to (^{t}butylbipy)Pd(CH_3)(CF_3). While five coordinate [(^{t}butylbipy)Pd(CH_3)$_2$(CF_3)]$^+$ has been observed via low temperature NMR experiments, five coordinate [(^{t}butylbipy)Pd(C_6H_5)$_2$(CF_3)]$^+$ cannot be observed at low temperature due to slow oxidation of (^{t}butylbipy)Pd(C_6H_5)(CF_3) at room temperature. The different rate of oxidation of these complexes can be observed in a competition experiment. Treatment of 0.5 equivalents of (^{t}butylbipy)Pd(C_6H_5)(CF_3) and 0.5 equivalents of (^{t}butylbipy)Pd(CH_3)(CF_3) with one equivalent of acylferrocenium resulted in the immediate formation of near quantitative yields of ethane. After 20 hours

at room temperature, approximately 50% yield of biphenyl is observed. Interestingly, trace amounts of toluene is also observed.

While the initial results from this work is promising, further work will be required to identify side products formed to provide insight into the reaction mechanism and determine why quantitative yields are not achieved.

3.2.2 Studies of C-H Activation with External Bases

C-H activation with Pt complexes bearing DAB ligands is well documented.[14,21,23] In particular, DAB Pt complexes with the aryl substituents 3,5-bis-trifluoromethylphenyl[14a] (Figure 3-3-**1**) and 3,5-ditertbutylphenyl[14b] (Figure 3-3-**2**) have been shown to activate methane.

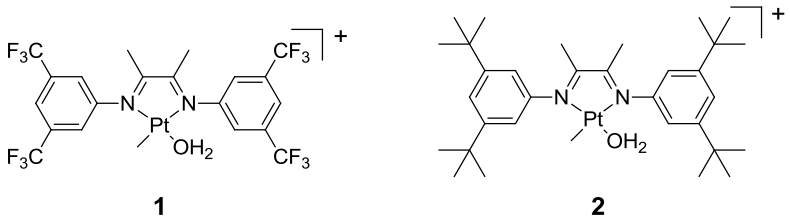

Figure 3-3. Monomethyl Pt complexes with a) 3,5-bis-trifluoromethylphenyl DAB and b) 3,5-ditertbutylphenyl DAB ligands.

The studies described here utilized Pt complexes with 3,5-bis-trifluoromethylphenyl DAB (DAB_{CF3}) due to low-cost of ligand starting materials and extensive prior work with these complexes. $DAB_{CF3}Pt(CH_3)_2$ was prepared following literature procedures.[14a] Protonolysis of $DAB_{CF3}Pt(CH_3)_2$ at -40^oC in wet dichloromethane with HBF_4•Et_2O

affords $[DAB_{CF3}Pt(CH_3)(H_2O)]^+$ (Figure 3-3-**1**). Removal of the reaction solvent results in an orange powder which is indefinitely stable in the glove box freezer at -35^oC.

Following literature procedures, initial C-H activation reactions were carried out in trifluoroethanol (TFE).[14] TFE is the frequently used solvent for these reactions because it is deactivated towards C-H activation, can solubilize the cationic complexes, and deuterated trifluoroethanol is commercially available. The aquo ligand in $[DAB_{CF3}Pt(CH_3)(H_2O)]^+$ is believed to be displaced by TFE prior to C-H activation.[24]

Rather than preparing samples under methane pressure, the studies were done using benzene due to the faster rate of C-H activation and easier sample preparation. In a typical experiment, a J. Young NMR tube is charged with a solution of complex 1 in TFE-d_3. A base is then added to the orange solution followed by benzene.

Bulky non-coordinating bases that are deactivated towards C-H activation were desired for these studies. The use of diisopropylethylamine for base assisted benzene activation has been previously reported.[25] For this reason, initial work focused on the use of bulky nitrogen-based bases such as 2,6-lutidine, 2,6-ditertbutylpyridine, diisopropylethylamine, triethylamine, proton sponge, and 1,8-diazabicyclo[5.4.0]undec-7-ene (DBU).

3.2.3 Attempts at Base Assisted C-H Activation with Pt DAB Complexes

Base assisted C-H activation of benzene was attempted with $[DAB_{CF3}Pt(CH_3)(H_2O)]^+$. The presence of an external base was hypothesized to deprotonate a Pt^{IV} hydride intermediate to give a Pt^{II} methyl phenyl product, Scheme 3-3.

Scheme 3-3. Proposed formation of a Pt^{II} methyl phenyl complex by base assisted C-H activation. N-N = 3,5-bis-trifluoromethylphenyl DAB

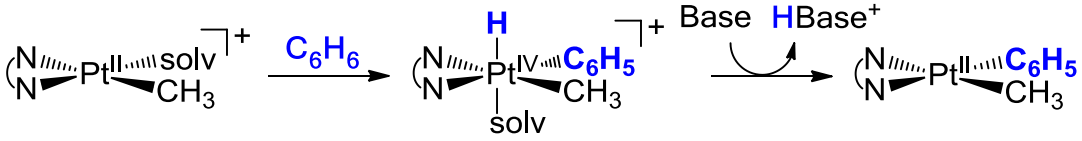

Addition of base to solutions of $[DAB_{CF3}Pt(CH_3)(H_2O)]^+$ in TFE-d_3 resulted in an immediate change in solution color from orange to brown-red. The ^{1}H-NMR spectrum of the reaction mixture showed an identical shift of the Pt-methyl resonance from δ 0.79 to δ 0.90 in all the samples. Addition of benzene to these solutions showed no C-H activation even after 24 hours at room temperature. Heating these solutions to 50^{o}C resulted in the formation of unidentified products.

The newly formed complex is unlikely to result from coordination of the base to Pt due to the use of bulky bases. An example of deprotonation of the DAB backbone methyl by sodium hydroxide has been reported in the literature,[26] but this is unlikely to be occurring based on the integration of the backbone methyl resonances. It is likely the base is deprotonating the aquo or TFE-d_3 ligand on Pt to afford a hydroxo or alkoxo complex as shown in Scheme 3-4.

Scheme 3-4. Deprotonation of protic ligands on a monomethyl-Pt complex. Ar = 3,5-bis-trifluoromethylphenyl

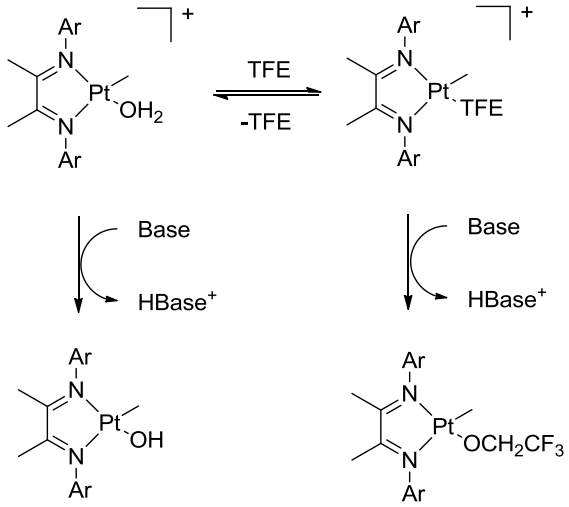

Hydroxide and alkoxide are strongly coordinating ligands which are not easily displaced and prevent oxidative addition of C-H bonds. Furthermore, solutions of $[DAB_{CF3}Pt(CH_3)(H_2O)]^+$ in acetonitrile-d_3, in which H_2O or TFE coordinated to Pt are expected to be displaced by acetonitrile-d_3, did not show any shift in the ^{1}H-NMR Pt-methyl signal upon addition of base.

3.2.4 Attempts at C-H Activation in Pentafluoropyridine

A weakly coordinating, aprotic solvent was desired for future experiments to avoid deprotonation by the external bases. Pentafluoropyridine has been used as a solvent for methane activation with tetramethylethylenediamine Pt complexes[27] and may be a suitable solvent for these reactions. Reaction mixtures of $[DAB_{CF3}Pt(CH_3)(H_2O)]^+$, benzene, and pentafluoropyridine heated to 85^{o}C did not show any C-H activation of benzene by ^{1}H-NMR spectroscopy even after 3 days. The lack of reactivity may be

explained by the strong coordination of the aquo ligand, which has been reported to hinder C-H activation.[14b]

In order to test this hypothesis, protonolysis of $DAB_{CF3}Pt(CH_3)_2$ was performed in the absence of H_2O. *p*-Trifluoromethylbenzonitrile was used as the ligand in the fourth coordination site as it has been reported as a labile ligand for benzene activation experiments.[28] However, C-H activation of benzene by this complex was not observed in TFE-d_3 or pentafluoropyridine solvents, suggesting that the benzonitrile ligand is not easily displaced to form the active species.

3.2.5 Attempts to Determine the Acidity of Pt Hydride Complexes

One concern in these studies was the unknown pK_a of the Pt hydride intermediate and whether the chosen bases are capable of deprotonating these intermediates. The pK_a of these complexes has not been previously studied due to the rapid reductive elimination of methane upon protonation of $(DAB)Pt(CH_3)_2$ complexes. Although dimethyl-Pt^{IV} hydride complexes have been observed via low temperature ^{1}H-NMR spectroscopy, they typically reductively eliminate to afford a monomethyl-Pt^{II} complex and methane at temperatures above -78^{o}C.[23b] Indeed, attempts to isolate a dimethyl-Pt^{IV} hydride via protonation of $DAB_{CF3}Pt(CH_3)_2$ with HBF_4•Et_2O in dichloromethane-d_2 at -78^{o}C and deprotonate with 2,6-lutidine were complicated by the rapid reductive elimination to afford methane and the monomethyl-Pt^{II} complex.

One strategy to slow the reductive elimination of methane is to protonate with a hydrogen halide to generate a 6-coordinate species with a halide bound trans to the

hydride.[29] Protonation of $DAB_{CF3}Pt(CH_3)_2$ with HCl in dichloromethane-d_2 at -78°C afforded the corresponding dimethyl-Pt^{IV} hydride complex. This species was characterized by low temperature ^{1}H-NMR spectroscopy at -78°C and a characteristic Pt-H signal at δ -21 with ^1J(Pt-H) = 1570 Hz was observed. Addition of 2,6-lutidine to this solution and warming to -50°C showed disappearance of the Pt-H resonance and appearance of the original dimethyl-Pt^{II} complex, some monomethyl-Pt^{II} chloride complex, and methane.

Although this experiment suggests 2,6-lutidine can deprotonate a platinum hydride complex as shown in Scheme 3-5 pathway **A**, a second pathway is possible since formation of the monomethyl-Pt^{II} chloride complex is observed. Due to decreased solubility of Pt complexes at -78°C, it is unclear if the protonation of dimethyl-Pt goes to completion. It is possible that the added base neutralizes the acid before it protonates the Pt complex that has not dissolved in solution. The Pt complexes dissolved in solution can be protonated and rapidly reductively eliminates methane before it can be deprotonated by the added base. These parallel pathways are shown in Scheme 3-5 pathways **B** and **C**.

Scheme 3-5. Possible reaction pathways for base addition to solutions of acid and $DAB_{CF3}Pt(CH_3)_2$. Ar = 3,5-bis-trifluoromethylphenyl

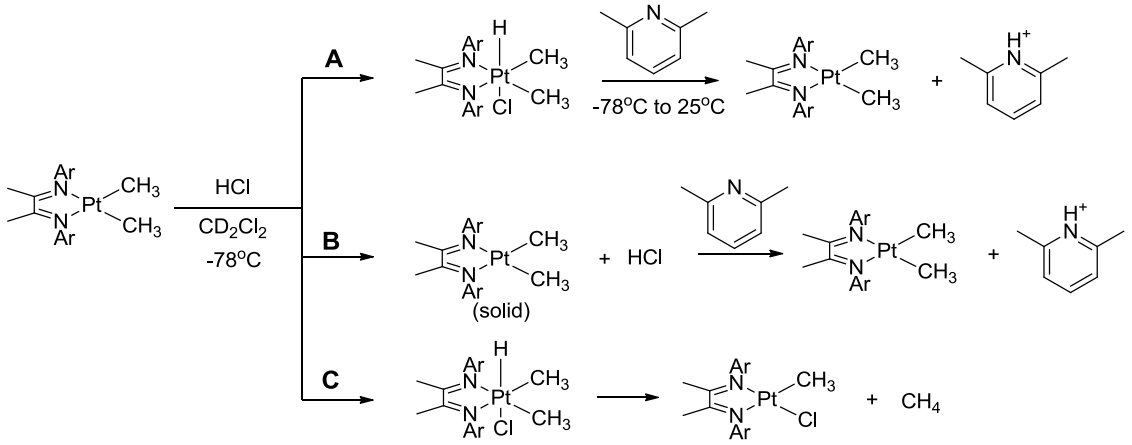

Although the pK_a of the chloride bound platinum hydride complex is likely to be very different from that without a chloride bound, this study gives some indication that deprotonation with an external base may be possible.

3.2.6 Attempts to Stabilize a Pt Hydride Complex with Facial Tridentate Ligands

Although our previously described studies suggested that Pt hydride complexes can be deprotonated using nitrogen-based bases, it is unknown if the deprotonation of a Pt hydride complex could occur faster than reductive elimination of methane from the reactive five coordinate intermediate. Facial coordinating tridentate ligands have been demonstrated to stabilize Pt hydride complexes after C-H activation by forming six-coordinate species.[30,31] It was hypothesized that a monomethyl-Pt^{II} complex with a tridentate ligand could be used to activate methane and form a six-coordinate dimethyl-

Pt^{IV} hydride complex. The addition of base would then give a desired dimethyl-Pt^{II} complex.

3.2.6.1 Dimethyl Pt Tripyridyl Amine

Reaction of 6-methyl-N,N-di-2-pyridinyl-2-pyridinamine (TPA) and dimeric $Pt(CH_3)_2(SMe_2)$ in toluene afforded (TPA)$Pt(CH_3)_2$, Figure 3-4, which was recovered by removal of the solvent and recrystallized to afford a yellow microcrystalline solid.

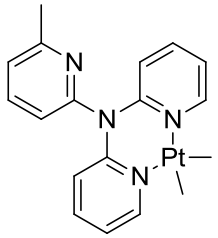

Figure 3-4. (6-methyl-N,N-di-2-pyridinyl-2-pyridinamine)$Pt(CH_3)_2$.

Sharp resonances in the ^{1}H-NMR spectrum suggested that ligand was not fluxional. X-ray quality crystals were obtained by layering CH_2Cl_2 solutions with pentane. X-ray crystallographic data can be found in Appendix A. C-H activation experiments with this complex have not yet been performed.

3.2.6.2 Dimethyl Pt Hydridotris(3,5-dimethylpyrazolyl)borate

Monomethyl-Pt^{II} hydridotris(3,5-dimethylpyrazolyl)borate (Tp') complexes have been demonstrated to activate the C-H bonds of benzene, cyclohexane, and pentane and form stable six-coordinate complexes.[31] It was hypothesized that the reaction solvent oxidatively adds to the reactive three-coordinate species to form a five-coordinate

monomethyl-Pt^{IV} alkyl hydride complex. This complex is then trapped by the third pyrazolyl ring to form the stable six-coordinate complex. Activation of methane with this complex is complicated by the fact that analogous reactions were performed in neat solvent and this cannot be achieved with methane under standard reaction conditions. It was hypothesized that reactions could be carried out in a solvent deactivated towards C-H activation with pressurized methane.

Following literature procedures, [K](Tp'Pt(CH_3)$_2$) was prepared by ligand exchange of dimeric Pt(CH_3)$_2$(SMe_2) with KTp' in tetrahydrofuran. Removal of the solvent afforded [K](Tp'Pt(CH_3)$_2$) as a colorless oil. Formation of the desired product was confirmed by ^{1}H-NMR spectroscopy. Addition of pentafluoropyridine to the colorless oil resulted in immediate formation of a white precipitate due to insolubility of the product. Attempts to synthesize [K](Tp'Pt(CH_3)$_2$) in pentafluoropyridine were also unsuccessful due to insolubility of the starting materials.

3.2.7 Pt Complexes with Pendant Bases and Large Bite Angles for C-H Activation

Extensive thermodynamic studies have been done with Pd and Pt catalysts with 9,9-dimethyl-4,5-bis(diethylphosphino)-xanthene (EtXantphos), Figure 3-5-**1**, for H_2 oxidation.[32] The large bite angles of these ligands result in a distortion from a square-planar to a distorted tetrahedral configuration. This distortion results in a lowered energy of the LUMO, which is the acceptor orbital for a hydride ligand. Thus larger ligand bite angles lead to lower energy for hydrogen activation.[33] Similar studies have also been

done for Ni catalysts with cyclic 1,5-diaza-3,7-diphospha-cyclooctane (P_2N_2) ligands, Figure 3-5-**2**.[34] These P_2N_2 ligands have pendant amines which act as bases in the second coordination sphere to aid in heterolytic cleavage of H_2. The C-H bond strength in methane is comparable to the H-H dihydrogen bond strength[35] and it is hypothesized that these ligands may allow for C-H activation of methane.

$[(EtXantphos)_2Pt](PF_6)_2$, $[(P^{Ph}{}_2N^{Bz}{}_2)_2Pt](PF_6)_2$, and $[(^tBuN)(CH_2PPh_2)_2Pt](PF_6)_2$ (ligands shown in Figure 3-5) complexes were prepared by ligand substitution with $PtCl_2SMe_2$ in the presence of $NaPF_6$. The preparation of the novel mixed ligand complex $[(EtXantphos)Pt(P^{Ph}{}_2N^{Bz}{}_2)](PF_6)_2$ was attempted, but resulted instead in formation of mixtures containing only $[(EtXantphos)_2Pt](PF_6)_2$ and $[(P^{Ph}{}_2N^{Bz}{}_2)_2Pt](PF_6)_2$. Attempts to synthesize $[(P^{tBu}{}_2N^{Bz}{}_2)_2Pt](PF_6)_2$ and $[(P^{tBu}{}_2N^{Ph}{}_2)_2Pt](PF_6)_2$ were also unsuccessful due to large steric demand by the tert-butyl substituents on phosphorus.[36]

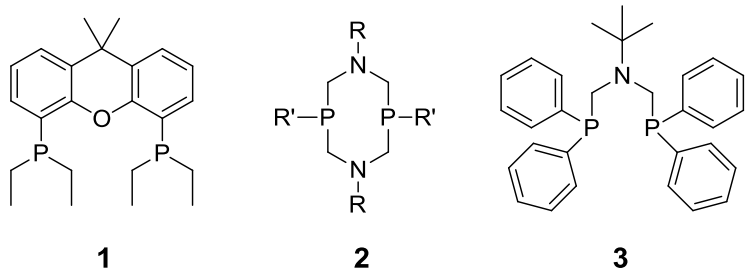

1 **2** **3**

Figure 3-5. 1) EtXantphos 2) General form of P_2N_2 type ligands 3) $(^tBuN)(CH_2PPh_2)_2$

NMR-scale reactions analogous to H_2 activation experiments reported in the literature were performed with methane.[32b,34a] Solutions of $[(EtXantphos)_2Pt](PF_6)_2$ and $[(P^{Ph}{}_2N^{Bz}{}_2)_2Pt](PF_6)_2$ in acetonitrile-d_3 were pressurized with 3 atm of methane. No

change in the ^{1}H-NMR spectra of the reaction solutions was observed after a week at room temperature. Solutions heated to 100^{o}C for ten days also did not show any reactivity. Complete decomposition of the Pt complexes was observed after heating solutions to 150^{o}C for one week.

While nitrogen containing ligands have pendant bases in the second coordination sphere to deprotonate methane upon heterolytic cleavage, C-H activation with $[(EtXantphos)_2Pt](PF_6)_2$ were anticipated to require additional bases. Rough thermodynamic calculations for C-H activation with $[(EtXantphos)_2Pt](PF_6)_2$ were performed to determine the strength of the base required for these reactions (Figure 3-6).

$$CH_4 \rightarrow CH_3^- + H^+ \qquad (1)\ 92\ kcal/mol$$
$$Pt^{2+} + CH_3^- \rightarrow Pt\text{-}CH_3^+ \qquad (2)\ -60\ to\ -50\ kcal/mol$$
$$H^+ + Base \rightarrow HBase^+ \qquad (3)\ ca.\ -30\ to\ -40\ kcal/mol\ (pKa > 22)$$
$$Pt^{2+} + CH_4 + Base \rightarrow Pt\text{-}CH_3^+ + HBase^+$$

Figure 3-6. Thermodynamic calculations for base assisted C-H activation of methane with $[(EtXantphos)_2Pt](PF_6)_2$. Reaction energy can be estimated as the sum of 1) Heterolytic cleavage of methane. 2) Pt-CH_3 bond formation. 3) Base protonation.

The net reaction can be thought of as heterolytic cleavage of methane, formation of a Pt-CH_3 bond, and protonation of a base. The heterolytic cleavage of methane is reported to require 92 kcal/mol in acetonitrile.[37] An estimation of the heterolytic cleavage of Pt-CH_3 can be calculated from the H^- affinity of $[(EtXantphos)_2Pt](PF_6)_2$ and a comparison of Pt-H and Pt-CH_3 bond dissociation energies.[38] Therefore, the formation of $[Pt\text{-}CH_3]^+$ from Pt^{2+} and CH_3^- is estimated to be between -60 and -50 kcal/mol. In order for the net C-H

activation reaction to be thermodynamically downhill, protonation of the base should be roughly -35 kcal/mol. This requires a base with pK_a of 25 or greater.

Guided by our thermodynamic calculations, methane activation with $[(EtXantphos)_2Pt](PF_6)_2$ and base was investigated in acetonitrile-d_3 under 3 atm of methane. Bases of pK_a's (in CH_3CN) between 13 and 41 were used in these studies. Immediate decomposition of $[(EtXantphos)_2Pt](PF_6)_2$ at room temperature was observed with bases above pK_a of 26 presumably due to initial deprotonation of the ligand. Solutions of $[(EtXantphos)_2Pt](PF_6)_2$ and tetramethylguanadine (pK_a 26) showed complex decomposition after 5 hours at 50°C. Reaction mixtures of $[(EtXantphos)_2Pt](PF_6)_2$ and diisopropylethylamine (pK_a 21) showed 40% decomposition after 10 days at 100°C.

The expected C-H activation product, $[(EtXantphos)_2Pt(CH_3)](PF_6)$, was independently synthesized via methylation of $[(EtXantphos)_2Pt](PF_6)_2$ with methyl magnesium bromide. The methyl resonance of the five-coordinate Pt complex was characterized by a quintet with ^{195}Pt satellites in the ^{1}H-NMR spectrum (^2J(Pt-H): 57 Hz, ^3J(P-H): 3.7 Hz) suggesting a square bipyramidal configuration. Efforts to recrystallize and fully characterize this material were unsuccessful. Although not fully characterized, this complex is potentially a rare example of a five-coordinate Pt^{II} complex that is not coordinated η^2 to an olefin.[39,40,41,42]

A solution of $[(EtXantphos)_2Pt(CH_3)](PF_6)$ and protonated diisopropylethylamine heated at 100°C for 10 days showed trace methane formation. However,

diisopropylethylamine and $[(EtXantphos)_2Pt](PF_6)_2$ were not observed. It is likely methane formation was the result of thermal decomposition of $[(EtXantphos)_2Pt(CH_3)](PF_6)$. The parallel experiments with $[(EtXantphos)_2Pt](PF_6)_2$ and diisopropylethylamine and $[(EtXantphos)_2Pt(CH_3)](PF_6)$ and protonated diisopropylethylamine show that the thermodynamic barrier for both reactions is uphill. The stability of $[(EtXantphos)_2Pt(CH_3)](PF_6)$ in the presence of protonated base suggests that base assisted C-H activation of methane could be a viable strategy. However, due to the incompatibility of $[(EtXantphos)_2Pt](PF_6)_2$ with strong bases, C-H activation of methane cannot be realized with these complexes.

3.3 Conclusion

Diaryl-Pt^{II} and monoaryl-Pd^{II} complexes have been studied for the development of catalytic aryl coupling reactions. Diaryl-Pt^{II} complexes do not follow the analogous chemistry of dimethyl-Pt^{II} complexes and do not afford biphenyl upon oxidation. Oxidation of monoaryl-Pd^{II} complexes results in the formation of Pd^{II} solvento complexes and biphenyl in roughly 50% yield. Although experiments with an oxidative phenyl transfer reagent suggest that biphenyl is formed via reductive elimination from a diaryl-Pd^{IV} species, more mechanistic studies are necessary to determine why yields are not quantitative. The use of stronger oxidants or elevated temperature NMR experiments may enable the mechanism of these reactions to be elucidated. If quantitative yields of biphenyl can be achieved with these complexes, these systems may be worth studying for

development of a complete catalytic cycle for C-C coupling of aromatics as regeneration of a monoaryl-Pd^{II} complex should be easier to achieve than diaryl-Pd^{II} complex.

Studies have suggested that bases such as 2,6-lutidine may be capable of deprotonating dimethyl-Pt^{IV} hydride complexes. However, protic solvents or ligands are not compatible with bases because they can be easily deprotonated when bound to Pt, inhibiting C-H activation. In pentafluoropyridine, $[DAB_{CF3}Pt(CH_3)]^+$ with *p*-trifluoromethylbenzonitrile bound was not found to C-H activate benzene because benzonitrile could not be displaced. In addition to being nonacidic, ligands used in this chemistry must also be labile to allow oxidative addition of an alkane/alkene to Pt for C-H activation to be possible. Base assisted C-H activation is unlikely to be successful for completing the catalytic cycle detailed in Scheme 3-1. The reductive elimination of methane from $[(DAB)Pt(CH_3)_2(H)]^+$ complexes is anticipated to be much faster than the deprotonation by an external base.

Facial tridentate ligands can aid in trapping five-coordinate Pt complexes and prevent reductive elimination. These ligands may make deprotonation more competitive with reductive elimination if the deprotonation of a five-coordinate Pt hydride with external base is kinetically competitive with reductive elimination. Methane activation experiments with $[K](Tp'Pt(CH_3)_2)$ could not be attempted due to its insolubility in pentafluoropyridine. It is unlikely that methane activation can be achieved with these complexes as C-H activation of compatible solvents is likely to be more facile.

C-H activation of methane was studied with $[(EtXantphos)_2Pt](PF_6)_2$ and various bases. Thermodynamic calculations and experimental results suggest a base with a pK_a above 26 is necessary for the activation of methane to be thermodynamically downhill. However, $[(EtXantphos)_2Pt](PF_6)_2$ was shown to be unstable in the presence of strong bases. While base assisted methane activation cannot be achieved with these catalysts, activation of weaker C-H bonds such as hydrofluorocarbons or higher alkanes may be thermodynamically favorable with weaker bases that are compatible with $[(EtXantphos)_2Pt](PF_6)_2$. Such studies may provide fundamental strategies in ligand design for future methane activation catalysts.

3.4 Experimental

General Procedures. All experiments were performed under an inert atmosphere using standard glovebox or Schlenk techniques.

Deuterated solvents were purchased from Cambridge Isotope Laboratories. Acetone-d_6, nitromethane-d_3, acetonitrile-d_3, and pentafluoropyridine were purified by vacuum distillation twice from $CaSO_4$. Dichloromethane-d_2 was purified by vacuum distillation from CaH_2. Sealed vials of trifluoroethanol-d_3 were used as purchased. Diethyl ether, benzene, pentane, and toluene were dried using a Seca Solvent System. Acetonitrile was purchased from Burdick and Jackson® (low-water brand) and stored in an argon pressurized stainless steel drum plumbed directly into a glove-box without further treatment. Pentane and diethyl ether were further purified by vacuum distillation from Na^0 and benzophenone.

2,6-lutidine, 2,6-ditertbutylpyridine, diisopropylethylamine, and triethylamine were purified by distillation from KOH. Proton sponge and 1,8-diazabicyclo[5.4.0]undec-7-ene (DBU) were used as received. All other chemicals were used as received.

^{1}H, ^{19}F and ^{31}P-NMR spectra were obtained using Bruker 500 and 300 MHz spectrometers. NMR quantification was performed by using 1,1,2-trichloroethane (TCE) as an internal integration standard.

Synthesis. (*N*,*N*′-diaryl-2,3-dimethyl-1,4-diaza-1,3-butadiene)Pt(C_6H_5)$_2$ complexes[43], (^{t}butylbipy)Pd(C_6H_5)(CF_3)[17], (^{t}butylbipy)Pd(C_6H_4F)(CF_3)[17], $DAB_{CF3}Pt(CH_3)_2$[17], $[DAB_{CF3}Pt(CH_3)(H_2O)]^{+}$[14a], [K](hydridotris(3,5-dimethylpyrazolyl)borate)Pt(CH_3)$_2$)[31], and [(9,9-dimethyl-4,5-bis(diethylphosphino)-xanthene)$_2$Pt](PF_6)$_2$[32b] were prepared as previously described in the literature.

(6-methyl-N,N-di-2-pyridinyl-2-pyridinamine)Pt(CH_3)$_2$. To a 50-mL round bottom flask was added 6-methyl-N,N-di-2-pyridinyl-2-pyridinamine (146 mg, 0.557 mmol), cis/trans-Pt(Cl)$_2$(SCH_3)$_2$ dimer (160 mg, 0.278 mmol), and 15 mL toluene. The solution was stirred under static vacuum overnight at room temperature to afford a yellow solution with yellow precipitate. The solvent was removed under removed under reduced pressure to afford a yellow solid. The solid was dissolved in 3 mL CH_2Cl_2, filtered through Celite, and layered with 20 mL pentane to crystallize out a yellow solid. The solution was filtered to collect on 230 mg of the product (84% yield). ^{1}H NMR (500 MHz, 25°C, Acetone-d_6): δ 0.73 (s, 6 H, PtC-H, ^{2}J(Pt-H): 87 Hz); δ 2.29 (s, 3 H, PyC-H); δ 6.39 (d, 1

H, Py-H), δ 6.81 (d, 1 H, Py-H), δ 7.45 (t, 2 H, Py-H), δ 7.50 (t, 1 H, Py-H) , δ 7.91 (d, 2 H, Py-H) , δ 8.16 (t, 2 H, Py-H) , δ 8.86 (d, 2 H, Py-H, ^{4}J(Pt-H): 23 Hz).

[($P^{Ph}_2N^{Bz}_2$)$_2$Pt](PF$_6$)$_2$. NMR scale solutions were prepared and used as needed. To a solution of $P^{Ph}_2N^{Bz}_2$ (4.0 mg, 0.0082 mmol) in 0.6 mL of acetonitrile-d_3 was added cis/trans-Pt(Cl)$_2$(SCH$_3$)$_2$ dimer (1.6 mg, 0.0020 mmol) and NaPF$_6$ (1.6 mg, 0.0094 mmol). The solution was allowed to stir at room temperature for 1 hour resulting in a light yellow solution with white precipitate. The precipitate was allowed to settle and the solution was decanted to a J. Young NMR tube and used without further purification. ^{1}H NMR (500 MHz, 25°C, CD$_3$CN): δ 3.67 (m, 16 H, PC-H); δ 4.08 (s, 8 H, PhC-H); δ 6.99 (br s, 8 H, Ar), δ 7.07 (t, 8 H, Ar), δ 7.29 (t, 4 H, Ar), δ 7.40 (m, 20 H, Ar). ^{31}P{^{1}H} NMR (202 MHz, 25°C, CD$_3$CN): δ -11.3 (^{1}J(Pt-P): 2080 Hz).

[(^{t}BuN(CH$_2$P(C$_6$H$_5$)$_2$)$_2$)$_2$Pt](PF$_6$)$_2$. NMR scale solutions were prepared and used as needed. To a solution of ^{t}BuN(CH$_2$P(C$_6$H$_5$)$_2$)$_2$ (3.9 mg, 0.0082 mmol) in 0.6 mL of acetonitrile-d_3 was added cis/trans-Pt(Cl)$_2$(SCH$_3$)$_2$ dimer (1.6 mg, 0.0020 mmol) and NaPF$_6$ (1.6 mg, 0.0094 mmol). The solution was allowed to sit at room temperature for 16 hour resulting in a colorless solution with white precipitate. The solution was condensed, taken up in CD$_3$CN and filtered through Celite to collect a clear, colorless solution that was used without further purification. ^{1}H NMR (500 MHz, 25°C, CD$_3$CN): δ 0.65 (s, 36 H, CC-H); δ 3.79 (t, 16 H, PC-H); δ 7.28 (t, 32 H, Ar), δ 7.35 (br s, 32 H, Ar), δ 7.48 (t, 16 H, Ar). ^{31}P{^{1}H} NMR (202 MHz, 25°C, CD$_3$CN): δ -9.75 (^{1}J(Pt-P): 2236 Hz).

[(EtXantphos)$_2$Pt(CH$_3$)](PF$_6$). To an oven dried 100-ml 2 neck round bottom flask was added [(EtXantphos)$_2$Pt](PF$_6$)$_2$ (120 mg, 0.095 mmol) and 20 mL THF. The orange slurry was stirred for 20 minutes before a solution of CH_3MgBr (35 μL of 3.0 M ether solution in 3 mL THF, 0.100 mmol) was added dropwise over 5 minutes. The orange slurry turned to a mostly clear yellow solution with small amounts of fine precipitate upon stirring for 30 minutes. 2 mL of 1,4-dioxane was added to the solution and the solution was partially condensed to about 12 mL. The solution was filtered through Celite and condensed to afford a yellow residue. The residue was washed with small portions of THF and pentane to afford a yellow powder. Attempts to recrystallize the product via vapor diffusion with THF/pentane and CH_3CN/ether, and layering solutions of benzonitrile/CH_3CN at -35^{o}C did not afford X-ray quality crystals. ^{1}H NMR (500 MHz, 25°C, CD_2Cl_2): δ 0.44 (quin, 3 H, PtC-H, ^2J(Pt-H): 57 Hz, ^3J(P-H): 3.7 Hz), δ 0.92 (s, 24 H, PCC-H), δ 1.66 (s, 12 H, xanthene C-H), δ 2.28 (s, 16 H, PC-H), δ 7.13 (br m, 4 H, Ar-H), δ 7.24 (t, 4 H, Ar-H), δ 7.59 (d, 4 H, Ar-H). ^{31}P{^{1}H} NMR (202 MHz, 25°C, CD_2Cl_2): δ -8.02 (^1J(Pt-P): 3587 Hz).

General procedure for oxidation of (*N*,*N*′-diaryl-2,3-dimethyl-1,4-diaza-1,3-butadiene)Pt(C$_6$H$_5$)$_2$. A J. Young NMR tube was charged with (DAB)Pt(C_6H_5)$_2$ (0.0035 mmol), acylferrocenium tetrafluoroborate (1.5 mg, 0.0035 mmol), and 0.60 mL acetone-d_6. The solution was left at room temperature for 6 hours resulting in the formation of benzene and several unidentified products.

Oxidation of (^{t}butylbipy)(Pd)(C_6H_5)(CF_3). In a typical reaction, a J. Young NMR tube was charged with (^{t}butylbipy)(Pd)(C_6H_5)(CF_3) (3.0 mg, 0.0058 mmol), acylferrocenium hexafluorophosphate (2.4 mg, 0.0063 mmol), and 0.60 mL acetone-d_6. 3 μL of 1,1,2-trichloroethane was added as an integration standard. The solution was left at room temperature overnight to afford a dark red solution. Monitoring these reactions by ^{19}F-NMR spectroscopy shows complete conversion of (^{t}butylbipy)(Pd)(C_6H_5)(CF_3) (s, δ -19.8) to (^{t}butylbipy)(Pd)(CF_3)(solvent) (br s, δ -31.8). ^{1}H NMR (500 MHz, 25°C, Acetone-d_6): δ 1.45 (br s, 18 H, C-CH_3), δ 7.8-8.1 (broad signals, 3 H, bipy-H), δ 8.6-8.8 (broad signals, 3 H, bipy-H).

Oxidation of (^{t}butylbipy)(Pd)(C_6H_4F)(CF_3). In a typical reaction, a J. Young NMR tube was charged with a solution of (^{t}butylbipy)(Pd)(C_6H_4F)(CF_3) (3.0 mg, 0.0056 mmol), acylferrocenium hexafluorophosphate (2.3 mg, 0.0062 mmol), and 0.60 mL acetone-d_6. 3 μL of 1,1,2-trichloroethane was added as an integration standard. The solution was left at room temperature overnight to afford a dark red solution. Monitoring these reactions by ^{19}F-NMR spectroscopy shows complete conversion of (^{t}butylbipy)(Pd)(C_6H_4F)(CF_3) (s, δ -19.8) to (^{t}butylbipy)(Pd)(CF_3)(solvent) (br s, δ -31.8), formation of 4,4'-difluorobiphenyl (br s, δ -116), and two unidentified F-Ph resonances (br s, δ -112 and δ -118).

Reaction of (^{t}butylbipy)Pd(C_6H_5)(CF_3) with diphenyliodonium triflate. In a typical experiment, a J. Young NMR tube was charged with (^{t}butylbipy)Pd(C_6H_5)(CF_3) (3.0 mg, 0.0058 mmol) and $(C_6H_5)_3I(CF_3SO_3)$ (2.5 mg, 0.0058 mmol), and 0.60 mL acetone-d_6.

The reaction was allowed to sit at room temperature for 72 hours prior to analysis by ^{1}H-NMR spectroscopy showing the formation of biphenyl and [(^{t}butylbipy)Pd(CF_3)]$^+$.

Attempts at base assisted C-H activation with [$DAB_{CF3}Pt(CH_3)(H_2O)$]$^+$. In a typical experiment, a J. Young NMR tube was charged with [$DAB_{CF3}Pt(CH_3)(H_2O)$]$^+$ (3.6 mg, 0.0044 mmol) and 0.50 mL trifluoroethanol-d_3 to afford a dark orange solution. The corresponding base (0.0044 mmol) and benzene (1.6 μL, 0.017 mmol) are added to the tube via a micropipette. Upon mixing, all solutions turned dark red and Pt-CH_3 resonances are observed to shift from δ 0.79 to δ 0.90. Bases studied were 2,6-lutidine, 2,6-ditertbutylpyridine, diisopropylethylamine, triethylamine, proton sponge, and 1,8-diazabicyclo[5.4.0]undec-7-ene (DBU).

Attempts at low temperature protonation and deprotonation of dimethyl-Pt^{II} $DAB_{CF3}Pt(CH_3)_2$. To a septa top NMR tube was added $DAB_{CF3}Pt(CH_3)_2$ (1.0 mg, 0.0014 mmol) in 0.50 mL CD_2Cl_2. The tube was inserted into a precooled NMR probe at 195 K and an initial ^{1}H-NMR spectrum was collected. The starting material was characterized by a Pt-CH_3 resonance (δ 0.92, Pt satellites not observed at low temperature). The tube was cooled in a dry ice/acetone bath and 1 μL H_2O and 36 μL of a 0.078 M solution of Me_3SiCl in CD_2Cl_2 were added via microsyringe to form 0.0028 mmol of HCl in situ. The tube was reinserted into the NMR probe at 195 K. The formation of $DAB_{CF3}Pt(CH_3)_2(Cl)(H)$ was indicated in the ^{1}H-NMR spectrum by a Pt-H resonance (δ -21 with ^1J(Pt-H) = 1570 Hz) and Pt-CH_3 resonance (δ 0.66 and ^2J(Pt-H) = 69 Hz). The

tube was returned to a dry ice/acetone bath and 32 μL of a 0.088 M solution of 2,6-lutidine in CD_2Cl_2. The tube was reinserted into the probe and warmed to 298 K. The ^{1}H-NMR spectrum showed disappearance of the Pt-H resonance and appearance of Pt-CH_3 resonances of $DAB_{CF3}Pt(CH_3)_2$ (δ 1.18 and ^2J(Pt-H) = 87 Hz) and $DAB_{CF3}Pt(CH_3)(Cl)$ (δ 0.98 and ^2J(Pt-H) = 80 Hz). Reactions performed without addition of base result in formation of only $DAB_{CF3}Pt(CH_3)(Cl)$. ^{1}H NMR of $DAB_{CF3}Pt(CH_3)(Cl)$ (500 MHz, 25°C, CD_2Cl_2): δ 0.98 (s, 3 H, PtC-H, ^2J(Pt-H): 80 Hz), δ 1.33 (s, 3 H, DAB-CH_3), δ 1.88 (s, 3 H, DAB-CH_3), δ 7.61 (s, 2 H, DAB Ar-H), δ 7.65 (s, 2 H, DAB Ar-H), δ 7.92 (s, 1 H, DAB Ar-H), δ 7.96 (s, 1 H, DAB Ar-H).

Base assisted methane activation with $[(EtXantphos)_2Pt](BPh_4)_2$. A medium-walled NMR tube was charged with $[(EtXantphos)_2Pt](BPh_4)_2$ (10.0 mg, 0.0062 mmol), diisopropylethylamine (1.6 μL, 0.0093 mmol), and 0.40 mL CD_3CN. The solution was freeze-pump-thaw degassed three times, pressurized with 5 atm methane, and the tube was flame-sealed. The tube was fully submerged in a 100^{o}C oil bath. The tube was removed from the bath, cleaned, and shaken prior to collection of ^{1}H-NMR spectra. 40% decomposition of $[(EtXantphos)_2Pt](BPh_4)_2$ to unidentified materials was observed after 10 days at 100^{o}C.

Protonated base with $[(EtXantphos)_2Pt(CH_3)](BPh_4)_2$. A J. Young NMR tube was charged with $[(EtXantphos)_2Pt(CH_3)](BPh_4)_2$ (8.1 mg, 0.0062 mmol), diisopropylethylaminium tetrafluoroborate (2.0 mg, 0.0093 mmol), and 0.40 mL CD_3CN.

The tube submerged up to the J. Young cap in a 100^{o}C oil bath. The tube was removed from the bath, cleaned, and shaken prior to collection of ^{1}H-NMR spectra.

3.5 Notes to Chapter 3

[1] For examples see: (a) Conley, B. L.; Tenn III, W. J.; Young, K. J. H.; Ganesh, S. K.; Meier, S. K.; Ziatdinov, V. R.; Mironov, O.; Oxgaard, J.; Gonzales, J.; Goddard Iii, W. A.; Periana, R. A. *J. Mol. Catal. A: Chem.* **2006**, *251*, 8-23. (b) Bergman, R. G. *Nature* **2007**, *446*, 391-393.

[2] U.S. Energy Information Administration, Department of Energy, *Annual Energy Review*, http://www.eia.doe.gov/totalenergy/data/annual/#resources (accessed Feb. 4, 2010).

[3] For example see: Crabtree, R. H. *Chem. Rev.* **1995**, *95*, 987-1007.

[4] Berkowitz, J.; Ellison, G. B.; Gutman, D. *J. Phys. Chem.* **1994**, *98*, 2744-2765.

[5] For example see: (a) Chen, G. S.; Labinger, J. A.; Bercaw, J. E. *Organometallics* **2009**, *28*, 4899-5292. (b) Periana, R. A.; Taube, D. J.; Gamble, S.; Taube, H.; Satoh, T.; Fujii, H. *Science* **1998**, *280*, 56-7.

[6] For example see: (a) Keller, G. E.; Bhasin, M. M. *J. Catal.* **1982**, *73*, 9-19. (b) Ito, T.; Lunsford, J. H. *Nature* **1985**, *314*, 721-722.

[7] (a) Lanci, M. P.; Remy, M. S.; Kaminsky, W.; Mayer, J. M.; Sanford, M. S. *J. Am. Chem. Soc.* **2009**, *131*, 15618-15620. (b) Lao, D. B.; Lanci, M. P.; Spettel, K. E.; Mayer, J. M. Manuscript in preparation.

[8] Lanci, M. P.; Remy, M. S.; Lao, D. B.; Sanford, M. S.; Mayer, J. M. *Organometallics* **2011**, *30*, 3704-3707.

[9] Brown, J. M.; Cooley, N. A. *Chem. Rev.* **1988**, *88*, 1031-1046.

[10] Hartwig, J. Reductive Elimination. In *Organotransition Metal Chemistry From Bonding to Catalysis*; University Science Books: Sausalito, CA, 2010; 331-338.

[11] (a) Hill, G. S.; Puddephatt, R. J. *Organometallics* **1997**, *16*, 4522-4524. (b) Hill, G. S.; Yap, G. P. A.; Puddephatt, R. J. *Organometallics* **1999**, *18*, 1408-1418.

[12] Fekl, U.; Goldberg, K. I. *J. Am. Chem. Soc.* **2002**, *124*, 6804-6805.

[13] (a) Moravskiy, A.; Stille, J. K. *J. Am. Chem. Soc.* **1981**, *103*, 4182-4186. (b) Brown, D. G.; Byers, P. K.; Canty, A. J. *Organometallics* **1990**, *9*, 1231-1235.

[14] (a) Johansson, L.; Ryan, O. B.; Tilset, M. *J. Am. Chem. Soc.* **1999**, *121*, 1974-1975. (b) Owen, J. S.; Labinger, J. A.; Bercaw, J. E. *J. Am. Chem. Soc.* **2006**, *128*, 2005-2016.

[15] Remy, M. S.; Cundari, T. R.; Sanford, M. S. *Organometallics* **2010**, *29*, 1522-1525.

[16] Lotz, M.; Sanford, M. S. Manuscript in preparation.

[17] Ball, N. D.; Gary, J. B.; Ye, Y.; Sanford, M. S. *J. Am. Chem. Soc.* **2011**, *133*, 7577-7584.

[18] Racowski, J. M.; Ball, N. D.; Sanford, M. S. *J. Am. Chem. Soc.* **2011**, *133*, 18022-18025.

[19] Lersch, M.; Tilset, M. *Chem Rev.* **2005**, *105*, 2471-2526. and references therein.

[20] (a) Johansson, L.; Tilset, M. *J. Am. Chem. Soc.* **2001**, *123*, 739-740. (b) Wik, B. J.; Lersch, M.; Tilset, M. *J. Am. Chem. Soc.* **2002**, *124*, 12116-12117.

[21] Johansson, L.; Tilset, M.; Labinger, J. A.; Bercaw, J. E. *J. Am. Chem. Soc.* **2000**, *122*, 10846-10855.

[22] Canty, A. J.; Patel, J.; Rodemann, T.; Ryan, J. H.; Skelton, B. W.; White, A. H. *Organometallics* **2004**, *23*, 3466-3473.

[23] Heiberg, H.; Johansson, L.; Gropen, O.; Ryan, O. B.; Swang, O.; Tilset, M. *J. Am. Chem. Soc.* **2000**, *122*, 10831-10845.

[24] Labinger, J. A.; Bercaw, J. E.; Tilset, M. *Organometallics* **2006**, *25*, 805-808.

[25] Harkins, S. B.; Peters, J. C. *Organometallics* **2002**, *21*, 1753-1755.

[26] Cavallo, L.; Macchioni, A.; Zuccaccia, C.; Zuccaccia, D.; Orabona, I.; Ruffo, F. *Organometallics* **2004**, *23*, 2137-2145.

[27] Holtcamp, M. W.; Labinger, J. A.; Bercaw, J. E. *J. Am. Chem. Soc.* **1997**, *119*, 848-849.

[28] Norris, C. M.; Templeton, J. L. *Organometallics* **2004**, *23*, 3101-3104.

[29] Hill, G. S.; Rendina, L. M.; Puddephatt, R. J. *Organometallics* **1995**, *14*, 4966-4968.

[30] Vedernikov, A. N.; Fettinger, J. C.; Mohr, F. *J. Am. Chem. Soc.* **2004**, *126*, 11160-11161.

[31] Wick, D. D.; Goldberg, K. I. *J. Am. Chem. Soc.* **1997**, *119*, 10235-10236.

[32] (a) Raebiger, J. W.; Miedaner, A.; Curtis, C. J.; Miller, S. M.; Anderson, O. P.; DuBois, D. L. *J. Am. Chem. Soc.* **2004**, *126*, 5502-5514. (b) Miedaner, A.; Raebiger, J. W.; Curtis, C. J.; Miller, S. M.; DuBois, D. L. *Organometallics* **2004**, *23*, 2670-2679.

[33] DuBois, M. R.; DuBois, D. L. *Chem. Soc. Rev.* **2009**, *38*, 62-72.

[34] (a) Fraze, K.; Wilson, A. D.; Appel, A. M.; DuBois, M. R.; DuBois, D. L. *Organometallics* **2007**, *26*, 3918-3924. (b) Wilson, A. D.; Shoemaker, R. K.; Miedaner, A.; Mukerman, J. T.; DuBois, D. L.; DuBois, M. R. *Proc. Nat. Acad. Sci.* **2007**, *104*, 6951-6956.

[35] Blanksby, S. J.; Ellison, G. B. *Acc. Chem. Res.* **2003**, *36*, 255-263.

[36] Wiedner, E. S.; Yang, J. Y.; Dougherty, W. G.; Kassel, W. S.; Bullock, R. M.; DuBois, M. R.; DuBois, D. L. *Organometallics* **2010**, *29*, 5390-5401.

[37] Warren, J. J.; Tronic, T. A.; Mayer, J. M. *Chem. Rev.* **2010**, *110*, 6961-7001.

[38] Goddard, W. A. *J. Am. Chem. Soc.* **1984**, *106*, 8321-8322.

[39] Clark, H. C.; Manzer, L. E. *J. Am. Chem. Soc.* **1973**, *95*, 3812-3813.

[40] Terheijden, J.; van Koten, G.; Mul, W. P.; Stufkens, D. J.; Muller, F.; Stam, C. H. *Organometallics* **1986**, *5*, 519-525.

[41] Cucciolito, M. E.; De Felice, V.; Panunzi, A.; Vitagliano, A. *Organometallics* **1989**, *8*, 1180-1187.

[42] Albano, V. G.; Natile, G.; Panunzi, A. *Coord. Chem. Rev.* **1994**, *133*, 67-114.

[43] Moret, M.; Chen, P. *J. Am. Chem. Soc.* **2009**, *131*, 5675-5690.

4 – Deoxygenation of Glycerol by Iridium Pincer Complexes

4.1 Introduction

4.1.1 General Introduction

Dwindling oil reserves have placed significant focus on the need for renewable sources for fuels and commodity chemicals. Due to its infrastructure compatibility with current transportation fuels, biodiesel has drawn considerable interest and production has grown in recent years. The rapid growth in biodiesel production has resulted in the generation of large quantities of the byproduct glycerol. While glycerol has many uses as a commodity chemical, the production scale of transportation fuels far exceeds that of commodity chemicals. As a result of high production quantities that exceed market demand and high purification costs, waste glycerol from biodiesel production is often burned onsite as fuel for the production process. The transformation of waste stream glycerol into a C-3 platform chemical would improve upon the atom efficiency and economics of the biodiesel industry.[1,2,3,4,5]

Potential C-3 target chemicals from glycerol are 1,3-propanediol (1,3-PD) and 1-propanol (1-PO). 1,3-PD is utilized in the production of polyesters, polyurethanes, and polyethers. The conversion of glycerol to 1,3-PD can be envisioned as a net deoxygenation via a tandem catalytic sequence with an initial acid catalyzed dehydration followed by metal catalyzed hydrogenation (Equation 4.1).

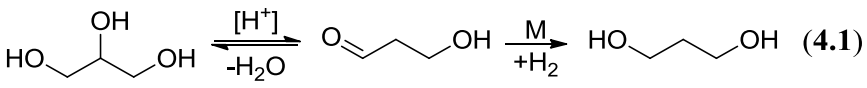

(**4.1**)

Deoxygenation of glycerol in the C2 and C3 positions would afford 1-PO, a useful solvent. Although 1-PO has lower value than 1,3-PD, it is still a value-added chemical made from glycerol, particularly so if generated from crude biodiesel byproduct glycerol.

4.1.2 Previous Work

Catalysts capable of these transformations must be stable in aqueous acidic solutions at extreme temperatures (above 180^{o}C) and pressures (above 40 bar). Many heterogeneous catalysts for glycerol conversion have been reported using metals ranging from Co[5], Ni[6,7], Cu[9,8], Pt[9,10,11,12], Pd[13,14], Ru[9,8,15,16], and Rh[32,17,18]. While many catalysts have been reported for conversion of glycerol to 1,2-propanediol (1,2-PD) with high selectivities, there are considerably fewer catalysts that give high conversion to 1,3-PD.

There are several Cu catalysts reported for glycerol deoxygenation. In general, Cu catalysts are selective for 1,2-PD formation and do not catalyze undesired C-C bond cleavage. Montassier has reported 85% conversion of aqueous solutions of glycerol with 66% selectivity to 1,2-PD using Raney Cu and Cu on carbon catalysts.[19] Even higher selectivities have been reported by Pinel, who have reported 100% selectivity for 1,2-PD from 20% conversion of glycerol using Cu-ZnO catalysts.[32] 100% selectivity for 1,2-PD has also been reported by Qiu, using Cu-Cr oxide catalysts with up to 51% conversion of glycerol. Formation of 1,3-PD was reported for gas-phase reactions in flow reactors with glycerol over Cu-$H_4SiW_{12}O_{40}$ on SiO_2 by Zhu et al.[20] Under these conditions, 84% conversion of glycerol was achieved with 32% selectivity for 1,3-PD and 22% selectivity for 1,2-PD.

Reported Ru catalysts are typically selective for 1,2-PD, but with lower selectivity than reported Cu catalysts. Tomishige has reported various studies with Ru on carbon with Amberlyst and has achieved 49% conversion of aqueous glycerol with 70% selectivity to 1,2-PD.[34,35] 1,3-PD is formed, but with less than 2% selectivity. Lingaiah has reported catalysts of Ru supported on titania for conversion of aqueous glycerol with up to 46% conversion and 63% selectivity for 1,2-PD.[21] These catalysts also result in approximately 20% selectivity to ethylene glycol as a result of C-C bond cleavage.

In order to achieve increased selectivities of 1,3-PD, tungsten trioxide or rhenium and/or organic solvents are typically used. Tomishige has reported the use of rhodium catalysts supported on silica modified with added rhenium to achieve up to 79% conversion of aqueous glycerol with 14% selectivity to 1,3-PD.[22] The catalyst favored 1,2-PD, with 41% selectivity. Chen has a number of reports on Pt catalysts with tungsten trioxide on zirconia and titania with silica.[10,37,23] Optimization of these catalysts have resulted in up to 70% conversion with 45% selectivity to 1,3-PD, 3% selectivity to 1,2-PD, and 32% selectivity for 1-PO. This report is one of the highest ratios of 1,3-PD to 1,2-PD to date. High selectivity for 1,3-PD has also been reported by Tomishige using iridium nanoparticles on silica with rhenium oxides.[24] These catalyst were able to achieve up to 63% conversion with 49% selectivity to 1,3-PD, 10% selectivity to 1,2-PD, and 33% to 1-PO. Reactions with these catalysts are heated to 120 ^{o}C, which is the lowest temperature reported for glycerol deoxygenation.

Despite many recent reports of heterogeneous catalysts, there are relatively few examples of homogeneous catalysts. The earliest report of a homogeneous catalyst was

by Che in 1987.[25] Using a $Rh(CO)_2$(acetylacetonate) complex under syngas pressure, glycerol was converted to 1,3-PD and 1,2-PD in a 1:1 ratio. Braca has reported a ruthenium iodocarbonyl catalyst for the deoxygenation of glycerol to 1-PO with up to 90% selectivity.[26] Schlaf has recently reported ruthenium aqua complexes with co-catalyst triflic acid for the deoxygenation of glycerol to 1-PO with up to 18% yield.[27,28] Under more forcing conditions, these catalysts convert glycerol completely to propene.

In addition to catalyst development, there have been various studies on the stability of glycerol deoxygenation intermediates in order to better understand how selectivity can be better controlled. Thermodynamic calculations for various mechanisms of acid catalyzed dehydration and intermediate stability have been reported by Johnson and co-workers.[29] Their calculations suggest formation of hydroxyacetone, via initial protonation at oxygen at the glycerol C1 position followed by a pinacol rearrangement, is more thermodynamically favorable than formation of 3-hydroxypropanal. This suggests formation of 1,2-PD is thermodynamically favored over 1,3-PD.

An extensive computational study on glycerol dehydration and hydrogenation was also performed by Sautet.[30] Similar to Johnson's calculations, their gas phase calculations suggest that the formation of hydroxyacetone and 1,2-aldol, the precursors to 1,2-PD, are more thermodynamically stable than 3-hydroxypropanal or 1,2-enol, the precursors to 1,3-PD. 1,3-enol and 2,3-enol were the least thermodynamically stable of the six possible intermediates. The stability of the dehydration intermediates changes when glycerol is first adsorbed onto a transition metal surface. Calculations showed that adsorption onto Ni and Rh did not change the relative stability of the intermediates. However, when

glycerol is adsorbed onto Pd, acid catalyzed dehydration to 1,2-enol is the most stable intermediate. These calculations suggest that the selectivity of the reaction to 1,3-PD can potentially be tuned by using an appropriate transition metal.

Schlaf has suggested that for acidic homogeneous systems, acrolein formation from glycerol is favored over 3-hydroxypropanal formation.[43] Schlaf also notes that in the reaction energy profile of glycerol deoxygenation, the initial acid catalyzed dehydration of glycerol has the highest activation barrier. Therefore, under conditions where glycerol can be dehydrated, all subsequent steps for dehydration and hydrogenation can proceed until propene is formed and 1,3-PD should not be formed selectively (propene would not be hydrogenated due to low solubility). In the case of heterogeneous catalysts, surface interactions with glycerol may cause reactions to be under kinetic control rather than thermodynamic control and various deoxygenated products can be formed.

Ahmed-Foskey recently reported the deoxygenation of the glycerol model substrate 1,2-PD to 1-PO using a homogeneous bis(phosphinite) (POCOP) iridium pincer catalyst (Figure 4-1-**1**).[31] Speciation studies showed that under the reaction conditions, the iridium carbonyl complex (Figure 4-1-**2**) was formed by alcohol decarbonylation. The iridium carbonyl complex was then shown to be an effective catalyst for the deoxygenation of 1,2-PD.

Herein, we report an extension of this work for catalytic deoxygenation of glycerol to 1-PO and 1,3-PD using the POCOP iridium carbonyl complex and derivatives

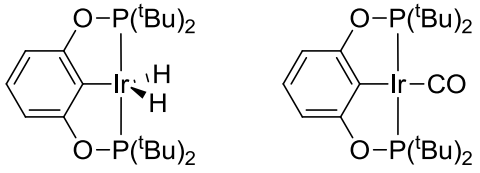

1 **2**

Figure 4-1. Bis(phosphinite) (POCOP) iridium pincer catalysts previously studied for the deoxygenation of 1,2-propanediol.

4.2 Results and Discussion

4.2.1 Increasing Solubility in Polar Reaction Mixtures

Consistent with our previous studies of deoxygenation of 1,2-PD, it was found that dioxane is a suitable solvent for this chemistry. However, in glycerol/water/dioxane mixtures, the unsubstituted POCOP iridium carbonyl complex has limited solubility at room temperature and 200°C. A series of pincer ligands were prepared to increase catalyst solubility in polar reaction mixtures containing glycerol and water. Novel ligands containing diethylene glycol monomethyl ether (Figure 4-2-**1**) and dimethyl amine (Figure 4-2-**2**) were prepared by synthesizing the corresponding 5-substituted resorcinol[32,33] followed by diphosphorylation.[34]

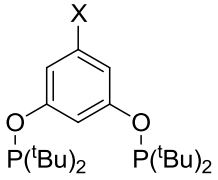

X =
$O(CH_2CH_2O)_2CH_3$ (**1**)
$N(CH_3)_2$ (**2**)

Figure 4-2. Bis(phosphinite) pincer ligands used for iridium catalysts.

Iridium carbonyl catalysts prepared from these ligands showed improved solubility over the unsubstituted POCOP iridium carbonyl complex in reaction mixtures

containing glycerol in aqueous dioxane. Complete catalyst solubility in reaction mixtures at room temperature enabled reliable reaction optimization experiments to be performed. Due to ease of ligand synthesis and improved solubility in acidic polar solutions, the dimethyl amine complex, Figure 4-3, formed from the dimethyl amine substituted ligand shown in Figure 4-2-**2** was used in all catalytic reactions described here.

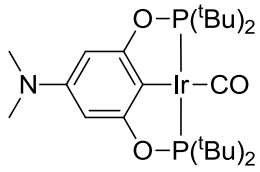

Figure 4-3. (5-Dimethylamine POCOP)Ir(CO) catalyst used for the deoxygenation of glycerol.

4.2.2 Deoxygenation of Glycerol

In a typical experiment, glycerol was converted to 1-PO and 1,3-PD in aqueous dioxane solutions of 0.125 mole% relative to glycerol (5-Dimethylamine POCOP)Ir(CO) and 1 mole% relative to glycerol sulfuric acid at 200^{o}C under 80 bar H_2. Reaction progress was monitored by quantitative and qualitative ^{13}C-NMR spectroscopy of neat reaction solutions (see experimental section for details). Approximately 45% conversion of glycerol to 1-PO and 1,3-PD was observed after 48 hours (Figure 4-4). Bubbling the reaction headspace gas through acetone-d_6 and characterizing by ^{1}H-NMR spectroscopy showed formation of propane and propylene. Possible gaseous byproducts propane and propene were not observed by ^{1}H-NMR spectroscopy. Weighing reaction vessels before and after heating and venting showed good mass balance suggesting that propane and

propylene were formed in trace amounts. No appreciable amounts of 1,2-PD were observed in these reactions.

We propose that 1,2-PD was not observed due to the rapid deoxygenation of 1,2-PD to 1-PO as determined in our previous studies[31] and in control reactions. Control reactions have also shown that under our reaction conditions, 1,3-PD was not deoxygenated to 1-PO. It is reasonable to then suggest that 1-PO is formed via deoxygenation at the glycerol C1 position followed by a subsequent deoxygenation at the C2 position of 1,2-PD. Our previous studies have shown that deoxygenation of 1,2-PD to 1-PO occurs at much lower temperatures (125^{o}C) than the reaction conditions used for the deoxygenation of glycerol. Deoxygenation at the glycerol C2 position leads to formation of 1,3-PD.

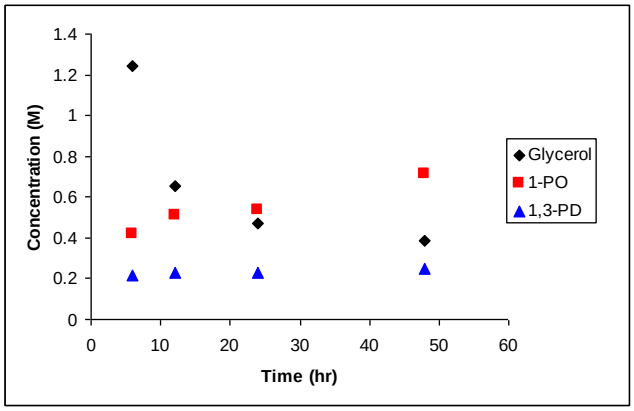

Figure 4-4. Time course of glycerol conversion to 1-propanol and 1,3-propanediol. Reactions with 0.0065 mmol (5-Dimethylamine POCOP)Ir(CO), 5.2 mmol glycerol, and 0.052 mmol H_2SO_4 in deionized water (0.197 g) and dioxane (1.22 g) under 80 bar H_2. Reactions heated to 200^{o}C. Concentrations measured by quantitative ^{13}C-NMR spectroscopy (see experimental section for details).

The selectivity of product formation appears to change over time (Figure 4-4). In the first 6 hours, 1,3-PD and 1-PO are formed in an approximate 1:2 ratio, respectively. Over the course of 48 hours, the 1,3-PD: 1-PO selectivity diminishes to 1:4. As noted previously, this decrease in 1,3-PD selectivity is not due to conversion of 1,3-PD to 1-PO or decomposition of products as shown by overall mass balance. One possible explanation for the change in selectivity may be a change in the catalyst over the course of the reaction. A change in the reaction medium over the course of the reaction may also result in the different selectivity with time.

The effect of reaction temperature on conversion and selectivity was investigated (Figure 4-5). Lowering the reaction temperature from 200 to 180^{o}C for 24 hours resulted in the reduction of glycerol conversion from ca. 35% to 9%. Further lowering the temperature to 170^{o}C resulted in reduction of glycerol conversion of only 4% within 24 hours.

The reaction selectivity is also a function of temperature. Reactions carried out at 180^{o}C show a 1:1 ratio of 1,3-PD to 1-PO. The selectivity increased to a 2:1 ratio of 1,3-PD to 1-PO when the reaction was carried out at 170^{o}C.

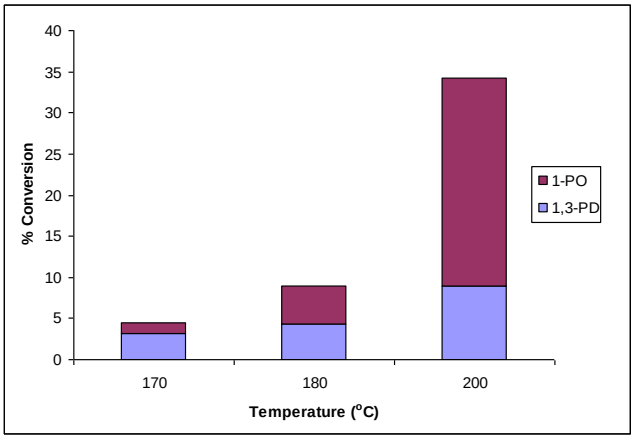

Figure 4-5. Conversion of glycerol to 1-propanol and 1,3-propanediol at different temperatures. Reactions with 0.0065 mmol (5-Dimethylamine POCOP)Ir(CO), 5.2 mmol glycerol, and 0.052 mmol H_2SO_4 in deionized water (0.197 g) and dioxane (1.22 g) under 80 bar H_2. Reactions heated for 24 hours. Concentrations measured by qualitative ^{13}C-NMR spectroscopy (see experimental section for details).

We have previously shown that deoxygenation of 1,2-propanediol at 185°C requires H_2 pressures above 40 bar to achieve high selectivities (90%) to 1-PO.[31] Comparable selectivities and conversions for glycerol deoxygenation at 200°C for 20 hours were observed when H_2 pressures between 40 and 80 bar were used (Figure 4-6). Notably, the use of a syngas-like mixture of 40 bar CO and 40 bar H_2 in our reactions resulted in a decrease of conversion from 24% to 3%, but maintained a 1,3-PD : 1-PO selectivity of *ca*. 1:3. The decrease in conversion in the presence of CO suggests that catalysis is hindered by CO coordination to the catalyst. The proposed reaction mechanism is discussed below.

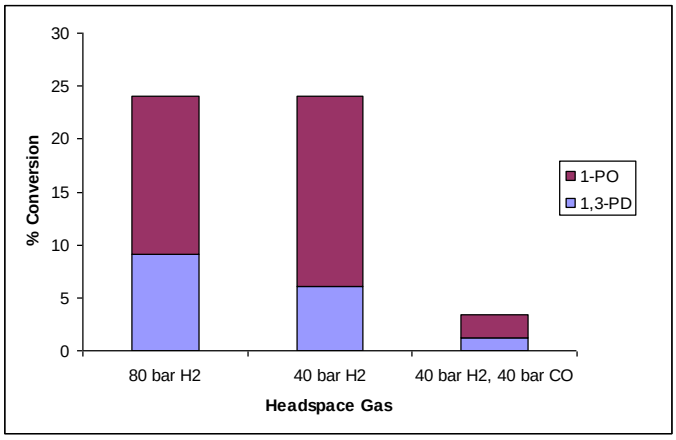

Figure 4-6. Conversion of glycerol to 1-propanol and 1,3-propanediol at different headspace pressures. Reactions with 0.0065 mmol (5-Dimethylamine POCOP)Ir(CO), 5.2 mmol glycerol, and 0.052 mmol H_2SO_4 in deionized water (0.197 g) and dioxane (1.22 g). Reactions heated at 200^{o}C for 20 hours. Concentrations measured by qualitative ^{13}C-NMR spectroscopy (see experimental section for details).

The effect of acid concentration was also studied (Figure 4-7). Acid concentration was varied from 0.25% to 4.0% versus glycerol. Acid concentrations below 4.0% were used to avoid the formation of acid catalyzed side products. An increase in acid concentration results in an increase in glycerol conversion from 8 to 38% over 24 hours at 200^{o}C. The increase in conversion with acid concentration is consistent with an initial acid catalyzed dehydration step. Selectivity for 1,3-PD decreased with increasing acid concentration. Increasing acid concentration from 0.25% to 4.0% led to a decrease in 1,3-PD to 1-PO selectivity from 2:1 to 1:4. Notably, with 0.25% acid, formation of 1,2-PD was also observed as a product. 1,2-PD was not observed with higher acid concentrations.

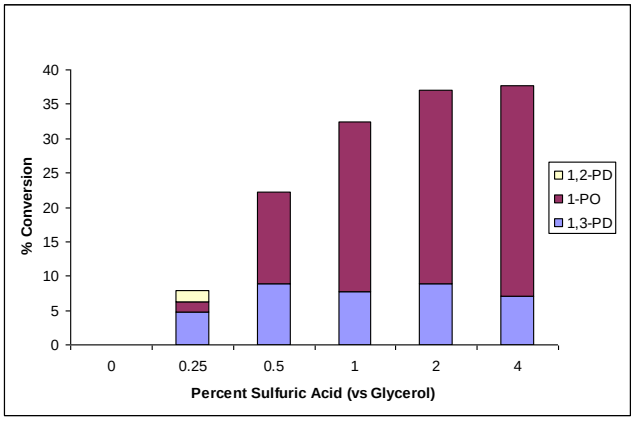

Figure 4-7. Conversion of glycerol to 1-propanol, 1,2-propanediol, and 1,3-propanediol with varying acid equivalents. Reactions with 0.0065 mmol (5-Dimethylamine POCOP)Ir(CO) and 5.2 mmol glycerol in deionized water (0.197 g) and dioxane (1.22 g) under 80 bar H_2. Reactions heated to 200^{o}C for 24 hours. Concentrations measured by qualitative ^{13}C-NMR spectroscopy (see experimental for details).

The dependence of selectivity on acid concentration is not fully understood at this time. A change in the protonation level of the catalyst may account for the increased selectivity for 1-PO at higher acid concentration. Studies are currently underway to determine the role of the catalyst on product selectivity.

In order to test the applicability of our reaction conditions to the development of a practical process, the deoxygenation of waste glycerol from biodiesel production was also studied. Waste stream glycerol contains impurities such as sodium hydroxide and methanol necessary for the transesterification process as well as carboxylates. While distillation is the most common method for purification on an industrial scale, it is an energy intensive process. In lieu of distillation, we have found that waste glycerol can be purified by acidifying with 1 M sulfuric acid, allowing the biphasic mixture to settle, and decanting the impurity layer containing various free acids. The resulting solution of

water, methanol and glycerol can be diluted in dioxane and used directly in deoxygenation reactions. In our initial test reactions, recycled waste glycerol was deoxygenated in 20% yield over 24 hrs, with a 1,3-PD to 1-PO selectivity of 1:9. The high selectivity for 1-PO in these reactions is due to the high acid concentration employed in the purification of crude glycerol.

4.2.3 Mechanistic Studies

In our previous work, we reported that the air and water stable iridium carbonyl precatalyst, (POCOP)Ir(CO), could be used in place of (POCOP)Ir$(H)_2$ for the deoxygenation of 1,2-propanediol.[31] We also discovered that upon the completion of these reactions, both (POCOP)Ir(CO) and *trans*-(POCOP)Ir(CO)$(H)_2$ were present in the reaction mixture. The presence of these two species was confirmed by NMR (^{1}H and ^{31}P) and IR spectroscopy. The proposed mechanism for formation of *trans*-(POCOP)Ir(CO)$(H)_2$ from (POCOP)Ir(CO) is shown in Scheme 4-1. Initial protonation of (POCOP)Ir(CO) forms a cationic monohydride species. Dihydrogen association and deprotonation affords *trans*-(POCOP)Ir(CO)$(H)_2$. It is hypothesized that the iridium dihydride and/or dihydrogen-hydride species are the active catalysts for the deoxygenation of glycerol.

Scheme 4-1. Proposed mechanism for formation of *trans*-(POCOP)Ir(CO)$(H)_2$ from (POCOP)Ir(CO).

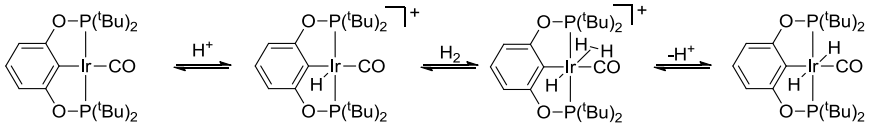

The formation of *trans*-(POCOP)Ir(CO)$(H)_2$ from (POCOP)Ir(CO) has been verified by pressurizing a THF solution of (POCOP)Ir(CO) under H_2 for 24 hours in the presence of 0.5 equivalents of anilinium tetrafluoroborate. In the absence of catalytic acid, the formation of *trans*-(POCOP)Ir(CO)$(H)_2$ is not observed. A linear relationship was observed for H_2 pressure and conversion to *trans*-(POCOP)Ir(CO)$(H)_2$. Under 110 bar of H_2, up to 80% conversion to *trans*-(POCOP)Ir(CO)$(H)_2$ could be achieved, but complete conversion was never observed. These observations are consistent with an equilibrium between *trans*-(POCOP)Ir(CO)$(H)_2$ and (POCOP)Ir(CO), with equilibration facilitated by acid. Upon neutralization of the acid by stirring solutions with K_2CO_3 and filtering, the resulting mixture is stable for weeks at ambient temperature without any change in composition.

Reaction of (POCOP)Ir(CO) with the bis-etherate of tetrakis[3,5-bis(trifluoromethyl)phenyl]boric acid ($[H(OEt_2)_2]B(C_6H_3(CF_3)_2)_4$) affords the cationic Ir(III) complex $[(POCOP)Ir(CO)(H)]^+$, identified by the observation of a triplet resonance in the ^{1}H NMR spectrum at δ -36 (^3J(P-H) = 10.4 Hz). The structure of this cationic complex was determined by X-ray diffraction (Figure 4-8).

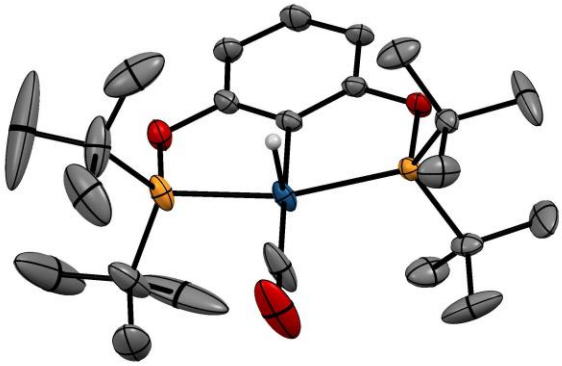

Figure 4-8. ORTEP of $[(POCOP)Ir(CO)(H)]^+$. Counter-anion and non hydride H atoms omitted for clarity. Significant bond distances: Ir-P = 2.3209(14) Å, 2.3196(12)Å; Ir-C_{Ph} = 2.033(5) Å; Ir-C_{CO}= 1.929(6) Å; Ir-H = 1.58(7) Å.

The cationic complex $[(POCOP)Ir(CO)(H)]^+$ is a rare example of a structurally characterized five coordinate Ir(III) complex.[35,36] For comparison, the structure of the neutral Ir(I) complex 2 was also determined. Surprisingly, it is very similar, with Ir-P = 2.2785(3) Å, 2.2800(3) Å; Ir-C_{Ph} = 2.0488(12) Å; Ir-C_{CO}= 1.8658(14)Å. Details of the X-ray data collection are found in the Appendix A.

To confirm the viability of cationic *trans*-$[(POCOP)Ir(CO)(H_2)(H)]^+$ as a potential intermediate, low temperature NMR experiments were performed. At 180 K, a solution containing *trans*-$(POCOP)Ir(CO)(H)_2$ in CD_2Cl_2 was treated with one equivalent of $[H(OEt_2)_2]B(C_6H_3(CF_3)_2)_4$. New broad resonances at δ -18.7, δ -23.3, and δ -23.0 are observed upon mixing. The resonances at δ -23.0 and δ -23.3 integrate to 2:1, respectively, but preliminary relaxation time measurements show these resonances to have T_1's of approximately 350 ms; much higher than expected for a metal dihydrogen complex. Upon warming the solutions to 223 K, hydrogen was evolved and the

resonances at δ -23.0 and δ -23.3 disappear. The resonance at δ -18.7 does not appear to correlate to the species observed at δ -23.0 and δ -23.3 as it is stable up to 273 K. This species may be an iridium hydride with ether coordinated trans to hydrogen. Complete formation of $[(POCOP)Ir(CO)(H)]^+$ was evident by disappearance of the resonances at δ -18.7, δ -23.3, and δ -23.0 and appearance of a resonance at δ -36 in the ^{1}H-NMR spectrum upon warming to 273 K. Further effort is currently underway to confirm the intermediacy of the proposed dihydrogen complex.

4.2.4 Proposed Mechanism

trans-$[(POCOP)Ir(CO)(H_2)(H)]^+$ is hypothesized to be a possible proton and hydride source for the deoxygenation of glycerol. A proposed catalytic cycle for glycerol deoxygenation to 1,3-propanediol via *trans*-$[(POCOP)Ir(CO)(H_2)(H)]^+$ is shown in the top portion of Scheme 4-2. Initial protonation of (POCOP)Ir(CO) to $[(POCOP)Ir(CO)(H)]^+$ followed by reaction with hydrogen generates *trans*-$[(POCOP)Ir(CO)(H_2)(H)]^+$. *trans*-$[(POCOP)Ir(CO)(H_2)(H)]^+$ can act as a proton and hydride source for the deoxygenation of glycerol. An alternative pathway is shown in the bottom of Scheme 4-2. Deprotonation of *trans*-$[(POCOP)Ir(CO)(H_2)(H)]^+$ affords *trans*-$(POCOP)Ir(CO)(H)_2$. An external acid can serve as a proton source and *trans*-$(POCOP)Ir(CO)(H)_2$ can serve as a hydride source for the deoxygenation of glycerol.

Formation of 1-propanol is hypothesized to proceed through an analogous mechanism for deoxygenation at the C1 position, leading to 1,2-PD, which is then rapidly deoxygenated to 1-propanol. The selectivity of the reaction (1,3-PD vs 1-PO product) was found to depend on the acid concentration, the reaction temperature and the reaction

time. Whether this is due to changes in the reaction medium as the reaction progresses or decomposition of the catalyst is not yet clear and is under further investigation.

Scheme 4-2. Proposed mechanism for formation of 1,3-propanediol from glycerol with *trans*-[(POCOP)Ir(CO)(H_2)(H)]$^+$.

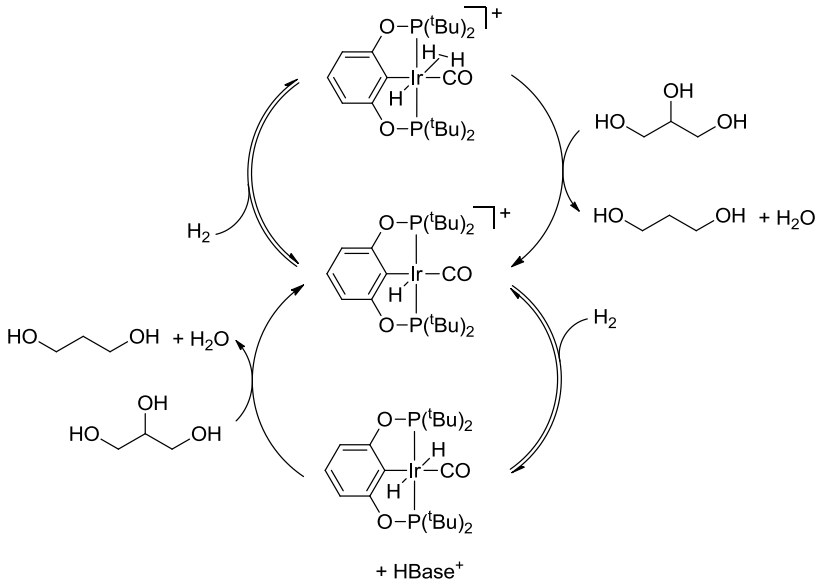

4.3 Conclusion

The catalyzed deoxygenation of glycerol to 1,3-propanediol and 1-propanol has been achieved with sulfuric acid and an iridium pincer complex. Conversions of up to 45% glycerol and selectivities of 1:4 1,3-propanol to 1-propanol have been achieved. The catalytic reactions can also be performed using acidified waste glycerol from biodiesel production. The transient *trans*-[(POCOP)Ir(CO)(H_2)(H)]$^+$ is proposed to be the active catalyst for these reactions.

While this is rare example of a catalytic homogeneous system for the conversion of glycerol to 1,3-propanediol and the compatibility with crude glycerol is encouraging, the modest yields leave room for improvement. The development of a more selective and

active catalyst is necessary. In addition, catalyst stability over extended periods must be increased. The pathways to catalyst decomposition must be fully investigated to enable development of more stable catalysts.

It is still unclear if the catalyst plays a role in the selectivity of these reactions. Studying a series of complexes with varying substituents at the para position on the ring of the POCOP ligand may reveal the role the catalyst plays in selectivity and aid in future catalyst design.

Finally, it would be interesting to study whether these catalysts can be developed into heterogeneous catalysts by anchoring them onto solid supports. Development of a recyclable heterogeneous catalyst may increase the viability of the adopting these systems for industrial processes.

4.4 Experimental

General Procedures. All experiments were performed under an inert atmosphere using standard glovebox or Schlenk techniques. All NMR solvents were dried using appropriate drying agents. All reaction solvents and reagents were used as received.

^{1}H, ^{31}P, and ^{13}C-NMR spectra were obtained using a Bruker 500 MHz spectrometer. IR spectra were obtained using a Bruker Vector 33 FT-IR spectrometer. X-ray crystal structures were collected at -173^{o}C on a Bruker APEX II single crystal X-ray diffractometer, Mo-radiation.

Reaction Quantification by ^{13}C-NMR Spectroscopy. Qualitative studies were performed by collecting ^{13}C-NMR spectra of neat reaction mixtures. Intensity

enhancement due to the nuclear Overhauser effect (nOe) was nullified by integration of carbons with equal number of protons.

Reaction mixtures were quantified by collecting ^{13}C-NMR spectra of neat reaction mixtures. A similar procedure for quantitative analysis of reaction mixtures was recently reported by Gagne.[37] Quantitative spectra were obtained by collecting inverse-gated decoupled NMR spectra to avoid nOe enhancement. To minimize integration problems associated with long relaxation times, delay times of 3 seconds were employed and the paramagnetic additive $Cr(acac)_3$ was used as a relaxation agent.[38] Sodium *p*-toluenesulfonate was used as an internal standard.

Upon heating, approximately 300-400 mg of material comes to rest in the reactor head assembly. Rinsing the reactor head assembly with D_2O and characterizing the solution by ^{1}H-NMR spectroscopy showed that the material composition was primarily dioxane and 1-propanol. The exact concentration of lost 1-propanol was not quantified. Some mass loss was also attributed to decomposition materials and gaseous products. Because the exact amount of lost material was not quantified, reported conversion percentages only account for the material in the reactor vessels.

Ligand and Catalyst Synthesis. (POCOP)Ir(H)(Cl)**[34]**, (POCOP)Ir(CO)[39], $Ir(CO)_2(Cl)$(*p*-toluidine)[40], and $[H(OEt_2)_2]B(C_6H_3(CF_3)_2)_4$[41] were prepared as previously described in the literature.

5-Diethylene glycol monomethyl ether resorcinol. Following a similar procedure as Marzo[32], to a stirring solution of phloroglucinol (0.63 g, 5.0 mmol), potassium fluoride (0.29 g, 5.0 mmol), and potassium carbonate (0.35 g, 2.5 mmol) in 4 mL DMSO under

argon was added 2-bromoethyl 2-methoxyethyl ether (0.92 g, 5.0 mmol) in 2 mL DMSO. The slurry solution was stirred under argon for 48 hours. After 48 hours, 10 mL of deionized water was added to the solution to afford a clear orange solution. The solution was neutralized to pH 7 with 10% HCl and the organics were extracted with chloroform. The organic extractions were combined, dried over $MgSO_4$, and condensed to afford an orange liquid. The crude product was purified by silica column chromatography eluted with 60:40 ethyl acetate:hexane to collect 0.090 g (8% yield) of an off-white solid. ^{1}H NMR (500 MHz, 25°C, DMSO-d_6): δ 9.17 (s, 2H, 2 x OH); δ 5.82 (m, 1 H, 2-H); δ 5.77 (m, 2 H, 4- and 6-H); glycol: δ 3.92 (t, 2 H), δ 3.67 (t, 2 H), δ 3.56 (t, 2 H), δ 3.45 (t, 2 H), δ 3.25 (s, 3 H).

5-Dimethylamine resorcinol. Following a similar procedure as Lusuardi[33], to a stirring solution of phloroglucinol (1.0 g, 7.9 mmol) in 9 mL H_2O and 14 mL DMF was added an aqueous solution of dimethylamine (1.3 mL 40% w:w solution, 10 mmol). The solution was stirred under argon for 48 hours and the solution was condensed to afford a dark red oil. A pink precipitate formed upon addition of ca. 30 mL of chloroform to the dark red oil. The solution was filtered and washed with small portions of cold chloroform to afford 0.59 g (49% yield) of a pink solid. ^{1}H NMR (500 MHz, 25°C, DMSO-d_6): δ 8.81 (s, 2 H, 2 x OH); δ 5.59 (s, 3 H, 2-, 4- and 6-H); δ 2.77 (s, 6 H, NC-H).

The general procedure for POCOP synthesis by Brookhart was followed.[39]

5-Diethylene glycol monomethyl ether POCOP. From 0.090 g (0.39 mmol) 5-diethylene glycol monomethyl ether resorcinol, 0.020 g (0.83 mmol) NaH, and 0.150 g (0.83 mmol) di-*tert*-butylchlorophosphine was obtained 0.20 g (99% yield) of 5-

Diethylene glycol monomethyl ether POCOP as a light yellow oil. ^{1}H NMR (500 MHz, 25°C, C_6D_6): δ 7.22 (m, 1 H, 2-H); δ 6.79 (m, 2 H, 4- and 6-H); glycol: δ 3.82 (t, 2 H), δ 3.50 (t, 2 H), δ 3.44 (t, 2 H), δ 3.32 (t, 2 H), δ 1.13 (s, 3 H); δ 3.82 (d, ^{3}J(P-H): 11.7 Hz, 36 H, PCC-H). ^{31}P{^{1}H} NMR (202 MHz, 25°C, C_6D_6): δ 151.

5-Dimethylamine POCOP. From 0.153 g (1.0 mmol) 5-dimethylamine resorcinol, 0.048 g (2.0 mmol) NaH, and 0.36 g (2.0 mmol) di-*tert*-butylchlorophosphine was obtained 0.44 g (99% yield) of 5-Dimethylamine POCOP as a light orange oil. ^{1}H NMR (500 MHz, 25°C, C_6D_6): δ 7.10 (m, 1 H, 2-H); δ 6.52 (m, 2 H, 4- and 6-H); δ 2.55 (s, 6 H, NC-H); δ 1.18 (d, ^{3}J(P-H): 12 Hz, 36 H, PCC-H). ^{31}P{^{1}H} NMR (202 MHz, 25°C, C_6D_6): δ 149.

General procedure for (5-X-POCOP)Ir(CO) was as follows: a solution of 1 equivalent 5-X-POCOP and 1 equivalent of $Ir(CO)_2(Cl)$(*p*-toluidine) in toluene was heated to reflux under argon for 16 hours. After 16 hours, the solution was condensed and the solid was washed with small portions of cold pentane and methanol.

(5-Diethylene glycol monomethyl ether POCOP)Ir(CO). Due to product solubility in pentane, the condensed residue was purified by neutral alumina column chromatography eluted with 10:90 Et_2O:Hexanes. From 0.192 g (0.37 mmol) 5-Diethylene glycol monomethyl ether POCOP and 0.132 g $Ir(CO)_2(Cl)$(*p*-toluidine) in 8 mL toluene was obtained 0.081 g (30% yield) (5-Diethylene glycol monomethyl ether POCOP)Ir(CO) as a yellow solid. ^{1}H NMR (500 MHz, 25°C, CD_2Cl_2): δ 6.20 (s, 2H, 3- and 5-H); glycol: δ 4.05 (t, 2 H), δ 3.76 (t, 2 H), δ 3.65 (t, 2 H), δ 3.52 (t, 2 H), δ 3.34 (s, 3 H); δ 1.35 (v t, *J*: 7.3 Hz, 36 H, PCC-H). ^{31}P{^{1}H} NMR (202 MHz, 25°C, CD_2Cl_2): δ 200.

(5-Dimethylamine POCOP)Ir(CO). From 0.300 g (0.68 mmol) 5-Dimethylamine POCOP and 0.266 g (0.68 mmol) $Ir(CO)_2(Cl)$(*p*-toluidine) in 10 mL toluene was obtained 0.160 g (35% yield) (5-Dimethylamine POCOP)Ir(CO) as a bright yellow powder. ^{1}H NMR (500 MHz, 25°C, CD_2Cl_2): δ 6.03 (s, 2H, 3- and 5-H); δ 2.90 (s, 6 H, NC-H); δ 1.36 (v t, *J*: 7.0 Hz, 36 H, PCC-H). ^{31}P{^{1}H} NMR (202 MHz, 25°C, CD_2Cl_2): δ 200.

***trans*-(POCOP)Ir(CO)(H)$_2$.** To a stirring solution of 0.31 g (0.50 mmol) (POCOP)Ir(H)(Cl) and 0.056 g (0.50 mmol) potassium tert-butoxide in 6 mL of benzene under argon was added 0.015 g (0.50 mmol) paraformaldehyde. The dark red solution was heated under static argon at 80^{o}C for 3 hours. After cooling, the solution was filtered through Celite and condensed to afford a brown-yellow solid. ^{1}H NMR (500 MHz, 25°C, CD_2Cl_2): δ 6.71 (t, ^3J(H-H): 8 Hz, 1 H, 4-H); δ 6.41 (d, ^3J(H-H): 8 Hz, 2 H, 3- and 5-H); δ 1.39 (v t, *J*: 6.8 Hz, 36 H, PCC-H), δ -9.9 (t, ^2J(P-H):15 Hz, 3 H, Ir-H). ^{31}P{^{1}H} NMR (202 MHz, 25°C, CD_2Cl_2): δ 183.

Glycerol Deoxygenation. Reactions for deoxygenation of glycerol were carried out in Parr reactors. In a typical reaction, 45 mL reactors equipped with Teflon stirbars were charged with ($N(CH_3)_2$POCOP)IrCO (4.3 mg, 0.0065 mmol) and a solution containing glycerol (0.479 g, 5.2 mmol), deionized water (0.197 g), and dioxane (1.22 g). A sulfuric acid solution with pH = 0 was added with a micropipette (52 microliters, 0.052 mmol). Reactors were stirred at 400 rpm, purged with H_2 for 4 minutes, pressurized to 80 bar, and heated to 200^{o}C over 20 minutes (pressure increases to 110 bar). After 24 hours, the reactor was allowed to cool to room temperature and then cooled in an ice water bath for 20 minutes before venting slowly. To analyze gaseous products, the vented gas was

bubbled slowly through acetone-d_6 in a J. Young NMR tube and analyzed by ^{1}H-NMR spectroscopy. To ensure gaseous products were not produced in appreciable amounts, the Parr reactors were weighed prior to pressurization and after venting using a balance scale accurate to *ca.* 50 mg to check mass balance.

Reaction conditions of heating time, gas pressure, acid concentration, and reaction temperature were varied. Time course studies were performed by setting up a series of identical reactions and stopping reactions at different times. For reactions with CO and H_2 mixtures, the reactors were purged with CO for 4 minutes, pressurized to 40 bar of CO followed by 40 bar of H_2 to increase the total pressure to 80 bar. For studies involving varying acid concentration, the mass of deionized water was adjusted to maintain the total water concentration.

Crude Glycerol Purification and Deoxygenation. To a stirring solution of crude glycerol from biodiesel production was added concentrated sulfuric acid until the solution became cloudy (ca. pH = 0). The cloudy solution was left overnight to allow formation of two distinct layers. The clear, colorless bottom layer was collected and filtered to remove any particulates.

The solution of purified glycerol (1.0 g) was diluted with dioxane (5.1 g). Standard deoxygenation procedures were carried out with 2.0 g of this solution and ($N(CH_3)_2$POCOP)IrCO (6.8 mg, 0.010 mmol).

Low Temperature Protonation of *trans*-(POCOP)Ir(CO)$(H)_2$. A J. Young NMR tube was charged with solid $[H(OEt_2)_2]B(C_6H_3(CF_3)_2)_4$ (9.8 mg, 0.0097 mmol) and *trans*-(POCOP)Ir(CO)$(H)_2$ (6.0 mg, 0.0097 mmol). The J. Young NMR tube was evacuated

and CD_2Cl_2 was vacuum distilled into the tube. The solution was kept frozen until immediately before NMR studies at which time, tubes were partially thawed quickly in a dry ice/isopropanol bath, inverted, and immediately injected into an NMR probe cooled to 180 K.

4.5 Notes to Chapter

[1] Schlaf, M. *Dalton Trans.* **2006**, 4625-4653.

[2] Johnson, T. D.; Taconi, K. A. *Environmental Progress* **2007**, *26*, 338-348.

[3] Cheda, J. N.; Huber, G. W.; Dumesic, J. A. *Angew. Chem., Int. Ed.* **2007**, *46*, 7164-7183.

[4] Dam, J. T.; Hanefeld, U. *ChemSusChem* **2011**, *4*, 1017-1034.

[5] Guo, X.; Li, Y.; Shi, R.; Liu, Q.; Zhan, E.; Shen, W. *Appl. Catal. A* **2009**, *371*, 108-113.

[6] Perosa, A.; Tundo, P. *Ind. Eng. Chem. Res.* **2005**, *44*, 8535-8537.

[7] Hosgun, H. L.; Yildiz, M.; Gercel, H. F. *Ind. Eng. Chem. Res.* **2012**, *51*, 3863-3869.

[8] Ruppert, A. M.; Weinberg, K.; Palkovits, R. *Angew. Chem. Int. Ed.* **2012**, *51*, 2564-2601. and references therein.

[9] Daniel, O. M.; DeLaRiva, A.; Kunkes, E. L.; Datye, A. K.; Dumesic, J. A.; Davis, R. J. *ChemCatChem* **2010**, *2*, 1107-1114.

[10] Gong, L.; Lu, Y.; Ding, Y.; Lin, R.; Li, J.; Dong, W.; Wang, T.; Chen, W. *Appl. Cat. A: Gen.* **2010**, *390*, 119–126.

[11] Oh, J.; Dash, S.; Lee, H. *Green Chem.* **2011**, *13*, 2004-2007.

[12] Qin, L.; Song, M.; Chen. C. *Green Chem.* **2010**, *12*, 1466-1472.

[13] Musolino, M. G.; Scarpino, L. A.; Mauriello, F.; Pietropaolo, R.; *Green Chem.* **2009**, *11*, 1511-1513.

[14] Chaminand, J.; Djakovitch, L.; Gallezot, P.; Marion, P.; Pinel, C.; Rosier, C. *Green Chem.* **2004**. *6*, 359-361.

[15] Miyazawa, T.; Koso, S.; Kunimori, K.; Tomishige, K.; *Appl. Cat. A: Gen.* **2007**, *318*, 244-251.

[16] Miyazawa, T.; Koso, S.; Kunimori, K.; Tomishige, K. *Appl. Cat. A: Gen.* **2007**, *329*, 30-35.

[17] Shimao, A.; Koso, S.; Ueda, N.; Shinmi, Y.; Furikado, I. Tomishige, K. *Chem. Lett.* **2009**, *38*, 540-541.

[18] Furiado, I.; Miyazawa, T.; Koso, S.; Shimao, A.; Kunimori, K.; Tomishige, K. *Green Chem.* **2007**, *9*, 582-588.

[19] Montassier, C.; Dumas, J. M.; Granger, P.; Barbier, *J. Appl. Cat. A: Gen.* **1995**, *121*, 231-244.

[20] Huang, L.; Zhu, Y.; Zheng, H.; Ding, G.; Li, Y. *Catal. Lett.* **2009**, *131*, 312-320.

[21] Balaraju, M.; Rekha, V.; Devi, B. L. A. P.; Prasad, R. B. N.; Prasad, P. S. S.; Lingaiah, N. Appl. Cat. A.: Gen. 2010, 384, 107-114.

[22] Shinmi, Y.; Koso, S.; Kubota, T.; Nakagawa, Y.; Tomishige, K. Appl. Cat. B: Enviro. 2010, 94, 318-326.

[23] Gong, L.; Lu, Y.; Ding, Y.; Lin, R.; Li, J.; Dong, W.; Wang, T.; Chen, W. Chin. J. Cat. 2009, 30, 1189-1191.

[24] Nakagawa, Y.; Shinmi, Y.; Koso, S.; Tomishige, K. *J. Catal.* **2010**, *272*, 191-194.

[25] Che, M. US Pat., 4642394, 1987.

[26] Braca, G.; Galletti, A. M. R.; Sbrana, G. *J. Organomet. Chem.* **1991**, *417*, 41-49.

[27] Thibault, M. E.; DiMondo, D. V.; Jennings, M.; Abdelnur, P. V.; Eberlin, M. N.; Schlaf, M. *Green Chem.* **2011**, *13*, 357-366.

[28] Taher, D.; Thibault, M. E.; DiMondo, D.; Jennings, M.; Schlaf, M. *Chem. Eur. J.* **2009**, *15*, 10132-10143.

[29] Nimlos, M. R.; Blanksby, S. J.; Qian, X.; Himmel, M. E.; Johnosn, D. K. *J. Phys. Chem. A.* **2006**, *110*, 6145-6156.

[30] Coll, D.; Delbecq, F.; Aray, Y.; Sautet, P. Phys. *Chem. Chem. Phys.* **2011**, *13*, 1448-1456.

[31] Ahmed-Foskey, T. J.; Heinekey, D. M.; Goldberg, K. I.; *ACS Catal.* **2012**, *2*, 1285-1289.

[32] Brizzi, A.; Brizzi, V.; Cascio, M. G.; Corelli, F.; Guida, F.; Ligresti, A.; Maione, S.; Martinelli, A.; Pasuini, S.; Tuccinardi, T.; Marzo, V. D. *J. Med. Chem.* **2009**, *52*, 2506-25-14.

[33] Petrzilka, T.; Lusuardi, W.G., *Helvetica Chimica Acta* **1973**, *56*, 510-518.

[34] Goettker-Schenetmann, I.; White, P.; Brookhart, M. *J. Am. Chem. Soc.* **2004**, *126*, 1804-1811.

[35] Ghosh, R.; Emge, T. J.; Krogh-Jespersen, K.; Goldman, A. S. *J. Am. Chem. Soc.* **2008**, *130*, 11317-11327.

[36] Bernskoetter, W. H.; Hanson, S. K.; Buzak, S. K.; Davis, Z.; White, P. S.; Swartz, R.; Goldberg, K. I.; Brookhart, M. *J. Am. Chem. Soc.* **2009**, *131*, 8603-8613.

[37] McLaughlin, M.P.; Adduci, L.L.; Becker, J.J.; Gagne, M.R.; *J. Am. Chem. Soc.* 2013, **135**, 1225-1227.

[38] Lamar, G.N.; *Chem. Phys. Lett.* **1971**, *10*, 230-232.

[39] Goettker-Schenetmann, I.; White, P.; Brookhart, M. *Organometallics* **2004**, *23*, 1766-1776.

[40] Roberto, D.; Cariati, E.; Psaro, R.; Ugo, R. *Organometallics* **1994**, *13*, 4227-4231.

[41] Brookhart, M.; Grant, B.; Volpe Jr., A. F. *Organometallics* **1992**, *11*, 3920-3922.

Bibliography

Ahmed-Foskey, T. J.; Heinekey, D. M.; Goldberg, K. I.; *ACS Catal.* **2012**, *2*, 1285-1289.

Albano, V. G.; Natile, G.; Panunzi, A. *Coord. Chem. Rev.* **1994**, *133*, 67-114.

Balaraju, M.; Rekha, V.; Devi, B. L. A. P.; Prasad, R. B. N.; Prasad, P. S. S.; Lingaiah, N. *Appl. Cat. A.: Gen.* **2010**, *384*, 107-114.

Bales, B. C.; Brown, P.; Dehestani, A.; Mayer, J. M. *J. Am. Chem. Soc.* **2005**, *127*, 2832-2833.

Ball, N. D.; Gary, J. B.; Ye, Y.; Sanford, M. S. *J. Am. Chem. Soc.* **2011**, *133*, 7577-7584.

Beckwith, A. L. J.; Bowry, V. W. *J. Am. Chem. Soc.* **1994**, *116*, 2710-2716.

Beckwith, A. L. J.; Moad, G. *J. Chem. Soc., Perkin Trans. 2* **1980**, 1473-1482.

Bergman, R. G. *Nature* **2007**, *446*, 391-393.

Berkowitz, J.; Ellison, G. B.; Gutman, D. *J. Phys. Chem.* **1994**, *98*, 2744-2765.

Bernskoetter, W. H.; Hanson, S. K.; Buzak, S. K.; Davis, Z.; White, P. S.; Swartz, R.; Goldberg, K. I.; Brookhart, M. *J. Am. Chem. Soc.* **2009**, *131*, 8603-8613.

Blanksby, S. J.; Ellison, G. B. *Acc. Chem. Res.* **2003**, *36*, 255-263.

Blasing, T. J.; Hand, K. *Tellus* **2007**, *59*, 15-21.

Braca, G.; Galletti, A. M. R.; Sbrana, G. *J. Organomet. Chem.* **1991**, *417*, 41-49.

Brizzi, A.; Brizzi, V.; Cascio, M. G.; Corelli, F.; Guida, F.; Ligresti, A.; Maione, S.; Martinelli, A.; Pasuini, S.; Tuccinardi, T.; Marzo, V. D. *J. Med. Chem.* **2009**, *52*, 2506-25-14.

Brookhart, M.; Grant, B.; Volpe Jr., A. F. *Organometallics* **1992**, *11*, 3920-3922.

Brown, D. G.; Byers, P. K.; Canty, A. J. *Organometallics* **1990**, *9*, 1231-1235.

Brown, J. M.; Cooley, N. A. *Chem. Rev.* **1988**, *88*, 1031-1046.

Bugarcic, Z.; Novokmet, S.; Kostic, V. J. *Serb. Chem. Soc.* **2005**, *70*, 681-686.

Buist, G. J.; Hipperson, W. C. P.; Lewis, J. D. *J. Chem. Soc. A* **1969**, 307-312.

Burton, G. W.; Ingold, K. U. *Acc. Chem. Res.* **1986**, *19*, 194-201.

Canty, A. J.; Patel, J.; Rodemann, T.; Ryan, J. H.; Skelton, B. W.; White, A. H. *Organometallics* **2004**, *23*, 3466-3473.

Carey, F. A.; Sundberg, R. J. *Advanced Organic Chemistry Part B: Reactions and Synthesis*; Fifth Edition ed.; Springer: Charlottesville, 2007.

Cavallo, L.; Macchioni, A.; Zuccaccia, C.; Zuccaccia, D.; Orabona, I.; Ruffo, F. *Organometallics* **2004**, *23*, 2137-2145.

Chaminand, J.; Djakovitch, L.; Gallezot, P.; Marion, P.; Pinel, C.; Rosier, C. *Green Chem.* **2004**. *6*, 359-361.

Che, M. US Pat., 4642394, 1987.

Cheda, J. N.; Huber, G. W.; Dumesic, J. A. *Angew. Chem., Int. Ed.* **2007**, *46*, 7164-7183.

Chen, G. S.; Labinger, J. A.; Bercaw, J. E. *Organometallics* **2009**, *28*, 4899-5292.

Claridge, T. D. W. *High-Resolution NMR Techniques in Organic Chemistry*; Elsevier: Boston, 1999; Vol. 19.

Clark, H. C.; Manzer, L. E. *J. Am. Chem. Soc.* **1973**, *95*, 3812-3813.

Climate Change 2007: The Physical Science Basis. Contribution of Working Group I to the Fourth Assessment Report of the Intergovernmental Panel on Climate Change; Solomon, S., D. Qin, M. Manning, Z. Chen, M. Marquis, K.B. Averyt, M.Tignor, H.L. Miller, Ed.; Cambridge University Press: New York, 2007.

Coll, D.; Delbecq, F.; Aray, Y.; Sautet, P. *Phys. Chem. Chem. Phys.* **2011**, *13*, 1448-1456.

Conley, B. L.; Tenn III, W. J.; Young, K. J. H.; Ganesh, S. K.; Meier, S. K.; Ziatdinov, V. R.; Mironov, O.; Oxgaard, J.; Gonzales, J.; Goddard III, W. A.; Periana, R. A. *J. Mol. Catal. A: Chem.* **2006**, 251, 8-23.

Crabtree, R. H. *Chem. Rev.* **1995**, *95*, 987-1007.

Crouthamel, C. E.; Hayes, A. M.; Martin, D. S. *J. Am. Chem. Soc.* **1951**, *73*, 82-87.

Cucciolito, M. E.; De Felice, V.; Panunzi, A.; Vitagliano, A. *Organometallics* **1989**, *8*, 1180-1187.

Dam, J. T.; Hanefeld, U. *ChemSusChem* **2011**, *4*, 1017-1034.

Daniel, O. M.; DeLaRiva, A.; Kunkes, E. L.; Datye, A. K.; Dumesic, J. A.; Davis, R. J. *ChemCatChem* **2010**, *2*, 1107-1114.

Davies, A. G.; Muggleton, B.; Godet, J.-Y.; Pereyre, M.; Pommier, J.-C. *J. Chem. Soc., Perkin Trans. 2* **1976**, 1719-1724.

Dehestani, A.; Lam, W. H.; Hrovat, D. A.; Davidson, E. R.; Borden, W. T.; Mayer, J. M. *J. Am. Chem. Soc.* **2005**, *127*, 3423-3432.

Dewkar, G. K.; Narina, S. V.; Sudalai, A. *Org. Lett.* **2003**, *5*, 4501-4504.

DuBois, M. R.; DuBois, D. L. *Chem. Soc. Rev.* **2009**, *38*, 62-72.

Elvidge, C.; Ziskin, D.; Baugh, K.; Tuttle, B.; Ghosh, T.; Pack, D.; Erwin, E.; Zhizhin, M. *Energies* **2009**, *2*, 595-622.

Fekl, U.; Goldberg, K. I. *J. Am. Chem. Soc.* **2002**, *124*, 6804-6805.

Fraze, K.; Wilson, A. D.; Appel, A. M.; DuBois, M. R.; DuBois, D. L. *Organometallics* **2007**, *26*, 3918-3924.

Furiado, I.; Miyazawa, T.; Koso, S.; Shimao, A.; Kunimori, K.; Tomishige, K. *Green Chem.* **2007**, *9*, 582-588.

Gesser, H. D.; Hunter, N. R. *Catalysis Today* **1998**, *42*, 183-189.

Ghosh, R.; Emge, T. J.; Krogh-Jespersen, K.; Goldman, A. S. *J. Am. Chem. Soc.* **2008**, *130*, 11317-11327.

Goddard, W. A. *J. Am. Chem. Soc.* **1984**, *106*, 8321-8322.

Goettker-Schenetmann, I.; White, P.; Brookhart, M. *J. Am. Chem. Soc.* **2004**, *126*, 1804-1811.

Goettker-Schenetmann, I.; White, P.; Brookhart, M. *Organometallics* **2004**, *23*, 1766-1776.

Gol'dshleger, N. F.; Es'kova, V. V.; Shilov, A. E.; Shteinman, A. A. *Zh. Fiz. Khim.* **1972**, *46*, 1353.

Gong, L.; Lu, Y.; Ding, Y.; Lin, R.; Li, J.; Dong, W.; Wang, T.; Chen, W. *Appl. Cat. A: Gen.* **2010**, *390*, 119–126.

Gong, L.; Lu, Y.; Ding, Y.; Lin, R.; Li, J.; Dong, W.; Wang, T.; Chen, W. *Chin. J. Cat.* **2009**, *30*, 1189-1191.

Griller, D.; Ingold, K. U. *Acc. Chem. Res.* **1980**, *13*, 317-323.

Guo, X.; Li, Y.; Shi, R.; Liu, Q.; Zhan, E.; Shen, W. Appl. Catal. A 2009, 371, 108-113.
Harkins, S. B.; Peters, J. C. *Organometallics* **2002**, *21*, 1753-1755.

Hartwig, J. *Organotransition Metal Chemistry From Bonding to Catalysis*; University Science Books: Sausalito, CA, 2010.

Heiberg, H.; Johansson, L.; Gropen, O.; Ryan, O. B.; Swang, O.; Tilset, M. *J. Am. Chem. Soc.* **2000**, *122*, 10831-10845.

Hill, A. E. *J. Am. Chem. Soc.* **1928**, *50*, 2678-2692.

Hill, G. S.; Puddephatt, R. J. *Organometallics* **1997**, *16*, 4522-4524.

Hill, G. S.; Rendina, L. M.; Puddephatt, R. J. *Organometallics* **1995**, *14*, 4966-4968.

Hill, G. S.; Yap, G. P. A.; Puddephatt, R. J. *Organometallics* **1999**, *18*, 1408-1418.

Holtcamp, M. W.; Labinger, J. A.; Bercaw, J. E. *J. Am. Chem. Soc.* **1997**, *119*, 848-849.

Hosgun, H. L.; Yildiz, M.; Gercel, H. F. *Ind. Eng. Chem. Res.* **2012**, *51*, 3863-3869.

Huang, L.; Zhu, Y.; Zheng, H.; Ding, G.; Li, Y. *Catal. Lett.* **2009**, *131*, 312-320.

Ito, T.; Lunsford, J. H. *Nature* **1985**, *314*, 721-722.

Itzel, H.; Fischer, H. *Tetrahedron Lett.* **1975**, *16*, 563-564.

IUPAC Solubility Data Series: Methane; Clever, H. L.; Young, C. L., Eds.; Pergamon Press: New York, **1987**; Vol. 27/28.

IUPAC Solubility Data Series: Oxygen and Ozone; Battino, R., Ed.; Pergamon Press: New York, **1987**; Vol. 7.

Jin, Y.; Lipscomb, J. D. *Biochimica et Biophysica Acta (BBA) - Protein Structure and Molecular Enzymology* **2000**, 1543, 47-59.

Johansson, L.; Ryan, O. B.; Tilset, M. *J. Am. Chem. Soc.* **1999**, *121*, 1974-1975.

Johansson, L.; Tilset, M. *J. Am. Chem. Soc.* **2001**, *123*, 739-740.

Johansson, L.; Tilset, M.; Labinger, J. A.; Bercaw, J. E. *J. Am. Chem. Soc.* **2000**, *122*, 10846-10855.

Johnson, T. D.; Taconi, K. A. *Environmental Progress* **2007**, *26*, 338-348.

Keller, G. E.; Bhasin, M. M. *J. Catal.* **1982**, *73*, 9-19.

Klaning, U. K.; Sehested, K. *J. Chem. Soc., Faraday Trans.* **1978**, *74*, 2818-2838.

Kraus, G. A. *Clean Soil Air Water* **2008**, *36*, 648-651.

Labinger, J. A.; Bercaw, J. E. *Nature* **2002**, *417*, 507-514.

Labinger, J. A.; Bercaw, J. E.; Tilset, M. *Organometallics* **2006**, *25*, 805-808.

Lamar, G.N.; *Chem. Phys. Lett.* **1971**, *10*, 230-232.

Lanci, M. P.; Remy, M. S.; Kaminsky, W.; Mayer, J. M.; Sanford, M. S. *J. Am. Chem. Soc.* **2009**, *131*, 15618-15620.

Lanci, M. P.; Remy, M. S.; Lao, D. B.; Sanford, M. S.; Mayer, J. M. *Organometallics* **2011**, *30*, 3704-3707.

Lao, D. B.; Lanci, M. P.; Spettel, K. E.; Mayer, J. M. Manuscript in preparation.

Lee, C.; Yoon, J. *J. Photochem. Photobiol. A* **2004**, *165*, 35-41.

Lei, M.; Hu, R.-J.; Wang, Y.-G. *Tetrahedron* **2006**, *62*, 8928-8932.

Lersch, M.; Tilset, M. *Chem Rev.* **2005**, *105*, 2471-2526.

Lotz, M.; Sanford, M. S. Manuscript in preparation.

Maillard, B.; Ingold, K. U.; Scaiano, J. C. *J. Am. Chem. Soc.* **1983**, *105*, 5095-5099.

Martinez, F. N.; Schlegel, H. B.; Newcomb, M. *J. Org. Chem.* **1998**, *63*, 3618-3623.

Mathew, L.; Warkentin, J. *J. Am. Chem. Soc.* **1986**, *108*, 7981-7984.

McLaughlin, M.P.; Adduci, L.L.; Becker, J.J.; Gagne, M.R.; *J. Am. Chem. Soc.* **2013**, *135*, 1225-1227.

Miedaner, A.; Raebiger, J. W.; Curtis, C. J.; Miller, S. M.; DuBois, D. L. *Organometallics* **2004**, *23*, 2670-2679.

Miyazawa, T.; Koso, S.; Kunimori, K.; Tomishige, K. *Appl. Cat. A: Gen.* **2007**, *329*, 30-35.

Miyazawa, T.; Koso, S.; Kunimori, K.; Tomishige, K. *Appl. Cat. A: Gen.* **2007**, *318*, 244-251.

Moghadam, M.; Tangestaninejad, S.; Mirkhani, V.; Karami, B.; Rashidi, N.; Ahmadi, H. *J. Iran. Chem. Soc.* **2006**, *3*, 64-68.

Montassier, C.; Dumas, J. M.; Granger, P.; Barbier, *J. Appl. Cat. A: Gen.* **1995**, *121*, 231-244.

Moravskiy, A.; Stille, J. K. *J. Am. Chem. Soc.* **1981**, *103*, 4182-4186.

Moret, M.; Chen, P. *J. Am. Chem. Soc.* **2009**, *131*, 5675-5690.

Musolino, M. G.; Scarpino, L. A.; Mauriello, F.; Pietropaolo, R.; *Green Chem.* **2009**, *11*, 1511-1513.

Nakagawa, Y.; Shinmi, Y.; Koso, S.; Tomishige, K. *J. Catal.* **2010**, *272*, 191-194.

Nakamoto, K. *Infared and Raman Spectra of Inorganic and Coordination Compounds*; 3rd ed.; Wiley-Interscience: New York, 1978.

Nandibewoor, S. T.; Hiremath, G. A. *J. Indian Chem. Soc.* **1999**, *76*, 250-252.

National Biodiesel Board Annual Estimates. Biodiesel.org (accessed Apr. 4, 2013).

Newcomb, M. *Tetrahedron* **1993**, *49*, 1151-1176.

Newcomb, M.; Horner, J. H.; Emanuel, C. J. *J. Am. Chem. Soc.* **1997**, *119*, 7147-7148.

Nimlos, M. R.; Blanksby, S. J.; Qian, X.; Himmel, M. E.; Johnosn, D. K. *J. Phys. Chem. A.* **2006**, *110*, 6145-6156.

Norris, C. M.; Templeton, J. L. *Organometallics* **2004**, *23*, 3101-3104.

Oh, J.; Dash, S.; Lee, H. *Green Chem.* **2011**, *13*, 2004-2007.

Osako, T.; Hayoun, R.; Mayer, J. M. 2007. Unpublished results.

Osako, T.; Watson, E. J.; Dehestani, A.; Bales, B. C.; Mayer, J. M. *Angew. Chem. Int. Ed.* **2006**, *45*, 7433-7436.

Panigrahi, G. P.; Misro, P. K. *Indian J. Chem., Sect. A: Inorg., Bio-inorg., Phys., Theor. Anal. Chem.* **1977**, *15*, 1066-1069.

Panigrahi, G. P.; Misro, P. K. *Indian J. Chem., Sect. A: Inorg., Bio-inorg., Phys., Theor. Anal. Chem.* **1978**, 16, 762-766.

Periana, R. A.; Taube, D. J.; Gamble, S.; Taube, H.; Satoh, T.; Fujii, H. *Science* **1998**, *280*, 56-7.

Perosa, A.; Tundo, P. *Ind. Eng. Chem. Res.* **2005**, *44*, 8535-8537.

Perrin, D. D.; Dempsey, B. *Buffers for pH and Metal Ion Control*; Halsted Press: New York, 1974.

Petrzilka, T.; Lusuardi, W.G., *Helvetica Chimica Acta* **1973**, *56*, 510-518.

Price, C. C.; Knell, M. *J. Am. Chem. Soc.* **1942**, *64*, 552-554.

Qin, L.; Song, M.; Chen. C. *Green Chem.* **2010**, *12*, 1466-1472.

Racowski, J. M.; Ball, N. D.; Sanford, M. S. *J. Am. Chem. Soc.* **2011**, *133*, 18022-18025.

Raebiger, J. W.; Miedaner, A.; Curtis, C. J.; Miller, S. M.; Anderson, O. P.; DuBois, D. L. *J. Am. Chem. Soc.* **2004**, *126*, 5502-5514.

Remy, M. S.; Cundari, T. R.; Sanford, M. S. *Organometallics* **2010**, *29*, 1522-1525.

Roberto, D.; Cariati, E.; Psaro, R.; Ugo, R. *Organometallics* **1994**, *13*, 4227-4231.

Ruppert, A. M.; Weinberg, K.; Palkovits, R. *Angew. Chem. Int. Ed.* **2012**, *51*, 2564-2601.

Sawyer, D. T. *Oxygen Chemistry*; Oxford University Press: New York, 1991.

Schlaf, M. *Dalton Trans.* **2006**, 4625-4653.

Shimao, A.; Koso, S.; Ueda, N.; Shinmi, Y.; Furikado, I. Tomishige, K. *Chem. Lett.* **2009**, *38*, 540-541.

Shinmi, Y.; Koso, S.; Kubota, T.; Nakagawa, Y.; Tomishige, K. *Appl. Cat. B: Enviro.* **2010**, *94*, 318-326.

Srivastava, S.; Srivastava, S.; Singh, S.; Parul *Int. J. Pure Appl. Chem.* **2008**, *3*, 17-20.

Stewart, R. *Oxidation Mechanisms: Applications to Organic Chemistry*; W. A. Benjamin, Inc.: New York, 1964.

Taher, D.; Thibault, M. E.; DiMondo, D.; Jennings, M.; Schlaf, M. *Chem. Eur. J.* **2009**, *15*, 10132-10143.

Tang, X.; Weavers, L. K. *J. Photochem. Photobiol., A* **2008**, *194*, 212-219.

Tanko, J. M.; Drumright, R. E.; Suleman, N. K.; Brammer, L. E. *J. Am. Chem. Soc.* **1994**, *116*, 1785-1791.

Terheijden, J.; van Koten, G.; Mul, W. P.; Stufkens, D. J.; Muller, F.; Stam, C. H. *Organometallics* **1986**, *5*, 519-525.

Thibault, M. E.; DiMondo, D. V.; Jennings, M.; Abdelnur, P. V.; Eberlin, M. N.; Schlaf, M. *Green Chem.* **2011**, *13*, 357-366.

U.S. Energy Information Administration, Department of Energy, Annual Energy Review. http://www.eia.doe.gov/totalenergy/data/annual/#resources (accessed Feb. 4, 2010).

Vedernikov, A. N.; Fettinger, J. C.; Mohr, F. *J. Am. Chem. Soc.* **2004**, *126*, 11160-11161.

Walborsky, H. M.; Plonsker, L. *J. Am. Chem. Soc.* **1961**, *83*, 2138-2144.

Wang, K.; Mayer, J. M. *J. Org. Chem.* **1997**, *62*, 4248-4252.

Warren, J. J.; Tronic, T. A.; Mayer, J. M. *Chem. Rev.* **2010**, *110*, 6961-7001.

Weizman, H. *J. Chem. Educ.* **2008**, *85*, 294.

Wick, D. D.; Goldberg, K. I. *J. Am. Chem. Soc.* **1997**, 119, 10235-10236.

Wiedner, E. S.; Yang, J. Y.; Dougherty, W. G.; Kassel, W. S.; Bullock, R. M.; DuBois, M. R.; DuBois, D. L. *Organometallics* **2010**, *29*, 5390-5401.

Wik, B. J.; Lersch, M.; Tilset, M. *J. Am. Chem. Soc.* **2002**, *124*, 12116-12117.

Wilson, A. D.; Shoemaker, R. K.; Miedaner, A.; Mukerman, J. T.; DuBois, D. L.; DuBois, M. R. *Proc. Nat. Acad. Sci.* **2007**, *104*, 6951-6956.

Appendix A: X-Ray Crystal Data for Chapter 3

X-ray Structure Analyses, Sample Preparation and Data Acquisition for (6-methyl-N,N-di-2-pyridinyl-2-pyridinamine)Pt(CH_3)$_2$:
A colorless plate, measuring 0.25 x 0.20 x 0.10 mm^3 was mounted on a glass capillary with oil. Data was collected at -173^{o}C on a Bruker APEX II single crystal X-ray diffractometer, Mo-radiation.

Crystal-to-detector distance was 40 mm and exposure time was 10 seconds per degree for all sets. The scan width was 0.5^o. Data collection was 99.9% complete to 25^o in ϑ. A total of 115725 (merged) reflections were collected covering the indices, h = -18 to 18, k = -17 to 17, l = -27 to 27. 8497 reflections were symmetry independent and the R_{int} = 0.0390 indicated that the data was good (average quality 0.07). Indexing and unit cell refinement indicated a monoclinic P lattice. The space group was found to be P 2_1/n (No.14).

X-ray Structure Analyses, Structure Determination and Data Refinement.
The data was integrated and scaled using SAINT, SADABS within the APEX2 software package by Bruker.[1]

Solution by direct methods (SHELXS, SIR97[2]) produced a complete heavy atom phasing model consistent with the proposed structure. The structure was completed by difference Fourier synthesis with SHELXL97.[3,4] Scattering factors are from Waasmair and Kirfel[5]. Hydrogen atoms were placed in geometrically idealized positions and constrained to ride on their parent atoms with C---H distances in the range 0.95-1.00 Angstrom. Isotropic thermal parameters U_{eq} were fixed such that they were 1.2U_{eq} of their parent atom U_{eq} for CH's and 1.5U_{eq} of their parent atom U_{eq} in case of methyl groups. All non-hydrogen atoms were refined anisotropically by full-matrix least-squares.

Table A-1. Crystallographic data for **(**6-methyl-N,N-di-2-pyridinyl-2-pyridinamine)Pt(CH_3)$_2$.

	(6-methyl-N,N-di-2-pyridinyl-2-pyridinamine)Pt(CH_3)$_2$
Empirical formula	$C_{18}H_{20}N_4Pt$
Formula weight	487.47
Temperature, K	100(2)
Wavelength, Å	0.71073
Crystal system	Monoclinic
Space group	P 21/n

a, Å	13.5583(8)
b, Å	12.9866(7)
c, Å	20.3367(14)
α, (º)	90°.
β, (º)	109.399(3)°.
γ, (º)	90°.
Volume, $Å^3$	3377.5(4)
Z	8
Density (calcd), mg/m^3	1.917
Absorption coefficient, mm^{-1}	8.313
F(000)	1872
Crystal size, mm^3	0.25 x 0.20 x 0.10
Theta range for data collection, (º)	1.59 to 28.47°.
Reflections collected	115725
Independent reflections	8497 [R(int) = 0.0390]
Completeness to theta = 25.00°	99. %
Max. and min. transmission	0.4903 and 0.2304
Refinement method	Full-matrix least-squares on F^2
Data / restraints / parameters	8497 / 0 / 421
Goodness-of-fit on F^2	1.049
Final R indices [I>2sigma(I)]	R1 = 0.0199, wR2 = 0.0436
R indices (all data)	R1 = 0.0235, wR2 = 0.0452

Table A-2. Bond lengths for (6-methyl-N,N-di-2-pyridinyl-2-pyridinamine)Pt$(CH_3)_2$.

Bond	Bond Distance (Å)
Pt(1)-C(17)	2.029(3)
Pt(1)-C(18)	2.044(3)
Pt(1)-N(1)	2.104(2)
Pt(1)-N(2)	2.104(2)
Pt(2)-C(36)	2.027(3)
Pt(2)-C(35)	2.034(3)
Pt(2)-N(6)	2.104(2)
Pt(2)-N(5)	2.109(2)
N(2)-C(6)	1.341(4)
N(2)-C(10)	1.347(3)
N(3)-C(11)	1.402(3)
N(3)-C(6)	1.418(4)
N(3)-C(5)	1.422(4)
N(1)-C(1)	1.340(4)
N(1)-C(5)	1.342(4)

N(4)-C(11)	1.329(4)
N(4)-C(15)	1.345(4)
N(5)-C(23)	1.330(4)
N(5)-C(19)	1.351(4)
N(7)-C(29)	1.402(4)
N(7)-C(24)	1.418(4)
N(7)-C(23)	1.426(4)
N(8)-C(29)	1.328(4)
N(8)-C(33)	1.343(4)
N(6)-C(24)	1.344(4)
N(6)-C(28)	1.347(4)
C(6)-C(7)	1.390(4)
C(5)-C(4)	1.382(4)
C(1)-C(2)	1.376(4)
C(1)-H(1)	0.95
C(2)-C(3)	1.380(5)
C(2)-H(2)	0.95
C(3)-C(4)	1.380(4)
C(3)-H(3)	0.95
C(4)-H(4)	0.95
C(11)-C(12)	1.398(4)
C(15)-C(14)	1.384(5)
C(15)-C(16)	1.502(5)
C(16)-H(16A)	0.98
C(16)-H(16B)	0.98
C(16)-H(16C)	0.98
C(14)-C(13)	1.388(5)
C(14)-H(14)	0.95
C(13)-C(12)	1.379(4)
C(13)-H(13)	0.95
C(12)-H(12)	0.95
C(7)-C(8)	1.378(4)
C(7)-H(7)	0.95
C(8)-C(9)	1.391(4)
C(8)-H(8)	0.95
C(9)-C(10)	1.376(4)
C(9)-H(9)	0.95
C(10)-H(10)	0.95
C(18)-H(18A)	0.98
C(18)-H(18B)	0.98
C(18)-H(18C)	0.98
C(17)-H(17A)	0.98
C(17)-H(17B)	0.98
C(17)-H(17C)	0.98
C(19)-C(20)	1.380(4)
C(19)-H(19)	0.95

C(20)-C(21)	1.384(4)
C(20)-H(20)	0.95
C(21)-C(22)	1.379(4)
C(21)-H(21)	0.95
C(22)-C(23)	1.392(4)
C(22)-H(22)	0.95
C(29)-C(30)	1.409(4)
C(33)-C(32)	1.384(5)
C(33)-C(34)	1.498(5)
C(32)-C(31)	1.380(5)
C(32)-H(32)	0.95
C(31)-C(30)	1.369(5)
C(31)-H(31)	0.95
C(30)-H(30)	0.95
C(34)-H(34A)	0.98
C(34)-H(34B)	0.98
C(34)-H(34C)	0.98
C(24)-C(25)	1.385(4)
C(25)-C(26)	1.378(4)
C(25)-H(25)	0.95
C(26)-C(27)	1.379(4)
C(26)-H(26)	0.95
C(27)-C(28)	1.376(4)
C(27)-H(27)	0.95
C(28)-H(28)	0.95
C(36)-H(36A)	0.98
C(36)-H(36B)	0.98
C(36)-H(36C)	0.98
C(35)-H(35A)	0.98
C(35)-H(35B)	0.98
C(35)-H(35C)	0.98

Table A-3. Bond angles for (6-methyl-N,N-di-2-pyridinyl-2-pyridinamine)Pt(CH_3)$_2$.

Bond	Bond Angle [°]
C(17)-Pt(1)-C(18)	89.47(12)
C(17)-Pt(1)-N(1)	91.95(11)
C(18)-Pt(1)-N(1)	177.85(10)
C(17)-Pt(1)-N(2)	176.64(11)
C(18)-Pt(1)-N(2)	93.50(10)
N(1)-Pt(1)-N(2)	85.04(9)
C(36)-Pt(2)-C(35)	86.96(12)
C(36)-Pt(2)-N(6)	94.97(11)
C(35)-Pt(2)-N(6)	177.45(11)

C(36)-Pt(2)-N(5)	178.46(11)
C(35)-Pt(2)-N(5)	94.07(11)
N(6)-Pt(2)-N(5)	84.03(9)
C(6)-N(2)-C(10)	117.9(2)
C(6)-N(2)-Pt(1)	119.88(18)
C(10)-N(2)-Pt(1)	121.86(19)
C(11)-N(3)-C(6)	122.2(2)
C(11)-N(3)-C(5)	122.3(2)
C(6)-N(3)-C(5)	114.8(2)
C(1)-N(1)-C(5)	117.7(3)
C(1)-N(1)-Pt(1)	122.6(2)
C(5)-N(1)-Pt(1)	119.12(19)
C(11)-N(4)-C(15)	118.2(3)
C(23)-N(5)-C(19)	118.5(2)
C(23)-N(5)-Pt(2)	119.56(19)
C(19)-N(5)-Pt(2)	121.89(19)
C(29)-N(7)-C(24)	123.8(2)
C(29)-N(7)-C(23)	120.2(2)
C(24)-N(7)-C(23)	115.8(2)
C(29)-N(8)-C(33)	118.7(3)
C(24)-N(6)-C(28)	117.7(2)
C(24)-N(6)-Pt(2)	120.12(19)
C(28)-N(6)-Pt(2)	121.78(19)
N(2)-C(6)-C(7)	122.9(3)
N(2)-C(6)-N(3)	115.4(2)
C(7)-C(6)-N(3)	121.6(3)
N(1)-C(5)-C(4)	122.9(3)
N(1)-C(5)-N(3)	116.2(2)
C(4)-C(5)-N(3)	120.8(3)
N(1)-C(1)-C(2)	122.8(3)
N(1)-C(1)-H(1)	118.6
C(2)-C(1)-H(1)	118.6
C(1)-C(2)-C(3)	119.0(3)
C(1)-C(2)-H(2)	120.5
C(3)-C(2)-H(2)	120.5
C(4)-C(3)-C(2)	119.0(3)
C(4)-C(3)-H(3)	120.5
C(2)-C(3)-H(3)	120.5
C(3)-C(4)-C(5)	118.5(3)
C(3)-C(4)-H(4)	120.7
C(5)-C(4)-H(4)	120.7
N(4)-C(11)-C(12)	123.7(3)
N(4)-C(11)-N(3)	115.3(2)
C(12)-C(11)-N(3)	120.9(3)
N(4)-C(15)-C(14)	122.3(3)
N(4)-C(15)-C(16)	116.3(3)

C(14)-C(15)-C(16)	121.4(3)
C(15)-C(16)-H(16A)	109.5
C(15)-C(16)-H(16B)	109.5
H(16A)-C(16)-H(16B)	109.5
C(15)-C(16)-H(16C)	109.5
H(16A)-C(16)-H(16C)	109.5
H(16B)-C(16)-H(16C)	109.5
C(15)-C(14)-C(13)	118.4(3)
C(15)-C(14)-H(14)	120.8
C(13)-C(14)-H(14)	120.8
C(12)-C(13)-C(14)	120.3(3)
C(12)-C(13)-H(13)	119.9
C(14)-C(13)-H(13)	119.9
C(13)-C(12)-C(11)	117.0(3)
C(13)-C(12)-H(12)	121.5
C(11)-C(12)-H(12)	121.5
C(8)-C(7)-C(6)	118.5(3)
C(8)-C(7)-H(7)	120.7
C(6)-C(7)-H(7)	120.7
C(7)-C(8)-C(9)	119.0(3)
C(7)-C(8)-H(8)	120.5
C(9)-C(8)-H(8)	120.5
C(10)-C(9)-C(8)	118.9(3)
C(10)-C(9)-H(9)	120.5
C(8)-C(9)-H(9)	120.5
N(2)-C(10)-C(9)	122.7(3)
N(2)-C(10)-H(10)	118.7
C(9)-C(10)-H(10)	118.7
Pt(1)-C(18)-H(18A)	109.5
Pt(1)-C(18)-H(18B)	109.5
H(18A)-C(18)-H(18B)	109.5
Pt(1)-C(18)-H(18C)	109.5
H(18A)-C(18)-H(18C)	109.5
H(18B)-C(18)-H(18C)	109.5
Pt(1)-C(17)-H(17A)	109.5
Pt(1)-C(17)-H(17B)	109.5
H(17A)-C(17)-H(17B)	109.5
Pt(1)-C(17)-H(17C)	109.5
H(17A)-C(17)-H(17C)	109.5
H(17B)-C(17)-H(17C)	109.5
N(5)-C(19)-C(20)	122.1(3)
N(5)-C(19)-H(19)	119
C(20)-C(19)-H(19)	119
C(19)-C(20)-C(21)	119.0(3)
C(19)-C(20)-H(20)	120.5
C(21)-C(20)-H(20)	120.5

C(22)-C(21)-C(20)	119.2(3)
C(22)-C(21)-H(21)	120.4
C(20)-C(21)-H(21)	120.4
C(21)-C(22)-C(23)	118.5(3)
C(21)-C(22)-H(22)	120.7
C(23)-C(22)-H(22)	120.7
N(5)-C(23)-C(22)	122.7(3)
N(5)-C(23)-N(7)	116.9(2)
C(22)-C(23)-N(7)	120.2(3)
N(8)-C(29)-N(7)	114.7(3)
N(8)-C(29)-C(30)	123.0(3)
N(7)-C(29)-C(30)	122.3(3)
N(8)-C(33)-C(32)	121.7(3)
N(8)-C(33)-C(34)	116.2(3)
C(32)-C(33)-C(34)	122.0(3)
C(31)-C(32)-C(33)	119.1(3)
C(31)-C(32)-H(32)	120.4
C(33)-C(32)-H(32)	120.4
C(30)-C(31)-C(32)	120.0(3)
C(30)-C(31)-H(31)	120
C(32)-C(31)-H(31)	120
C(31)-C(30)-C(29)	117.4(3)
C(31)-C(30)-H(30)	121.3
C(29)-C(30)-H(30)	121.3
C(33)-C(34)-H(34A)	109.5
C(33)-C(34)-H(34B)	109.5
H(34A)-C(34)-H(34B)	109.5
C(33)-C(34)-H(34C)	109.5
H(34A)-C(34)-H(34C)	109.5
H(34B)-C(34)-H(34C)	109.5
N(6)-C(24)-C(25)	122.2(3)
N(6)-C(24)-N(7)	115.9(2)
C(25)-C(24)-N(7)	121.7(3)
C(26)-C(25)-C(24)	119.4(3)
C(26)-C(25)-H(25)	120.3
C(24)-C(25)-H(25)	120.3
C(25)-C(26)-C(27)	118.6(3)
C(25)-C(26)-H(26)	120.7
C(27)-C(26)-H(26)	120.7
C(28)-C(27)-C(26)	119.1(3)
C(28)-C(27)-H(27)	120.5
C(26)-C(27)-H(27)	120.5
N(6)-C(28)-C(27)	122.9(3)
N(6)-C(28)-H(28)	118.5
C(27)-C(28)-H(28)	118.5
Pt(2)-C(36)-H(36A)	109.5

Pt(2)-C(36)-H(36B)	109.5
H(36A)-C(36)-H(36B)	109.5
Pt(2)-C(36)-H(36C)	109.5
H(36A)-C(36)-H(36C)	109.5
H(36B)-C(36)-H(36C)	109.5
Pt(2)-C(35)-H(35A)	109.5
Pt(2)-C(35)-H(35B)	109.5
H(35A)-C(35)-H(35B)	109.5
Pt(2)-C(35)-H(35C)	109.5
H(35A)-C(35)-H(35C)	109.5
H(35B)-C(35)-H(35C)	109.5

Notes to Appendix A.

[1] Bruker (**2007**) APEX2 (Version 2.1-4), SAINT (version 7.34A), SADABS (version 2007/4), BrukerAXS Inc, Madison, Wisconsin, USA.

[2] (a) Altomare, A.; Burla, C.; Camalli M.; Cascarano L.; Giacovazzo C.; Guagliardi A.; Moliterni A.G.G.; Polidori G.; Spagna R. J. Appl. Cryst. 1999, **32**, 115-119. (b) Altomare, A., Cascarano, G., Giacovazzo, C., Guagliardi, A., J. Appl. Cryst. 1993, **26**, 343.

[3] Sheldrick, G. M. SHELXL-97: Program for the Refinement of Crystal Structures 1997 University of Gottingen, Germany.

[4] Mackay, S.; Edwards, C.; Henderson, A.; Gilmore, C.; Stewart, N.; Shankland, K.; Donald, A.; *MaXus: a computer program for the solution and refinement of crystal structures from diffraction data*. University of Glasgow, Scotland, 1997.

[5] Waasmaier, D.; Kirfel, A. Acta Crystallogr. A. 1995, **51**, 416.

Appendix B: X-Ray Crystal Data for Chapter 4

X-ray Structure Analyses, Sample Preparation and Data Acquisition for (POCOP)Ir(CO)(H):
An orange prism, measuring 0.1 x 0.07 x 0.03 mm^3 was mounted on a glass capillary with oil. Data was collected at -173^{o}C on a Bruker APEX II single crystal X-ray diffractometer, Mo-radiation.

Crystal-to-detector distance was 40 mm and exposure time was 10 seconds per frame for all sets. The scan width was 0.5^o. Data collection was 98.1% complete to 25^o in ϑ. A total of 20425 (merged) reflections were collected covering the indices, h = -12 to 12, k = -18 to 18, l = -20 to 20. 9169 reflections were symmetry independent and the R_{int} = 0.0565 indicated that the data was good (average quality 0.07). Indexing and unit cell refinement indicated a triclinic lattice. The space group was found to be P $\bar{1}$ (No.2).

X-ray Structure Analyses, Sample Preparation and Data Acquisition for $[(POCOP)Ir(CO)(H)]^+$:
An orange piece, measuring 0.20 x 0.10 x 0.03 mm^3 was mounted on a loop with oil. Data was collected at -173^{o}C on a Bruker APEX II single crystal X-ray diffractometer, Mo-radiation.

Crystal-to-detector distance was 45 mm and exposure time was 10 seconds per frame for all sets. The scan width was 0.5^o. Data collection was 100% complete to 25^o in ϑ. A total of 259706 reflections were collected covering the indices, h = -22 to 22, k = -24 to 24, l = -53 to 53. 15581 reflections were symmetry independent and the R_{int} = 0.0858 indicated that the data was of slightly less than average quality (0.07). Indexing and unit cell refinement indicated a C-centered monoclinic lattice. The space group was found to be C 2/c (No.15).

X-ray Structure Analyses, Structure Determination and Data Refinement.
The data were integrated and scaled using SAINT and SADABS within the APEX2 software package by Bruker.[1] Solution by direct methods (SHELXS, SIR97)[2,3] produced a complete heavy atom phasing model consistent with the proposed structure. The structure was completed by difference Fourier synthesis with SHELXL97.[4,5] Scattering factors are from Waasmair and Kirfel.[6] Hydrogen atoms were placed in geometrically idealized positions and constrained to ride on their parent atoms with C---H distances in the range 0.95-1.00 Å. Isotropic thermal parameters U_{eq} were fixed such that they were 1.2U_{eq} of their parent atom U_{eq} for CH's and 1.5U_{eq} of their parent atom U_{eq} in case of methyl groups. All non-hydrogen atoms were refined anisotropically by full-matrix least-squares.

Table B-1. Crystallographic data for (POCOP)Ir(CO) and $[(POCOP)Ir(CO)(H)]^+$.

	(POCOP)Ir(CO)	$[(POCOP)Ir(CO)(H)]^+$
Empirical formula	$C_{23}H_{39}IrO_3P_2$	$C_{55}H_{52}BF_{24}IrO_3P_2$
Formula weight	617.68	1481.9
Temperature, K	100(2)	100(2)
Wavelength, Å	0.71073	0.71073
Crystal system	Triclinic	Monoclinic
Space group	P $\bar{1}$	C 2/c
a, Å	8.288(7)	16.707(2)
b, Å	11.990(9)	18.088(2)
c, Å	13.424(10)	39.933(5)
α, (º)	100.742(15)°.	90°.
β, (º)	95.96(3)°.	96.480(10)°.
γ, (º)	103.708(14)°.	90°.
Volume, $Å^3$	1258.0(16)	11991(3)
Z	2	8
Density (calcd), mg/m^3	1.631	1.642
Absorption coefficient, mm^{-1}	5.454	2.397
F(000)	616	5872
Crystal size, mm^3	0.10 x 0.07 x 0.03	0.20 x 0.10 x 0.03
Theta range for data collection, (º)	1.79 to 33.21°.	1.67 to 29.51°.
Reflections collected	20425	259706
Independent reflections	9169 [R(int) = 0.0565]	15581 [R(int) = 0.0858]
Completeness to theta = 25.00°	98.1 %	100.0 %
Max. and min. transmission	0.8535 and 0.6115	0.9316 and 0.6457
Refinement method	Full-matrix least-squares on F^2	Full-matrix least-squares on F^2
Data / restraints / parameters	9169 / 0 / 274	15581 / 0 / 791
Goodness-of-fit on F^2	0.978	1.115
Final R indices [I>2sigma(I)]	R1 = 0.0422, wR2 = 0.0696	R1 = 0.0537, wR2 = 0.1069
R indices (all data)	R1 = 0.0665, wR2 = 0.0772	R1 = 0.0709, wR2 = 0.1138

Table B-2. Bond lengths for (POCOP)Ir(CO).

Bond	Bond Distance (Å)
C(1)-C(6)	1.386(5)
C(1)-C(2)	1.402(5)
C(1)-Ir(1)	2.060(4)
C(2)-C(3)	1.380(5)
C(2)-O(1)	1.389(4)
C(3)-C(4)	1.385(5)
C(3)-H(3)	0.9500
C(4)-C(5)	1.395(5)
C(4)-H(4)	0.9500
C(5)-C(6)	1.393(5)
C(5)-H(5)	0.9500
C(6)-O(2)	1.402(4)
C(7)-C(10)	1.526(6)
C(7)-C(9)	1.527(6)
C(7)-C(8)	1.531(6)
C(7)-P(1)	1.850(4)
C(8)-H(8A)	0.9800
C(8)-H(8B)	0.9800
C(8)-H(8C)	0.9800
C(9)-H(9A)	0.9800
C(9)-H(9B)	0.9800
C(9)-H(9C)	0.9800
C(10)-H(10A)	0.9800
C(10)-H(10B)	0.9800
C(10)-H(10C)	0.9800
C(11)-C(12)	1.522(7)
C(11)-C(13)	1.525(6)
C(11)-C(14)	1.526(6)
C(11)-P(1)	1.858(4)
C(12)-H(12A)	0.9800
C(12)-H(12B)	0.9800
C(12)-H(12C)	0.9800
C(13)-H(13A)	0.9800
C(13)-H(13B)	0.9800
C(13)-H(13C)	0.9800
C(14)-H(14A)	0.9800
C(14)-H(14B)	0.9800
C(14)-H(14C)	0.9800

C(15)-C(18)	1.532(6)
C(15)-C(17)	1.537(6)
C(15)-C(16)	1.538(6)
C(15)-P(2)	1.857(4)
C(16)-H(16A)	0.9800
C(16)-H(16B)	0.9800
C(16)-H(16C)	0.9800
C(17)-H(17A)	0.9800
C(17)-H(17B)	0.9800
C(17)-H(17C)	0.9800
C(18)-H(18A)	0.9800
C(18)-H(18B)	0.9800
C(18)-H(18C)	0.9800
C(19)-C(22)	1.517(6)
C(19)-C(20)	1.535(6)
C(19)-C(21)	1.539(6)
C(19)-P(2)	1.862(4)
C(20)-H(20A)	0.9800
C(20)-H(20B)	0.9800
C(20)-H(20C)	0.9800
C(21)-H(21A)	0.9800
C(21)-H(21B)	0.9800
C(21)-H(21C)	0.9800
C(22)-H(22A)	0.9800
C(22)-H(22B)	0.9800
C(22)-H(22C)	0.9800
C(23)-O(3)	1.153(5)
C(23)-Ir(1)	1.884(4)
O(1)-P(1)	1.667(3)
O(2)-P(2)	1.666(3)
P(1)-Ir(1)	2.2848(17)
P(2)-Ir(1)	2.2794(17)

Table B-3. Bond angles for (POCOP)Ir(CO).

Bond	Bond Angle [°]
C(6)-C(1)-C(2)	115.6(3)
C(6)-C(1)-Ir(1)	122.0(3)
C(2)-C(1)-Ir(1)	122.4(3)
C(3)-C(2)-O(1)	119.4(3)
C(3)-C(2)-C(1)	123.4(4)

O(1)-C(2)-C(1)	117.2(3)
C(2)-C(3)-C(4)	118.4(3)
C(2)-C(3)-H(3)	120.8
C(4)-C(3)-H(3)	120.8
C(3)-C(4)-C(5)	121.3(4)
C(3)-C(4)-H(4)	119.3
C(5)-C(4)-H(4)	119.3
C(6)-C(5)-C(4)	117.6(4)
C(6)-C(5)-H(5)	121.2
C(4)-C(5)-H(5)	121.2
C(1)-C(6)-C(5)	123.7(3)
C(1)-C(6)-O(2)	118.2(3)
C(5)-C(6)-O(2)	118.1(3)
C(10)-C(7)-C(9)	107.4(4)
C(10)-C(7)-C(8)	108.4(4)
C(9)-C(7)-C(8)	111.0(4)
C(10)-C(7)-P(1)	105.3(3)
C(9)-C(7)-P(1)	115.1(3)
C(8)-C(7)-P(1)	109.4(3)
C(7)-C(8)-H(8A)	109.5
C(7)-C(8)-H(8B)	109.5
H(8A)-C(8)-H(8B)	109.5
C(7)-C(8)-H(8C)	109.5
H(8A)-C(8)-H(8C)	109.5
H(8B)-C(8)-H(8C)	109.5
C(7)-C(9)-H(9A)	109.5
C(7)-C(9)-H(9B)	109.5
H(9A)-C(9)-H(9B)	109.5
C(7)-C(9)-H(9C)	109.5
H(9A)-C(9)-H(9C)	109.5
H(9B)-C(9)-H(9C)	109.5
C(7)-C(10)-H(10A)	109.5
C(7)-C(10)-H(10B)	109.5
H(10A)-C(10)-H(10B)	109.5
C(7)-C(10)-H(10C)	109.5
H(10A)-C(10)-H(10C)	109.5
H(10B)-C(10)-H(10C)	109.5
C(12)-C(11)-C(13)	109.5(4)
C(12)-C(11)-C(14)	107.3(4)
C(13)-C(11)-C(14)	109.6(4)
C(12)-C(11)-P(1)	105.3(3)
C(13)-C(11)-P(1)	110.2(3)

C(14)-C(11)-P(1)	114.8(3)
C(11)-C(12)-H(12A)	109.5
C(11)-C(12)-H(12B)	109.5
H(12A)-C(12)-H(12B)	109.5
C(11)-C(12)-H(12C)	109.5
H(12A)-C(12)-H(12C)	109.5
H(12B)-C(12)-H(12C)	109.5
C(11)-C(13)-H(13A)	109.5
C(11)-C(13)-H(13B)	109.5
H(13A)-C(13)-H(13B)	109.5
C(11)-C(13)-H(13C)	109.5
H(13A)-C(13)-H(13C)	109.5
H(13B)-C(13)-H(13C)	109.5
C(11)-C(14)-H(14A)	109.5
C(11)-C(14)-H(14B)	109.5
H(14A)-C(14)-H(14B)	109.5
C(11)-C(14)-H(14C)	109.5
H(14A)-C(14)-H(14C)	109.5
H(14B)-C(14)-H(14C)	109.5
C(18)-C(15)-C(17)	110.2(4)
C(18)-C(15)-C(16)	108.0(4)
C(17)-C(15)-C(16)	108.5(4)
C(18)-C(15)-P(2)	114.7(3)
C(17)-C(15)-P(2)	110.2(3)
C(16)-C(15)-P(2)	105.0(3)
C(15)-C(16)-H(16A)	109.5
C(15)-C(16)-H(16B)	109.5
H(16A)-C(16)-H(16B)	109.5
C(15)-C(16)-H(16C)	109.5
H(16A)-C(16)-H(16C)	109.5
H(16B)-C(16)-H(16C)	109.5
C(15)-C(17)-H(17A)	109.5
C(15)-C(17)-H(17B)	109.5
H(17A)-C(17)-H(17B)	109.5
C(15)-C(17)-H(17C)	109.5
H(17A)-C(17)-H(17C)	109.5
H(17B)-C(17)-H(17C)	109.5
C(15)-C(18)-H(18A)	109.5
C(15)-C(18)-H(18B)	109.5
H(18A)-C(18)-H(18B)	109.5
C(15)-C(18)-H(18C)	109.5
H(18A)-C(18)-H(18C)	109.5

H(18B)-C(18)-H(18C)	109.5
C(22)-C(19)-C(20)	108.8(4)
C(22)-C(19)-C(21)	110.0(4)
C(20)-C(19)-C(21)	108.5(4)
C(22)-C(19)-P(2)	114.8(3)
C(20)-C(19)-P(2)	105.2(3)
C(21)-C(19)-P(2)	109.2(3)
C(19)-C(20)-H(20A)	109.5
C(19)-C(20)-H(20B)	109.5
H(20A)-C(20)-H(20B)	109.5
C(19)-C(20)-H(20C)	109.5
H(20A)-C(20)-H(20C)	109.5
H(20B)-C(20)-H(20C)	109.5
C(19)-C(21)-H(21A)	109.5
C(19)-C(21)-H(21B)	109.5
H(21A)-C(21)-H(21B)	109.5
C(19)-C(21)-H(21C)	109.5
H(21A)-C(21)-H(21C)	109.5
H(21B)-C(21)-H(21C)	109.5
C(19)-C(22)-H(22A)	109.5
C(19)-C(22)-H(22B)	109.5
H(22A)-C(22)-H(22B)	109.5
C(19)-C(22)-H(22C)	109.5
H(22A)-C(22)-H(22C)	109.5
H(22B)-C(22)-H(22C)	109.5
O(3)-C(23)-Ir(1)	178.1(4)
C(2)-O(1)-P(1)	115.5(2)
C(6)-O(2)-P(2)	114.5(2)
O(1)-P(1)-C(7)	99.88(18)
O(1)-P(1)-C(11)	100.81(17)
C(7)-P(1)-C(11)	114.0(2)
O(1)-P(1)-Ir(1)	106.22(11)
C(7)-P(1)-Ir(1)	116.64(14)
C(11)-P(1)-Ir(1)	116.04(15)
O(2)-P(2)-C(15)	100.11(17)
O(2)-P(2)-C(19)	100.62(17)
C(15)-P(2)-C(19)	113.26(19)
O(2)-P(2)-Ir(1)	106.42(11)
C(15)-P(2)-Ir(1)	116.18(14)
C(19)-P(2)-Ir(1)	117.02(14)
C(23)-Ir(1)-C(1)	179.47(18)
C(23)-Ir(1)-P(2)	100.81(13)

C(1)-Ir(1)-P(2)	78.89(12)
C(23)-Ir(1)-P(1)	101.65(13)
C(1)-Ir(1)-P(1)	78.66(12)
P(2)-Ir(1)-P(1)	157.51(4)

Table B-4. Bond lengths for $[(POCOP)Ir(CO)(H)]^{+}$.

Bond	Bond Distance (Å)
C(1)-C(2)	1.392(6)
C(1)-C(6)	1.392(7)
C(1)-Ir(1)	2.033(5)
C(2)-C(3)	1.387(6)
C(2)-O(1)	1.391(6)
C(3)-C(4)	1.381(7)
C(3)-H(3)	0.9500
C(4)-C(5)	1.387(7)
C(4)-H(4)	0.9500
C(5)-C(6)	1.394(7)
C(5)-H(5)	0.9500
C(6)-O(2)	1.392(6)
C(7)-C(8)	1.516(12)
C(7)-C(9)	1.538(11)
C(7)-C(10)	1.542(11)
C(7)-P(2)	1.852(7)
C(8)-H(8A)	0.9800
C(8)-H(8B)	0.9800
C(8)-H(8C)	0.9800
C(9)-H(9A)	0.9800
C(9)-H(9B)	0.9800
C(9)-H(9C)	0.9800
C(10)-H(10A)	0.9800
C(10)-H(10B)	0.9800
C(10)-H(10C)	0.9800
C(11)-C(12)	1.506(13)
C(11)-C(14)	1.512(8)
C(11)-C(13)	1.540(12)
C(11)-P(2)	1.853(7)
C(12)-H(12A)	0.9800
C(12)-H(12B)	0.9800
C(12)-H(12C)	0.9800
C(13)-H(13A)	0.9800

C(13)-H(13B)	0.9800
C(13)-H(13C)	0.9800
C(14)-H(14A)	0.9800
C(14)-H(14B)	0.9800
C(14)-H(14C)	0.9800
C(15)-C(16)	1.517(7)
C(15)-C(18)	1.519(7)
C(15)-C(17)	1.544(7)
C(15)-P(1)	1.852(5)
C(16)-H(16A)	0.9800
C(16)-H(16B)	0.9800
C(16)-H(16C)	0.9800
C(17)-H(17A)	0.9800
C(17)-H(17B)	0.9800
C(17)-H(17C)	0.9800
C(18)-H(18A)	0.9800
C(18)-H(18B)	0.9800
C(18)-H(18C)	0.9800
C(19)-C(20)	1.519(7)
C(19)-C(22)	1.520(8)
C(19)-C(21)	1.523(8)
C(19)-P(1)	1.851(5)
C(20)-H(20A)	0.9800
C(20)-H(20B)	0.9800
C(20)-H(20C)	0.9800
C(21)-H(21A)	0.9800
C(21)-H(21B)	0.9800
C(21)-H(21C)	0.9800
C(22)-H(22A)	0.9800
C(22)-H(22B)	0.9800
C(22)-H(22C)	0.9800
C(23)-O(3)	1.132(7)
C(23)-Ir(1)	1.929(6)
C(24)-C(25)	1.398(7)
C(24)-C(29)	1.399(7)
C(24)-B(1)	1.636(7)
C(25)-C(26)	1.400(7)
C(25)-H(25)	0.9500
C(26)-C(27)	1.379(8)
C(26)-C(30)	1.505(10)
C(27)-C(28)	1.371(8)
C(27)-H(27)	0.9500

C(28)-C(29)	1.391(7)
C(28)-C(31)	1.485(7)
C(29)-H(29)	0.9500
C(30)-F(1)	1.260(10)
C(30)-F(3)	1.277(9)
C(30)-F(2)	1.357(10)
C(31)-F(6)	1.233(7)
C(31)-F(4)	1.306(7)
C(31)-F(5)	1.415(8)
C(32)-C(37)	1.395(6)
C(32)-C(33)	1.399(6)
C(32)-B(1)	1.637(7)
C(33)-C(34)	1.392(6)
C(33)-H(33)	0.9500
C(34)-C(35)	1.387(6)
C(34)-C(38)	1.501(7)
C(35)-C(36)	1.382(7)
C(35)-H(35)	0.9500
C(36)-C(37)	1.400(7)
C(36)-C(39)	1.492(7)
C(37)-H(37)	0.9500
C(38)-F(8)	1.318(7)
C(38)-F(7)	1.327(6)
C(38)-F(9)	1.336(6)
C(39)-F(12)	1.312(8)
C(39)-F(10)	1.332(7)
C(39)-F(11)	1.349(8)
C(40)-C(45)	1.386(6)
C(40)-C(41)	1.409(6)
C(40)-B(1)	1.641(7)
C(41)-C(42)	1.383(6)
C(41)-H(41)	0.9500
C(42)-C(43)	1.383(7)
C(42)-C(46)	1.503(7)
C(43)-C(44)	1.386(7)
C(43)-H(43)	0.9500
C(44)-C(45)	1.397(7)
C(44)-C(47)	1.494(7)
C(45)-H(45)	0.9500
C(46)-F(14)	1.294(6)
C(46)-F(15)	1.331(6)
C(46)-F(13)	1.334(6)

C(47)-F(16)	1.324(7)
C(47)-F(17)	1.335(7)
C(47)-F(18)	1.340(7)
C(48)-C(49)	1.391(7)
C(48)-C(53)	1.407(6)
C(48)-B(1)	1.644(7)
C(49)-C(50)	1.394(7)
C(49)-H(49)	0.9500
C(50)-C(51)	1.389(7)
C(50)-C(54)	1.494(8)
C(51)-C(52)	1.382(8)
C(51)-H(51)	0.9500
C(52)-C(53)	1.388(7)
C(52)-C(55)	1.496(8)
C(53)-H(53)	0.9500
C(54)-F(20)	1.333(6)
C(54)-F(19)	1.334(7)
C(54)-F(21)	1.336(6)
C(55)-F(24)	1.283(8)
C(55)-F(23)	1.293(9)
C(55)-F(22)	1.311(8)
O(1)-P(1)	1.645(3)
O(2)-P(2)	1.638(4)
P(1)-Ir(1)	2.3196(12)
P(2)-Ir(1)	2.3209(14)
Ir(1)-H(1I)	1.58(7)

Table B-5. Bond angles for $[(POCOP)Ir(CO)(H)]^{+}$.

Bond	Bond Angle [°]
C(2)-C(1)-C(6)	116.7(4)
C(2)-C(1)-Ir(1)	121.5(4)
C(6)-C(1)-Ir(1)	121.8(3)
C(3)-C(2)-O(1)	118.5(4)
C(3)-C(2)-C(1)	122.8(5)
O(1)-C(2)-C(1)	118.8(4)
C(4)-C(3)-C(2)	117.8(5)
C(4)-C(3)-H(3)	121.1
C(2)-C(3)-H(3)	121.1
C(3)-C(4)-C(5)	122.6(5)
C(3)-C(4)-H(4)	118.7

C(5)-C(4)-H(4)	118.7
C(4)-C(5)-C(6)	117.2(5)
C(4)-C(5)-H(5)	121.4
C(6)-C(5)-H(5)	121.4
O(2)-C(6)-C(1)	118.4(4)
O(2)-C(6)-C(5)	118.7(4)
C(1)-C(6)-C(5)	122.9(4)
C(8)-C(7)-C(9)	109.4(10)
C(8)-C(7)-C(10)	108.9(6)
C(9)-C(7)-C(10)	110.9(8)
C(8)-C(7)-P(2)	106.0(5)
C(9)-C(7)-P(2)	111.7(5)
C(10)-C(7)-P(2)	109.7(6)
C(7)-C(8)-H(8A)	109.5
C(7)-C(8)-H(8B)	109.5
H(8A)-C(8)-H(8B)	109.5
C(7)-C(8)-H(8C)	109.5
H(8A)-C(8)-H(8C)	109.5
H(8B)-C(8)-H(8C)	109.5
C(7)-C(9)-H(9A)	109.5
C(7)-C(9)-H(9B)	109.5
H(9A)-C(9)-H(9B)	109.5
C(7)-C(9)-H(9C)	109.5
H(9A)-C(9)-H(9C)	109.5
H(9B)-C(9)-H(9C)	109.5
C(7)-C(10)-H(10A)	109.5
C(7)-C(10)-H(10B)	109.5
H(10A)-C(10)-H(10B)	109.5
C(7)-C(10)-H(10C)	109.5
H(10A)-C(10)-H(10C)	109.5
H(10B)-C(10)-H(10C)	109.5
C(12)-C(11)-C(14)	110.0(8)
C(12)-C(11)-C(13)	110.5(10)
C(14)-C(11)-C(13)	108.2(6)
C(12)-C(11)-P(2)	105.6(5)
C(14)-C(11)-P(2)	110.4(5)
C(13)-C(11)-P(2)	112.2(6)
C(11)-C(12)-H(12A)	109.5
C(11)-C(12)-H(12B)	109.5
H(12A)-C(12)-H(12B)	109.5
C(11)-C(12)-H(12C)	109.5
H(12A)-C(12)-H(12C)	109.5

H(12B)-C(12)-H(12C)	109.5
C(11)-C(13)-H(13A)	109.5
C(11)-C(13)-H(13B)	109.5
H(13A)-C(13)-H(13B)	109.5
C(11)-C(13)-H(13C)	109.5
H(13A)-C(13)-H(13C)	109.5
H(13B)-C(13)-H(13C)	109.5
C(11)-C(14)-H(14A)	109.5
C(11)-C(14)-H(14B)	109.5
H(14A)-C(14)-H(14B)	109.5
C(11)-C(14)-H(14C)	109.5
H(14A)-C(14)-H(14C)	109.5
H(14B)-C(14)-H(14C)	109.5
C(16)-C(15)-C(18)	110.3(5)
C(16)-C(15)-C(17)	108.0(5)
C(18)-C(15)-C(17)	109.6(6)
C(16)-C(15)-P(1)	106.4(4)
C(18)-C(15)-P(1)	113.0(4)
C(17)-C(15)-P(1)	109.3(3)
C(15)-C(16)-H(16A)	109.5
C(15)-C(16)-H(16B)	109.5
H(16A)-C(16)-H(16B)	109.5
C(15)-C(16)-H(16C)	109.5
H(16A)-C(16)-H(16C)	109.5
H(16B)-C(16)-H(16C)	109.5
C(15)-C(17)-H(17A)	109.5
C(15)-C(17)-H(17B)	109.5
H(17A)-C(17)-H(17B)	109.5
C(15)-C(17)-H(17C)	109.5
H(17A)-C(17)-H(17C)	109.5
H(17B)-C(17)-H(17C)	109.5
C(15)-C(18)-H(18A)	109.5
C(15)-C(18)-H(18B)	109.5
H(18A)-C(18)-H(18B)	109.5
C(15)-C(18)-H(18C)	109.5
H(18A)-C(18)-H(18C)	109.5
H(18B)-C(18)-H(18C)	109.5
C(20)-C(19)-C(22)	107.9(5)
C(20)-C(19)-C(21)	109.7(5)
C(22)-C(19)-C(21)	110.6(6)
C(20)-C(19)-P(1)	105.9(4)
C(22)-C(19)-P(1)	112.9(4)

C(21)-C(19)-P(1)	109.7(4)
C(19)-C(20)-H(20A)	109.5
C(19)-C(20)-H(20B)	109.5
H(20A)-C(20)-H(20B)	109.5
C(19)-C(20)-H(20C)	109.5
H(20A)-C(20)-H(20C)	109.5
H(20B)-C(20)-H(20C)	109.5
C(19)-C(21)-H(21A)	109.5
C(19)-C(21)-H(21B)	109.5
H(21A)-C(21)-H(21B)	109.5
C(19)-C(21)-H(21C)	109.5
H(21A)-C(21)-H(21C)	109.5
H(21B)-C(21)-H(21C)	109.5
C(19)-C(22)-H(22A)	109.5
C(19)-C(22)-H(22B)	109.5
H(22A)-C(22)-H(22B)	109.5
C(19)-C(22)-H(22C)	109.5
H(22A)-C(22)-H(22C)	109.5
H(22B)-C(22)-H(22C)	109.5
O(3)-C(23)-Ir(1)	179.7(9)
C(25)-C(24)-C(29)	115.3(4)
C(25)-C(24)-B(1)	123.6(4)
C(29)-C(24)-B(1)	120.9(4)
C(24)-C(25)-C(26)	122.4(5)
C(24)-C(25)-H(25)	118.8
C(26)-C(25)-H(25)	118.8
C(27)-C(26)-C(25)	120.3(5)
C(27)-C(26)-C(30)	119.6(5)
C(25)-C(26)-C(30)	120.0(6)
C(28)-C(27)-C(26)	118.5(5)
C(28)-C(27)-H(27)	120.8
C(26)-C(27)-H(27)	120.8
C(27)-C(28)-C(29)	121.2(5)
C(27)-C(28)-C(31)	119.9(5)
C(29)-C(28)-C(31)	118.9(5)
C(28)-C(29)-C(24)	122.2(5)
C(28)-C(29)-H(29)	118.9
C(24)-C(29)-H(29)	118.9
F(1)-C(30)-F(3)	113.2(8)
F(1)-C(30)-F(2)	100.1(8)
F(3)-C(30)-F(2)	101.9(9)
F(1)-C(30)-C(26)	113.2(8)

F(3)-C(30)-C(26)	114.2(7)
F(2)-C(30)-C(26)	112.9(6)
F(6)-C(31)-F(4)	114.4(6)
F(6)-C(31)-F(5)	99.5(6)
F(4)-C(31)-F(5)	101.8(5)
F(6)-C(31)-C(28)	115.9(5)
F(4)-C(31)-C(28)	114.6(4)
F(5)-C(31)-C(28)	108.1(6)
C(37)-C(32)-C(33)	115.9(4)
C(37)-C(32)-B(1)	122.4(4)
C(33)-C(32)-B(1)	121.6(4)
C(34)-C(33)-C(32)	122.4(4)
C(34)-C(33)-H(33)	118.8
C(32)-C(33)-H(33)	118.8
C(35)-C(34)-C(33)	120.9(4)
C(35)-C(34)-C(38)	119.0(4)
C(33)-C(34)-C(38)	120.0(4)
C(36)-C(35)-C(34)	117.7(4)
C(36)-C(35)-H(35)	121.2
C(34)-C(35)-H(35)	121.2
C(35)-C(36)-C(37)	121.3(4)
C(35)-C(36)-C(39)	120.4(5)
C(37)-C(36)-C(39)	118.3(5)
C(32)-C(37)-C(36)	121.8(4)
C(32)-C(37)-H(37)	119.1
C(36)-C(37)-H(37)	119.1
F(8)-C(38)-F(7)	107.6(5)
F(8)-C(38)-F(9)	106.5(5)
F(7)-C(38)-F(9)	106.0(4)
F(8)-C(38)-C(34)	111.9(4)
F(7)-C(38)-C(34)	112.4(4)
F(9)-C(38)-C(34)	112.1(5)
F(12)-C(39)-F(10)	106.9(6)
F(12)-C(39)-F(11)	107.7(6)
F(10)-C(39)-F(11)	105.0(6)
F(12)-C(39)-C(36)	112.8(6)
F(10)-C(39)-C(36)	113.3(5)
F(11)-C(39)-C(36)	110.6(5)
C(45)-C(40)-C(41)	115.8(4)
C(45)-C(40)-B(1)	122.8(4)
C(41)-C(40)-B(1)	121.3(4)
C(42)-C(41)-C(40)	122.1(4)

C(42)-C(41)-H(41)	119
C(40)-C(41)-H(41)	119
C(41)-C(42)-C(43)	121.4(4)
C(41)-C(42)-C(46)	119.3(4)
C(43)-C(42)-C(46)	119.3(4)
C(42)-C(43)-C(44)	117.4(4)
C(42)-C(43)-H(43)	121.3
C(44)-C(43)-H(43)	121.3
C(43)-C(44)-C(45)	121.2(4)
C(43)-C(44)-C(47)	120.4(5)
C(45)-C(44)-C(47)	118.4(5)
C(40)-C(45)-C(44)	122.0(4)
C(40)-C(45)-H(45)	119
C(44)-C(45)-H(45)	119
F(14)-C(46)-F(15)	107.0(5)
F(14)-C(46)-F(13)	107.7(5)
F(15)-C(46)-F(13)	103.2(4)
F(14)-C(46)-C(42)	113.8(4)
F(15)-C(46)-C(42)	112.2(4)
F(13)-C(46)-C(42)	112.3(4)
F(16)-C(47)-F(17)	105.2(5)
F(16)-C(47)-F(18)	107.3(5)
F(17)-C(47)-F(18)	105.6(5)
F(16)-C(47)-C(44)	112.2(5)
F(17)-C(47)-C(44)	112.9(4)
F(18)-C(47)-C(44)	113.1(5)
C(49)-C(48)-C(53)	115.5(4)
C(49)-C(48)-B(1)	123.1(4)
C(53)-C(48)-B(1)	121.3(4)
C(48)-C(49)-C(50)	123.0(5)
C(48)-C(49)-H(49)	118.5
C(50)-C(49)-H(49)	118.5
C(51)-C(50)-C(49)	120.0(5)
C(51)-C(50)-C(54)	120.6(5)
C(49)-C(50)-C(54)	119.5(5)
C(52)-C(51)-C(50)	118.3(5)
C(52)-C(51)-H(51)	120.8
C(50)-C(51)-H(51)	120.8
C(51)-C(52)-C(53)	121.2(5)
C(51)-C(52)-C(55)	119.5(5)
C(53)-C(52)-C(55)	119.3(5)
C(52)-C(53)-C(48)	121.9(5)

C(52)-C(53)-H(53)	119.1
C(48)-C(53)-H(53)	119.1
F(20)-C(54)-F(19)	106.9(5)
F(20)-C(54)-F(21)	106.5(5)
F(19)-C(54)-F(21)	106.5(5)
F(20)-C(54)-C(50)	112.2(5)
F(19)-C(54)-C(50)	112.0(4)
F(21)-C(54)-C(50)	112.3(5)
F(24)-C(55)-F(23)	106.8(7)
F(24)-C(55)-F(22)	105.3(6)
F(23)-C(55)-F(22)	103.4(6)
F(24)-C(55)-C(52)	112.9(5)
F(23)-C(55)-C(52)	114.0(5)
F(22)-C(55)-C(52)	113.6(6)
C(2)-O(1)-P(1)	115.7(3)
C(6)-O(2)-P(2)	115.8(3)
C(24)-B(1)-C(32)	112.3(4)
C(24)-B(1)-C(40)	104.8(4)
C(32)-B(1)-C(40)	111.7(4)
C(24)-B(1)-C(48)	111.3(4)
C(32)-B(1)-C(48)	105.1(4)
C(40)-B(1)-C(48)	111.8(4)
O(1)-P(1)-C(19)	101.9(2)
O(1)-P(1)-C(15)	101.5(2)
C(19)-P(1)-C(15)	115.9(2)
O(1)-P(1)-Ir(1)	104.65(13)
C(19)-P(1)-Ir(1)	113.28(17)
C(15)-P(1)-Ir(1)	116.80(15)
O(2)-P(2)-C(7)	101.0(3)
O(2)-P(2)-C(11)	102.0(2)
C(7)-P(2)-C(11)	116.9(4)
O(2)-P(2)-Ir(1)	104.90(13)
C(7)-P(2)-Ir(1)	115.5(2)
C(11)-P(2)-Ir(1)	113.6(3)
C(23)-Ir(1)-C(1)	179.9(3)
C(23)-Ir(1)-P(1)	100.65(19)
C(1)-Ir(1)-P(1)	79.32(14)
C(23)-Ir(1)-P(2)	101.00(19)
C(1)-Ir(1)-P(2)	79.04(14)
P(1)-Ir(1)-P(2)	158.33(4)
C(23)-Ir(1)-H(1I)	80(3)
C(1)-Ir(1)-H(1I)	100(3)

P(1)-Ir(1)-H(1I)	90(3)
P(2)-Ir(1)-H(1I)	95(3)

Notes to Appendix B.

[1] Bruker (2007), APEX2 (Version 2.1-4), SAINT (Version 7.34A) SADABS (Version 2007/4), Bruker AXS Inc, Madison, Wisconsin, USA.

[2] Altomare, A.; Burla, C.; Camalli, M.; Cascarano, L.; Giacovazzo, C.; Guagliardi, A.; Moliterni, A. G. G.; Polidori, G.; Spagna, R. J. *J. Appl. Cryst.* **1999**, *32*, 115-119.

[3] Altomare, A.; Cascarano, L.; Giacovazzo, C.; Guagliardi, A. *J. Appl. Cryst.* **1993**, *26*, 343-350.

[4] Mackay, S.; Edwards, C.; Henderson, A.; Gillmore, C.; Sterwart, N.; Shankland, K.; Donald, A. *MaXus; a computer program for the solution and refinement of crystal structures from diffraction data*, University of Glasgow, Scotland, 1997.

[5] Sheldrick, G. M. SHELXL-97: Program for the Refinement of Crystal Structures, 1997, University of Gottigen, Germany.

[6] Waasmaier, D.; Kirfel, A. *Acta Crystallogr. A* **1995**, *51*, 416-431.

Vita

David B. Lao was born and raised in Seattle, WA. In 2007, he earned his B.S. in Chemical Engineering from the University of Washington. From 2004-2008 he performed undergraduate research in the labs of Prof. Larry Dalton and Prof. Philip Reid. In 2008, he began graduate studies at the University of Washington in Chemistry working with Prof. James Mayer and Prof. D. Michael Heinekey. David earned his Ph.D. in Chemistry in 2013.